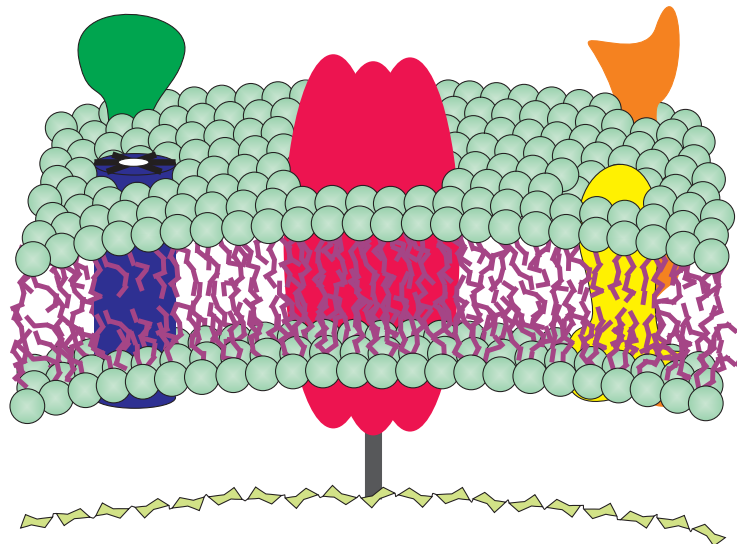




Effect of energy metabolism and membrane structure on single β -receptor motility

PhD Thesis
Tabita Winther Ryder
The Niels Bohr Institute
University of Copenhagen

Supervisor: Lene Broeng Oddershede



Contents

1	Introduction	1
1.0.1	Thesis outline	2
1.1	Acknowledgements	4
2	Methodology: Optical setup	5
2.1	Introduction	5
2.2	Theory	5
2.2.1	Calibration of the optical trap	6
2.3	Our setup	8
2.4	The photodiodes	9
3	The biological system	11
3.1	Introduction	11
3.1.1	The λ -receptor	11
3.1.2	The outer membrane	13
3.1.3	The peptidoglycan layer	14
3.2	The bacterial strains used	15
4	Protein and membrane diffusion	17
4.1	Introduction	17
4.2	Brownian motion	17
4.2.1	Anomalous diffusion	18
4.3	Diffusion in eukaryotes	19
4.4	Diffusion in prokaryotes	20
5	The effect of energy metabolism on the λ-receptor motility	23
5.1	Introduction	23
5.2	Biology	23
5.3	Model	26
5.4	Experimental procedures	29
5.5	Results	31
5.6	Summary	33

6	The effect of the peptidoglycan layer, using ampicillin	35
6.1	Introduction	35
6.2	Biology	35
6.3	Experimental procedures	36
6.4	Results	38
6.5	Summary	40
7	The effect of the peptidoglycan layer, using vancomycin	41
7.1	Introduction	41
7.2	Biology	41
7.3	P1 transduction protocol	43
7.3.1	Getting a single phage colony	43
7.3.2	Getting a P1 transduction solution	44
7.3.3	P1 transduction NR701	44
7.3.4	Purification and testing of the bacteria	45
7.3.5	Getting a P1 transduction solution	46
7.3.6	P1 transduction MCR106	46
7.3.7	P1 transduction into S1964	47
7.3.8	Testing and purification	48
7.3.9	Inserting of the plasmid	48
7.4	Experimental procedures	48
7.5	Results	51
7.6	Summary and conclusion	55
8	The influence of antimicrobial peptides on the λ-receptor motility	57
8.1	Introduction	57
8.2	Biology	57
8.3	Experimental procedures	60
8.4	Results	62
8.4.1	PMB results	62
8.4.2	PMBN results	63
8.5	Summary	63
9	Motility of the inner membrane protein, DsbB	65
9.1	Introduction	65
9.2	Biology	66
9.3	Problems and current status of the project	66
10	Ejection of the DNA of bacteriophage λ	69
10.1	Introduction	69
10.2	Biology	70
10.3	Experimental procedures for <i>in vitro</i> investigations	71
10.4	<i>In vitro</i> results	72

10.5 <i>In vivo</i> results	73
10.6 Summary	75
11 Discussion and conclusion	77
11.1 Outlook	79
A Appendix	81
A.1 Biological dictionary	81
A.2 Stock solutions Media	81
A.2.1 Frozen stocks	82
A.2.2 Vancomycin P1 transduction	82
A.2.3 Arsenate and azide experiments	84
A.2.4 DsbB experiments	84
A.3 DsbB experimental procedures	85
A.3.1 Phage ejection experiments	89

Chapter 1

Introduction

The main purpose of this thesis has been to study the motility of the outer membrane protein, the λ -receptor, in *Escherichia coli* and its dependence on energy metabolism and membrane structure.

E. coli is a gram negative bacterium having three membranes; an inner membrane, the peptidoglycan layer and the outer membrane. The outer membrane is an asymmetric structure where the outer side is mostly composed of lipopolysaccharides (LPS) and proteins and the inner side is composed of phospholipids. The peptidoglycan layer beneath the outer membrane is a rigid structure composed of glycan strands crosslinked by peptide bonds. The λ -receptor is an integral outer membrane protein responsible for transport of maltodextrins across the membrane and used by the bacteriophage lambda as receptor. In the presence of maltose thousands of receptors can be present. The λ -receptor is proposed to be attached to peptidoglycan layer [1].

The motility of proteins is very important for understanding the role of nutrient uptake and regulatory mechanisms of a cell. For prokaryotes (bacteria) this is also important for understanding the action of antibiotics. Single protein diffusion in eukaryotic cells has been studied since the 1970'ties. For a review of single molecule diffusion experimental highlights, see [2]. Only few studies exist on single protein motility in the outer membrane of bacteria. Theoretically it has been shown that there is a connection between the energetic activation of membrane proteins and membrane compartmentalization [3]. The spatial organization of the protein bacteriorhodopsin has been shown to depend on photoactivation. At a specific concentration of protein motility decreased upon photoactivation [4].

The first experiments performed on single molecule mobility in the outer membrane of living bacteria were performed in the optical tweezers group at the Niels Bohr Institute, Copenhagen University [5]. The mobility of an outer membrane protein, the λ -receptor, in *Escherichia coli* was recorded with optical tweezers and single particle tracking. Oddershede et al. observed that the λ -receptor performed a small wiggling motion and that this movement was confined within an area of 50 nm [5].

The experiments performed by Oddershede et al. left the question open of why the λ -receptor performs a wiggling motion and why the motion is area confined. Another interesting discovery made was that in the absence of glucose no receptor mobility was

seen.

In this thesis we have explored the nature of the wiggling motion of the λ -receptor using optical tweezers to follow the receptor motility. We investigated if the motion of the λ -receptor is energy dependent or purely thermal by poisoning the cells with arsenate and azide, which instantaneously stop the energy metabolism.

Previously, most investigations of the working mechanism of antibiotics have been performed as bacterial ensemble studies. The last decade's single molecule experiments have provided an alternative option. Single molecule studies can be used to reveal spatial and temporal inhomogeneities hidden in ensemble measurements, as in the case of polymerase, where single molecule studies have resulted in new information on the mechanism of energy turnover [6].

To further pinpoint the biological mechanism of the "wiggling" motion of the λ -receptor, the motility of single proteins was recorded in the presence or absence of ampicillin. Ampicillin is a commonly used antibiotic, which hinders the crosslinking of peptides in the peptidoglycan layer, blocking the transpeptidase action. Here the motility of the receptor was measured either in the presence or absence of ampicillin.

The influence of the peptidoglycan layer was further investigated by studying the effect of another antibiotic, vancomycin on the receptor motility. Vancomycin binds to the end of the peptide chains (the D-ala-D-ala terminal) hindering further peptidoglycan synthesis. Here we followed the development in time of individual λ -receptor motility upon vancomycin exposure.

Antimicrobial peptides are an alternative to common antibiotics. We have therefore investigated the influence of polymyxin B and polymyxin B nonapeptide on the motility of the λ -receptor.

The motility of the outer protein the λ -receptor is now very well studied. These studies were performed in metabolic competent cells. We therefore wanted to investigate how an inner membrane protein DsbB diffuses in a metabolic incompetent cell. The aim was to use the same techniques to follow the motility of an inner membrane protein as used for the the experiments with the λ -receptor.

The main focus of this thesis has been the motility of the λ -receptor. Since the λ -receptor serves as both the recognition site of bacteriophage λ (a bacterial virus) and involved in uptake of the carbon source maltose. We have also studied the interaction of bacteriophage λ with the λ -receptor both *in vitro* and *in vivo*.

1.0.1 Thesis outline

A large part of the work presented here has involved a great proportion of biology and this will hence be reflected in the thesis. The experimental procedure for the optical tweezers measurements are very similar in chapters 5, 6, 7 and 8, but for the sake of completion the entire description is explained stepwise in each chapter. This way each chapter can be read independently. The thesis is divided into the following chapters:

Chapter 2 : Introduction to our optical setup. Calibration of the optical trap. The two

different photodiodes used in this thesis will be described briefly here.

Chapter 3 : A brief description of the the biological system and the bacterial strains can be found here.

Chapter 4 : A short introduction to diffusion.

Chapter 5 : The influence of energy on the λ -receptor motility has been investigated, using arsenate and azide. Two different theoretical models are proposed to explain the motility pattern of the receptor.

Chapter 6 : The influence of the peptidoglycan layer has been investigated, using the very well known beta-lactamate antibiotic ampicillin.

Chapter 7 : The influence of the peptidoglycan layer has been investigated, using vancomycin. For these experiments a bacterial strain with increased outer membrane permeability has been made.

Chapter 8 : The influence of antimicrobial peptides on the motility of the receptor has been investigated using polymyxin B and polymyxin B nonapeptide.

Chapter 9 : Investigation of the motility of the inner membrane protein DsbB. This project turned out to be more challenging than expected. The chapter provides a short description of the current status of the project.

Chapter 10 : The ejection of DNA of bacterio phage λ has been studied here both *in vitro* and *in vivo*.

Chapter 11 : The obtained results are summarized here and an outlook for further experiments is presented.

1.1 Acknowledgements

The work presented in this thesis has mainly been done in the Optical Tweezers group at the Niels Bohr Institute. I would here especially like to thank my supervisor Dr. Lene Oddershede for guidance throughout the project. I would also like to thank her for her enthusiasm in establishing this group and for making experimental biophysics a vital and growing field at this institute. I would like to thank Kirstine Berg-Sørensen for her work done on developing the two proposed theoretical models on the mobility of the λ -receptor. I would especially like to thank Lei Xu for his work done on the photosensitive diode. I would like to thank the rest of the Optical Tweezers group for creating a lively working environment and for interesting discussion.

The work with the P1 transduction was done at the Institute of Molecular biology at Copenhagen University in collaboration with Dr. Stanley Brown. I would like to thank him for the laboratory training and his suggestions throughout this project.

The work done on bacteriophage λ was carried out at California Technical Institute in the group of professor Rob Phillips. I would here like to thank my close collaborators: Paul Grayson for his excellent laboratory training, Lin Han and Dawe Wu for his matlab expertise. I would also like to thank the rest of the Rob Phillips group for creating an extraordinary working environment.

I would like to thank Christian P. Ryder, Arne S. Madsen, Lars P. Ryder, Heidi Lentge and Kamilla Busk for proofreading and their moral support through this project.

Finally I would like to express my gratitude for the financial support from BioNet supported by the Kann Villum Rasmussen foundation.

Chapter 2

Methodology: Optical setup

2.1 Introduction

Optical traps were first invented by Athur Ashkin in 1970 [7]. He did pioneer work in the invention of the optical trap. Many people have since contributed to the further development of the optical trap. Today optical tweezers are fairly common laboratory equipment. The working mechanism will be described briefly in this chapter. As well as the setup used during my experiments.

The optical trap uses the momentum of light to trap small objects. The forces possible to exert with an optical trap are in the order of piconewton. Many biological processes take place in this force regime, and the technique is hence well suited to monitor biological processes. Using low intensity light in the optical tweezers, and by using a laser in the infrared regime, the damage on biological systems is limited. However, biological damage is seen on trapped bacteria [8], but at higher laser powers and longer time scales than used during my experiment. Optical tweezers also have the advantage that they are able to trap objects within living cells.

2.2 Theory

The interaction between light and matter is not trivial. The scope is here to give a short introduction to the basic principles of optical trapping. The optical tweezers can trap particles of sizes ranging from nanometer to micrometer. Visible and infrared light is normally used for the trapping. The interactions between the particles and the light can be put into three regimes: The Rayleigh-regime, the middle regime and the Mie-regime. In the Rayleigh regime the size of the particle is significantly smaller than the wavelength of the light. The particle can hence be treated as a point dipole source interacting with an electrical field. In the Mie-regime the size of the particle is significantly larger than the wavelength of the light, and the light can be considered as a set of light rays being reflected within the particle. The force acting on the particle can then be found as the sum of all forces on the particle. The situation gets more complicated in the middle area where the

size of the particle and the wavelength of the light are comparable in size. The calculation is here much more complicated. The force on a particle in an arbitrary electromagnetic field can be found by integration of the area surrounding the particle in space [9]

$$F_i = \left\langle \oint_s T_{ij} n_j da \right\rangle, \quad (2.1)$$

where T_{ij} is the Maxwell stress tensor, n_j the normal to the surface and da the area around the particle which is to be integrated. The stress tensor in a stable electromagnetic field in the Minkowsky form is given as

$$T_{ij} = \frac{1}{4\pi} [\epsilon E_i E_j + B_i B_j - \frac{1}{2} (\epsilon E_i E_i + B_i B_i) \delta_{ij}]. \quad (2.2)$$

Here, ϵ is the electric permittivity and E_i and B_i are the electric and the magnetic fields. This equation is very complicated and in our experiments the force of the laser is instead found by experimental calibration.

2.2.1 Calibration of the optical trap

We use the Brownian motion of small particles to calibrate the optical tweezers. Small particles in a media like water perform a wiggling motion due to thermal collision with the surrounding molecules. This movement was first observed and described by the botanist Robert Brown (1827). The Brownian motion of the particles can be described by the Langevin equation:

$$m\ddot{x} = -\gamma\dot{x} + F(t). \quad (2.3)$$

Here m is the mass of the particle, γ the drag coefficient, and $F(t)$ is the thermal noise term. For simplicity the calculations are done in one dimension but the two other dimension could be treated similarly. The thermal noise term is assumed to be white noise, i.e. having vanishing expectation value and delta-function auto-correlation. The drag force $\gamma\dot{x}$ can for small velocities be found by Stokes law: For a sphere moving in a liquid $\gamma = 6\pi\eta R$ where η is the viscosity of the fluid and R is the radius of the sphere. The influence of the optical trap can for small forces be included as a harmonic spring potential giving the equation:

$$m\ddot{x} = -\gamma\dot{x} - \kappa x + F(t) \quad (2.4)$$

with κ being the spring constant. The spring constant can be found from the equipartition theorem as $\frac{1}{2}\kappa\langle x^2 \rangle = \frac{1}{2}\frac{\kappa}{\sigma_x^2} = \frac{1}{2}K_B T$, rearranging gives the spring constant of the trap:

$$\kappa = \frac{K_B T}{\sigma_x^2} \quad (2.5)$$

The left side of equation 2.4 can be neglected due to the small Reynolds number. Fourier transforming equation 2.4 while neglecting the left side of the equation gives the power

spectrum:

$$P(f) = \frac{K_B T}{\pi^2 \gamma} \frac{1}{(f^2 + f_c^2)} \quad (2.6)$$

with the corner frequency $f_c = \frac{\kappa}{2\pi\gamma}$. At low frequencies (long time scales) the movement of the particle is dominated by the influence of the optical trap. At high frequencies (short time scales) the movement of the particle is governed by the Brownian motion. The corner frequency is the turning point between the low frequency and the high frequency regime, and it is illustrated in figure 2.1. This gives another way to find the spring constant of the trap.

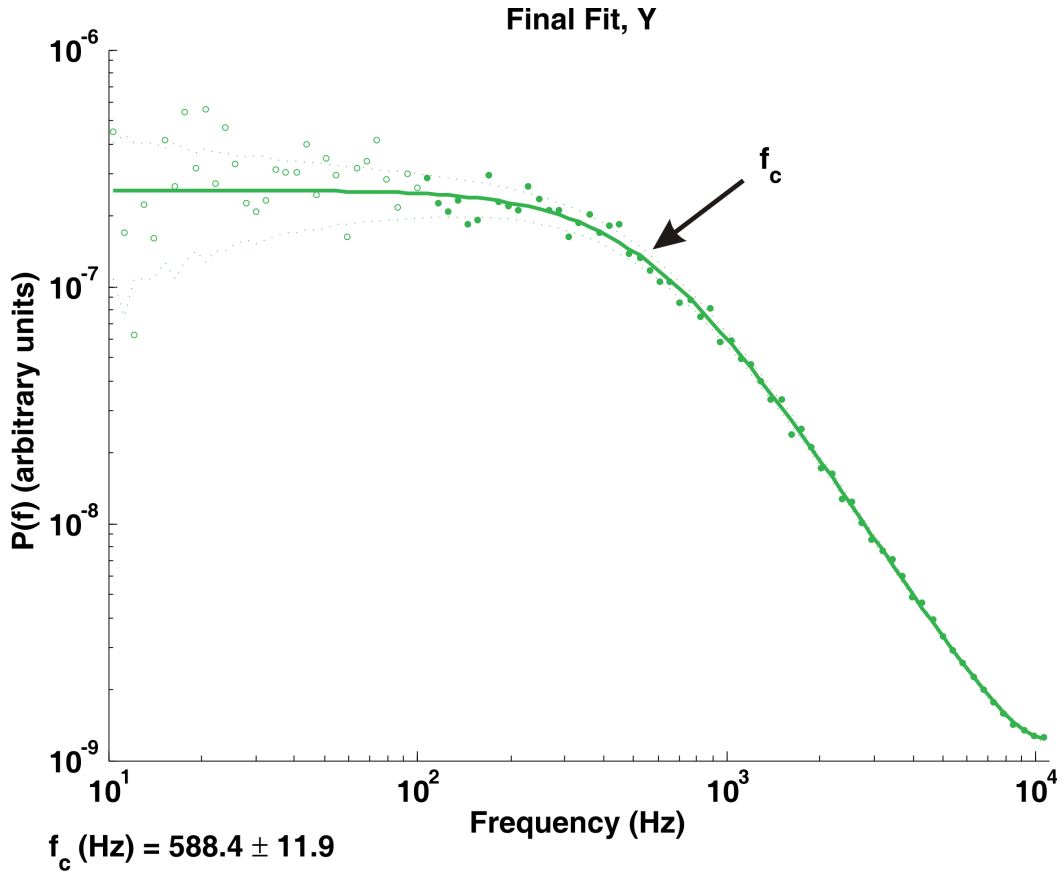


Figure 2.1: A power spectrum of a free bead in an optical trap is shown here. The fit of the power spectrum is used to find the conversion factor between the voltage output and the nanometers displacement. The turning point of the power spectrum is termed the corner frequency.

During my experiments the voltage signal recorded by a photodiode had to be converted into a nanometer displacement. This can be done as long as the movement fulfills Boltzmann statistics, which the freely moving bead does. The probability distribution for

a particle in a harmonic potential is given as:

$$P(x) = P_0 \frac{1}{\sqrt{2\pi}\sigma_x} e^{-\frac{(x-x_0)^2}{2\sigma_x^2}}. \quad (2.7)$$

Here $P(x)$ is the Gaussian distribution with the standard deviation σ_x . For low laser power the voltage signal from the photodiode is linearly related to the actual position of the particle. The voltage distribution is therefore assumed to be Gaussian with the standard deviation σ_V . The conversion factor between the recorded voltage signal and the nanometer movement is then given as $A = \frac{\sigma_x}{\sigma_V}$ with $\sigma_x = \sqrt{\frac{K_B T}{2\pi\gamma f_c}}$. The conversion factor is later used to convert the recorded voltage signal of the bead-receptor complex to a nanometer displacement.

2.3 Our setup

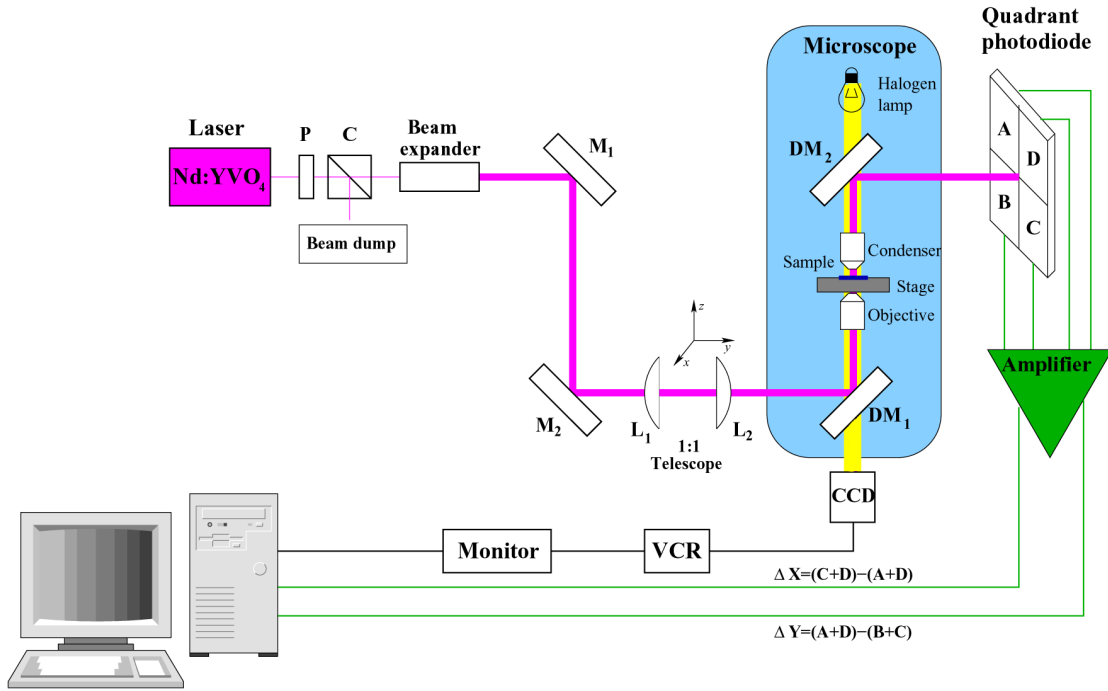


Figure 2.2: A schematic figure of the experimental tweezers setup. The laser light can here be followed through the electronic devices. The laser light is detected by the quadrant photodiode and the signal send to a computer. The microscope is illuminated by a halogen lamp. [10]

The optical tweezers setup is almost identical to the setup described in [10]. A schematic drawing of our setup can be seen in figure 2.2. Our optical tweezers are implemented in

an inverted microscope from Leica (Leica DM IRB HC). The laser is a Nd:YVO₄ laser (10 W Spectra Physics Millennia, = 1064 nm, TEM₀₀). It enters the microscope through the epifluorescence port in the back of the microscope and it is deflected by a custom made dichroic mirror placed in the epifluorescence prism well. After entering the microscope the laser light follows the path of the illuminating light. The laser output (diameter < 1 mm) is sent through a commercial beam expander (16 x, Casix, China). The beam is then steered into a 1:1 telescope, which is used to move the trap in the specimen plane [9]. The telescope consists of two lenses with identical focal lengths of 100 mm, which together images the laser on the back focal plane of the microscope objective. One of the lenses is mounted on a translator, which can move the beam axis in z direction. Translation in x and y directions are motorized by use of two orthogonally mounted Newport DC transducers (model M-MFN25CC) operating with a joystick control. The microscope objective is 100x/1.4 NA oil plan apochromat infinity corrected (Leica) with a back aperture of ~7 mm. The laser light is expanded so that it slightly overfills the back aperture to ensure that the light converges a diffraction limited spot [9]. The microscope has been equipped with a spring-loaded translation stage (750-MS Rolyn Optics, CA) for coarse movements of the sample and a piezoelectric stage (PI 731.20, Physik Instrumente, Germany) with a capacitive feedback control and nm position resolution, used for fine adjustments. Imaging is done by a CCD camera (Sony ES50), its output is sent to S-VHS (Sony SVT S3050P) and to a computer by a National Instrument frame-grabber card (IMAQ PCI 1407). High spatial and temporal resolution is obtained by a non-imaging technique focusing the laser onto a quadrant photodiode (S5981, Hamamatsu) or a photosensitive diode. After focusing the laser by the microscope objective the laser beam is collected by a 1.4 NA oil condenser. The condenser is aligned according to Köhler illumination. By using a dichotic mirror (Oriel) the laser light is passed through a condensing lens and a density filter onto the photodiode. The photodiode is positioned in the back focal plane of the condenser. The size of the beam at the photodiode has a size of 7-8 mm to maximize detector output. The lateral displacement (x and y) of a trapped bead is recorded. The z direction could in principle also be recorded but it is not needed for the measurements of this thesis. The signal from the photodiode enters a custom-built electronics box and is digitized by a 12-bit A/D board (PCI-MOI-16E-4, National Instruments).

2.4 The photodiodes

The signal from the optical trap was either detected by a quadrant photodiode or by a position sensitive detector. The detector is placed on the back focal plane of the objective. When a particle is trapped in the optical tweezers the light is scattered by the particle. Movements of the particle within the trap can by the detector be measured as a change in the light intensity of the scattered light. The mobility of the bead can therefore be measured below the wavelength of the light.

During the work presented in this thesis the setup has been equipped with two different photodiodes. The diode mostly used was a quadrant photodiode. The position signal is

here recorded as the intensity differences between the left and the right halves on the diode $(A+B)-(C+D)$ and the difference between the top and the bottom halves given as $(A+D)-(B+C)$, as shown in figure 2.2. For small displacement of the particle, the signal is a linear response of the displacement of the particle away from the center of the trap.

The quadrant photodiode used in our setup had an unintended high frequency filtering effect [11]. The quadrant photodiode used was of silicon, a material which is highly transparent to our infrared laser. The light is therefore not only absorbed in the depletion region of the diode as intended but also in the n-layer behind it. The electron hole pairs created in the depletion area are actively transported and detected within nanoseconds and a voltage created is measured "instantaneously". On the contrary the valence holes created in the n-layer have to diffuse to the depletion layer before they are recorded, see figure 2.3, this creates a delay of $\sim 20 \mu\text{s}$ [11]. In the frequency regime, this corresponds to a high frequency filtering with a frequency of roughly 10 kHz. The filtering of the photodiode is taken into account during data analysis [12].

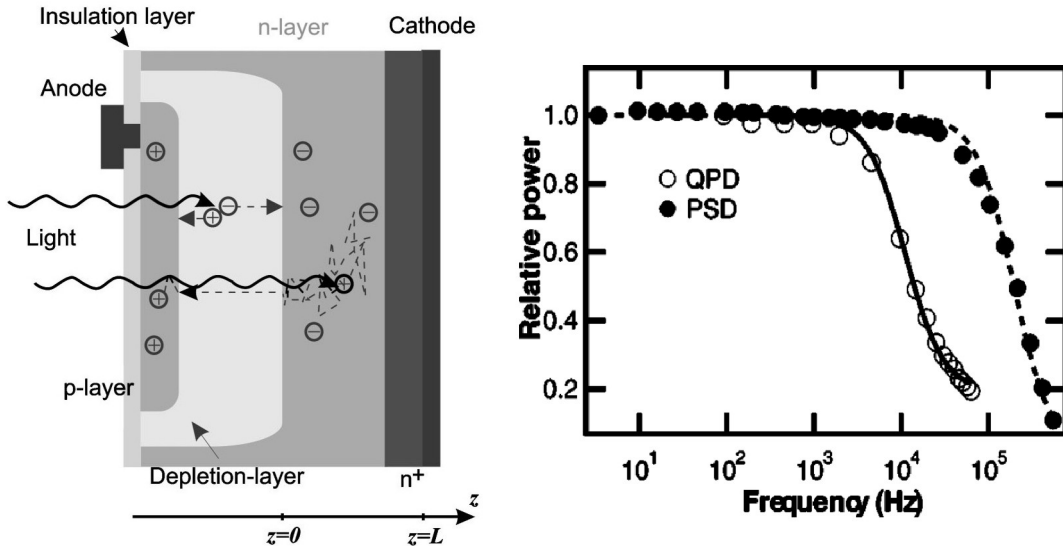


Figure 2.3: Left, a schematic drawing of a typical construction of a quadrant photodiode, seen from the side (the image is not to scale [11]). Right, a comparison between a quadrant photodiode (QP50-6sD, Pacific Silicon Sensor, open circles) and a position sensitive detector (DL 100-7PCBA, Pacific Silicon Sensor, solid circles) [13]. The high frequency filtering of the position sensitive diode is further out than for the quadrant photodiode.

The photo sensitive detector still has a high frequency filtering but further out than the quadrant photodiode, around 100 kHz [13] and shown to the right in figure 2.3.

Chapter 3

The biological system

3.1 Introduction

Escherichia coli is a gram negative bacteria. The natural inhabitation of *E. coli* is the lower intestines of warmblooded animals. It is rod shaped and is roughly $0.8 \mu\text{m}$ in diameter and $2.5 \mu\text{m}$ long, see figure 3.1. During growth it elongates, doubles its DNA and divides into two new cells at the middle. Under warm conditions and in nutrition rich media it can divide as fast as every 20 min. Gram negative bacteria have three membranes, the inner membrane, the outer membrane and the peptidoglycan layer. The inner membrane is a lipid-lipid bilayer with proteins embedded. The outer membrane is more complex; it consists mainly of phospholipids, proteins and lipopolysaccharides (LPS). Between these two membranes is the peptidoglycan layer, which maintains cell shape and gives rigidity. The three membranes will be described in further detail below. The particular *E. coli* strain I have used through most of my studies is a common laboratory strain *E. coli* K12. It was first isolated in 1922 from a diphtheria patient. Since then it has modified so much that it is no longer able to live in the lower human intestines.

3.1.1 The λ -receptor

In this thesis the motility of the λ -receptor has been monitored. The λ -receptor is also termed the malto porin or LamB. The λ -receptor is a pore which transports maltose and maltodextrins across the outer membrane of the bacteria [16]. In the presence of maltose, the λ -receptor is synthesized in great numbers. It is thought to be anchored in the peptidoglycan layer [1]. The λ -receptor is termed after bacteriophage λ , which uses it as a recognition site on *E. coli*. Crystal structures have revealed that the λ -receptor is a trimer, where each monomer consists of a 18-stranded β -barrel, see figure 3.2. Each pore has a diameter of 5-6 Å [17]. In 1975 Ryter et al. analyzed the distribution of the λ -receptor in the outer membrane of *E. coli*. This was done by analyzing electron microscopy pictures of the attachment of bacteriophage λ to the bacteria. The bacteria was exposed to the phage λ after 9 minutes of maltose induction (stimulation of λ -receptor growth). Using an electron microscope, images were taken and the distribution of the receptor on the bacteria

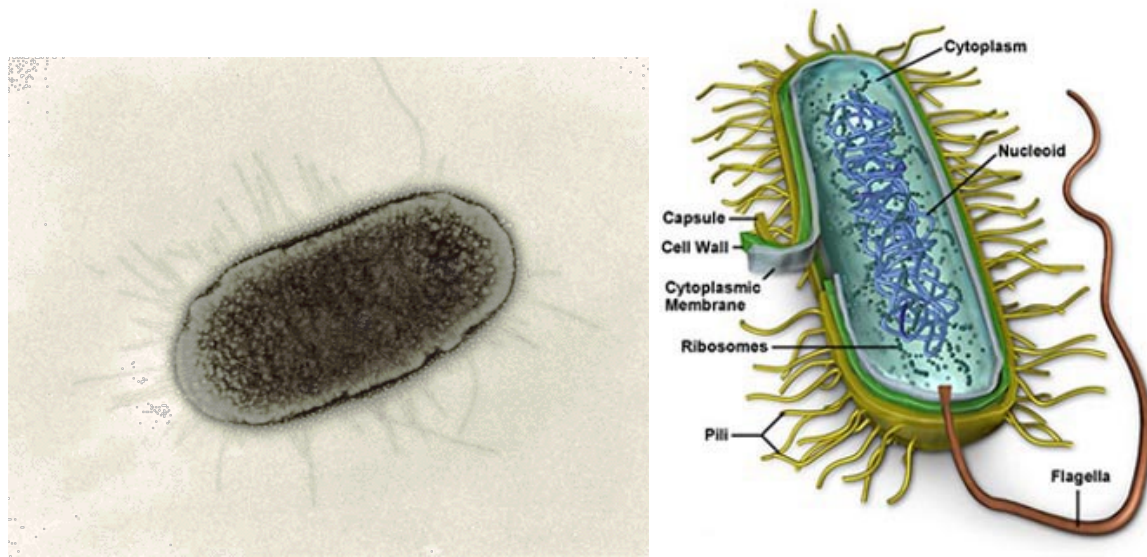


Figure 3.1: Left a electron microscope picture on an *E. coli* cell [14]. Right, a schematic drawing of a gram negative bacterium [15]. Showing the three membranes, the "hairy" structure of pili on the surface and the flagella (used to propel the bacteria forward). The inner membrane surrounds the cytoplasm which ribosomes and the genetic material of the bacteria.

analyzed and found to be present mainly localized at one pole or at the septum (which is only present in dividing cells). In cells induced with maltose for more than one generation the distribution of receptors was homogeneous across the entire cell [18]. The distribution and insertion of the λ -receptor was reinvestigated in 1984 by Vos-Scheperkeuter et al. [19]. Here they used antibody labelled gold beads to see the distribution of receptors. They studied the insertion of λ -receptors in normal *E. coli* cells and the insertion of λ -receptors in *E. coli* cells where the receptor is under the regulation of the lac promoter (it can be stimulated by the presence of IPTG, as we also use). The insertion of the receptor is studied after short induction 4-6 minutes, and in both cases they see a random insertion of the receptor. The only difference between the two types of cells seem to be that there are fewer receptors present in the surface of the strain where the receptor is controlled by the lac promoter. In 2004 Gibbs et al. [20] studied the distribution of λ -receptors in living cells. They did this by attaching fluorescent labelled bacteriophage λ receptors. It is unclear if and for how long the expression of the receptor was done. Fluorescent images were taken every 20 seconds for 5 minutes, the images were averaged to find the distribution of the receptors. Here they see a inhomogeneous distribution of the receptors and in 39 % of the case this distribution is described as helical.

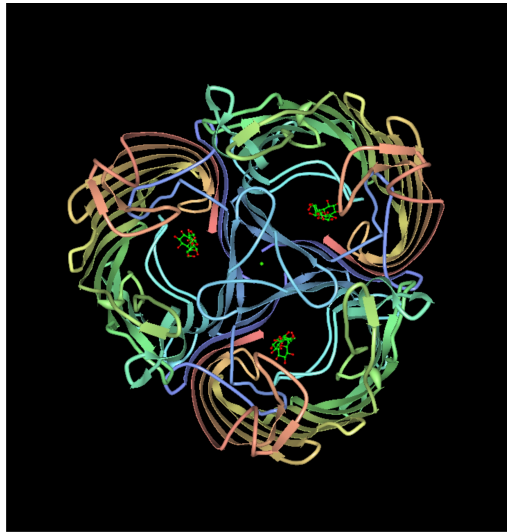


Figure 3.2: A computer generated top view of the λ -receptor trimer.

3.1.2 The outer membrane

The outer membrane is an asymmetrical lipid membrane. It contains two types of lipids: lipopolysaccharides (LPS) and phospholipids. The outer site consists of LPS and the inner site mainly of phospholipids and some LPS. Inserted into the membrane are also proteins (as the λ -receptor) and external organelles as pili and flagella. Pili is a hair-like structure that is used to make the cell adhere to a surface; the cells used for the experiments on the mobility of the λ -receptor are without pili. The flagellum is a long organelle used for transport. A small "motor" within the cell can make the flagellum rotate and thereby propel the cell forward.

The LPS is a unique structure of the gram negative bacteria. It consists of three domains: lipid A, the core, and the O-antigen, see figure 3.3. The *E. coli* K12 used in the mobility experiments for the λ -receptor lacks the O-antigen. The lipid A is the hydrophobic domain of the LPS embedded into the outer membrane. Lipid A is a glucosamine based phospholipid. The O-antigen is a hydrophilic sugar tail that extends into the surrounding media. A large variety is seen between different bacterial species. The O-antigen is composed of repeating units, each composed of up to 7 sugar groups. There can be up to 40 units in a single O-antigen chain, each lined by a glycosidic bond. The core of the LPS is composed of an inner part and an outer part. The outer core is mainly made up of hexose, but the sugar composition varies for different species. The inner core consists of heptose (an unusual monosaccharide with 7 carbon atoms), other monosaccharides, and charged entities as phosphate and ethanolamine. The LPS structure can be seen in figure 3.3

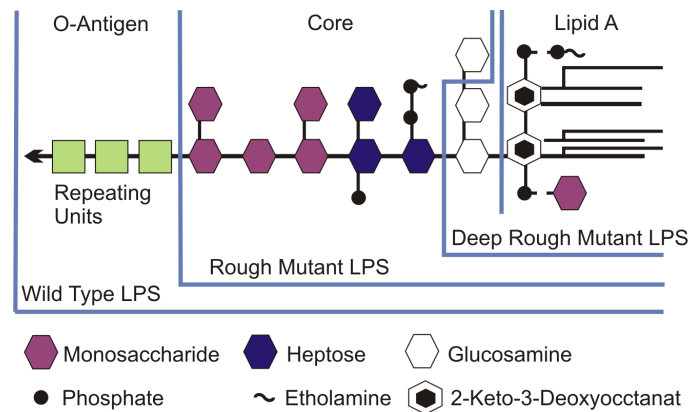


Figure 3.3: A schematic picture of the LPS. To the very left the O-antigen is shown, this part is not present in *E. coli* K12. In the middle is the core, composed of different sugars. To the right is the lipid A, the part of the LPS anchored in the outer membrane. The strains used in this thesis lack the outer repeating unit, of the O-antigen.

3.1.3 The peptidoglycan layer

The peptidoglycan layer consist of long glycan strands cross linked by peptide bonds. Specifically the single glycan strands consist of N-acetylglucosamine (GlcNAc) bound to N-acetylmuramic acid (MurNAc) by a β 1 \rightarrow 4 bond. The carboxyl group of the MurNAc has been exchanged for a residue of peptides (4-5 residues of D-alanine, D-glutamic acid, and meso-diaminopimelic acid in *E. coli*). The peptidoglycan layer is mainly a monolayer in *E. coli*.

The peptidoglycan layer undergo a constant dynamic ATP consuming remodelling. The synthesis of new peptidoglycan is a process of several steps. In figure 3.4 an overview of the whole process of the peptidoglycan synthesis is shown. The synthesis can however be divided into three main domains according to where it takes place in the cell:

- In the cytoplasm, synthesis of individual not finished strands (UDP-MurNAc) is done.
- The unfinished strands are then connected to the inner site of the inner membrane in *E. coli*; attached to a phospholipid forming the complex lipid I. A DlcNAc group is attached to the strand. The strand is thereafter transported to the outer site of the inner membrane.
- The last part takes place on the outer site of the inner membrane, here the newly synthesized strands are attached to existing strands, and afterwards the strands are cross linked.

The peptidoglycan layer has been a very successful target for antibiotics, as it is not present in eukaryotic cells. In this thesis I have investigated how effecting the peptidoglycan

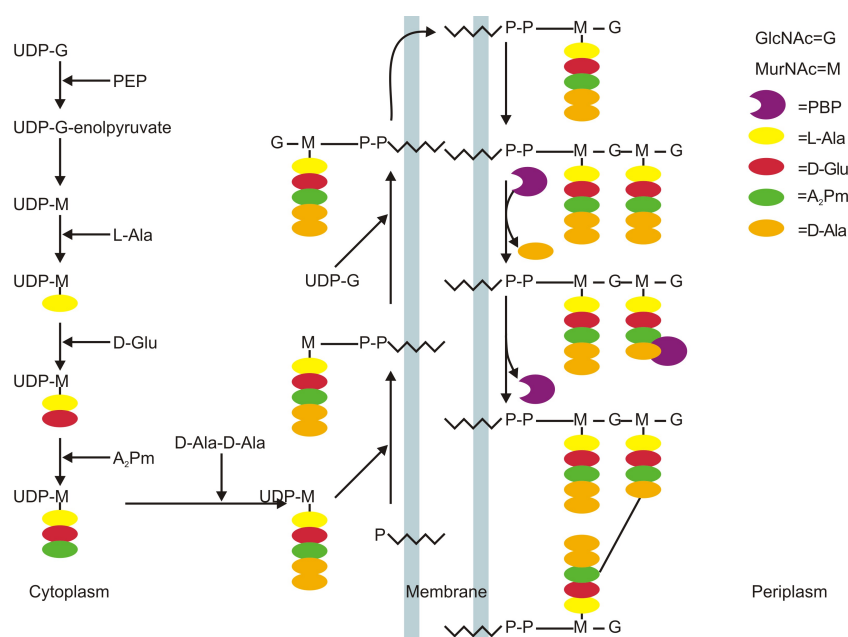


Figure 3.4: The purpose of this figure is to give a schematic view of the peptidoglycan synthesis (for a detailed description see [21], [22], [23], [24]). The short handed notation in the figure is the following: *N*-acetylglucosamine (GlcNAc)=G, *N*-acetylmuramic acid (MurNAc)=M, PEP=phosphoenolpyruvate, Ala=alanine, Glu=glucose, A₂M= meso-diaminopimelic acid, P=phosphogroup, UDP=uridine diphosphate, UMP=uridine monophosphate, PBP=penicillin binding protein.

layer influences the mobility of the λ -receptor, by ampicillin and vancomycin poisoning. Ampicillin and vancomycin hinder the last steps in the peptidoglycan synthesis; a more thorough description of their action can be found in chapter 6 and 7.

3.2 The bacterial strains used

The λ -receptor is in itself so small that we can not follow it with the optical tweezers or single particle tracking without a marker. In the experiments performed in my thesis this marker has been a polystyrene bead of the size of roughly 0.5 μm . The bead is attached to the λ -receptor by a biotin streptavidin binding, which is known to be very strong and specific [25]. In a normal *E. coli* cell there are no outer membrane proteins which have biotin attached. I have used a modified λ -receptor in all experiments. The gene modification was done by Lene Oddershede in collaboration with Dr. Stanley Brown [5]. A very short biotin-acceptor site [26] is inserted on the extracellular site of LamB, between codon 155 and 156 in pSB2267 [27], producing the new plasmid pLO16 ([5]). The biotinylated λ -receptor is still able to use maltodextrins as carbon source [5]. The λ -receptor is synthesized in the cytoplasm of the cell. The *in vivo* biotinylation system of

the cell recognized the inserted biotin-acceptor site and attached biotin to the receptor. The biotinylated λ -receptor is then transported to the outer membrane of the bacteria. However, the conjugation of biotin to the protein is inefficient [28], the number of λ -receptors able to bind streptavidin is fewer than one per cell on average [5]. The promoter of the λ -receptor has been replaced with *P_{tac}* allowing expression of the receptor to be enhanced by adding lactose or Isopropyl- β -D-thiogalactoside (IPTG) [29]. To make sure that the receptor motility in our experiments is not influenced by the bacteria pili, a strain lacking pili has been used for these type of experiments.

For the arsenate and azide, the ampicillin, and the polymyxin experiments, the host strain used was S2188: F⁻ *lacI^Q* Δ *lamB106* *endA* *hsdR17* *supE44* *thi1* *relA1* *gyrA96* Δ *fimB-H::kan* [27], it lacks the entire gene of the λ -receptor and it has no pili on the surface. The experiments with vancomycin were performed with the same plasmid as described above, but with a different bacterial strain; this strain is termed TM14 and was made with a P1 transduction. The bacteria TM14 is Δ *malB101* Δ *fimB-H::kan* *mini-tet* *imp4213*, this means that it has no pili, it has no λ -receptor, and finally it has increased outer membrane permeability. The increased outer membrane permeability makes the cells sensitive to larger molecules as vancomycin, which normally cannot pass the outer membrane.

Chapter 4

Protein and membrane diffusion

4.1 Introduction

Proteins in a biological membrane can behave in different ways. If the protein is firmly anchored to the underlying membrane structure it might not move at all. If the protein is not limited by membrane structures it would perform a two dimensional Brownian motion, but it is also possible that the movement of the protein is slowed down by obstacles. The protein could also be confined within an area in the membrane caused by underlying membrane structure. However, if the protein is actively transported it would move faster than normal diffusion. A brief introduction to diffusion will be given in this chapter.

4.2 Brownian motion

Small particles that are in a viscous fluid, e.g. water, perform a random motion due to the thermal noise. This random movement was first observed by a botanist Robert Brown (1827). Brownian motion is described in various textbooks. The Brownian motion is used for calibration of the optical trap and in the description of the λ -receptor motion in the outer *E. coli* membrane. The movement of a particle in a liquid can be described by the equation:

$$m\ddot{r} = -\gamma\dot{r} + F(t). \quad (4.1)$$

Here m is the mass of the particle, r the position of the particle and $F(t)$ is the thermal noise term. The thermal noise term is assumed to have zero mean as there is no preferred direction for molecular collision. The drag force $\gamma\dot{r}$ can for small velocities be found by Stokes law. For a sphere moving in a liquid, γ can be found from Stokes law, as $\gamma = 6\pi\eta R$ where η is the viscosity of the fluid and R is the radius of the sphere.

Solving the equation of motion in three dimensions for the particle gives

$$\langle r^2 \rangle = \frac{6k_B T}{\gamma} t. \quad (4.2)$$

As the molecular collision of a particle has no preferred direction, the motion of the particle will be equal to a random. The mean square displacement of a random walk is equal to:

$$\langle r^2 \rangle = 6Dt. \quad (4.3)$$

Comparing the two equations 4.2 and 4.3 for the motion of the particle gives the diffusion constant as $D = \frac{k_B T}{\gamma}$.

4.2.1 Anomalous diffusion

Transport within living cells can either be active, as transport along filaments by molecular motors, or passive like diffusion. The diffusion can either be random, as in a liquid (as described above), or be hindered by obstacles, as diffusion in a biological membrane with proteins, or a particle moving in a polymeric network. To take this into account an additional term, $F'(t)$, including the viscoelastic properties of the media is included in the equation of motion:

$$m\ddot{r} = -\gamma\dot{r} + F(t) + F'(t). \quad (4.4)$$

Here $F'(t)$ includes the elastic response on the particle. The mean square displacement of the particle in this case will then depend on an exponent with

$$\langle r^2 \rangle \propto t^\alpha. \quad (4.5)$$

- If $\alpha = 1$ the particle performs normal diffusion.
- If $\alpha < 1$ it is termed subdiffusion; this could be describing a motion where the particle meet obstacles.
- If $\alpha > 1$ it is termed superdiffusion. Superdiffusion describes a motion that is directed. This could be a particle transported by a molecular motor, or a particle being pushed by polymerization.

A graphical overview of the different types of diffusion is given in figure 4.1.

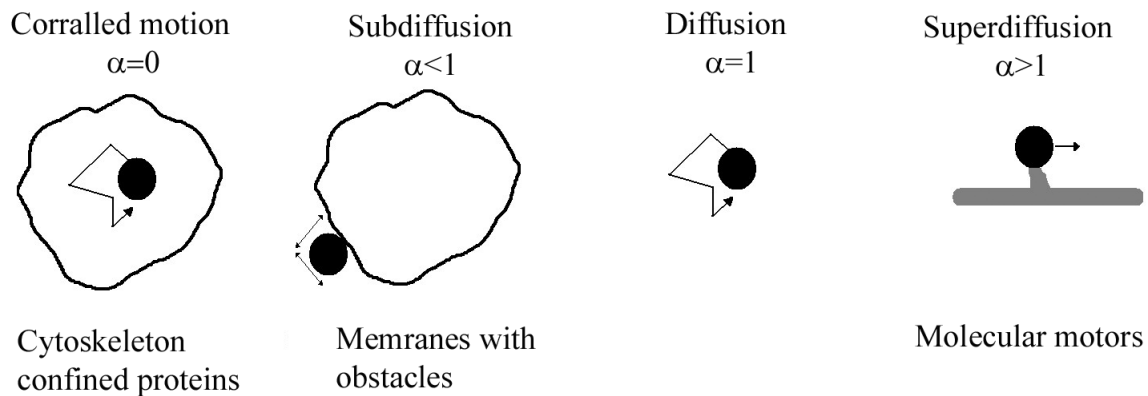


Figure 4.1: The first image from left shows corralled motion (confined diffusion): here a particle performs diffusion within a confined area. The second figure shows subdiffusion: here the particle is slowed down in its motion by obstacles, and the exponent will be $\alpha < 1$. The third picture shows a normal diffusing particle, hence $\alpha = 1$. The last picture shows superdiffusion, where the particle moves faster than normal diffusion, and the exponent is $\alpha > 1$.

4.3 Diffusion in eukaryotes

Diffusion in the membranes of eukaryotic cells has been studied for decades. Many types of different behaviors have been observed, ranging from free Brownian motion, subdiffusion (diffusion slower than Brownian motion), super diffusion (diffusion faster than Brownian motion often due to motor transport), or diffusion confined within an area. A nice review within experimental highlight of single molecule membrane diffusion is given in [2]. In the following a few experimental findings of diffusion in eukaryotic membranes will be presented.

In an early work within single molecule diffusion of eukaryotic cells the diffusion of glycoproteins in fish epidermal keratocytes was followed by attaching 40 nm gold particles [30]. It was found that the glycoproteins performed both random diffusion and forwarded transport (super diffusion). Single glycoproteins was seen to shift between random and forward directed transport.

Several studies have been carried out on diffusion within the membrane of normal rat kidney fibroblasts (NRK). Recently the diffusion of the μ -opiod receptor (μ OR) in (NRK) was extensively studied using single particle tracking (SPT) [31]. The movement of the receptor was followed both by using either green fluorescent protein (GFP) or by attaching a 40 nm gold particle. The (μ OR) receptor performed a diffusional behavior influenced by the underlying membrane skeleton structures. The structure of the membrane skeleton confined the motion of the protein within an area for a shorter time, but the particle can cross these membrane structures on longer time scales. The compartment size of the underlying membrane skeleton was found. Two compartment sized were found a 210

nm compartment included in larger compartments of 750 nm. The smallest compartment size could only be seen using very fast SPT with a frame rate of 40 kHz. The diffusion trajectories of the μ OR protein in NRK are shown in figure 4.2 [31].

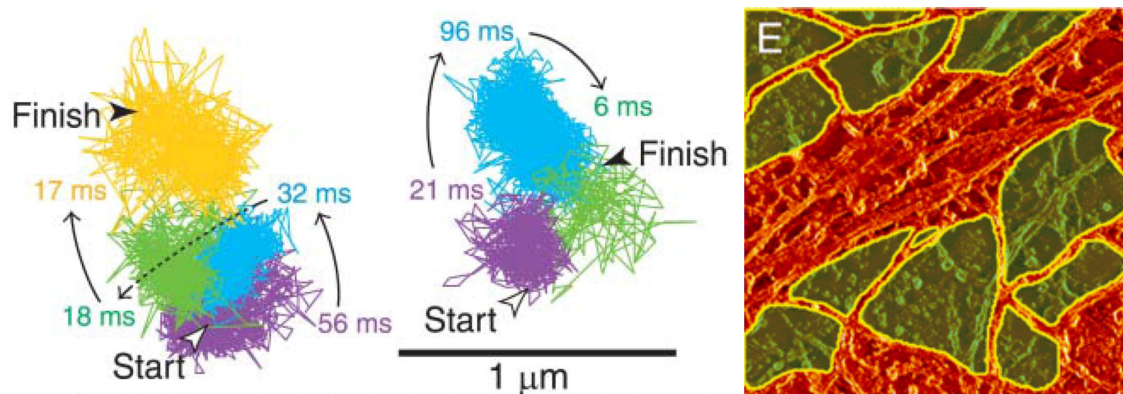


Figure 4.2: The left figures show two individual diffusion trajectories of a gold tagged μ OR protein in NRK cells. The protein undergo diffusion within compartments of 210 nm with the colours (purple, blue, green and yellow) indicating possible compartments [31]. To the right is a 3D construction achieved by electron microscopy tomography of the membrane skeleton (in orange) with the compartments shown in green. The image is 670 nm \times 670 nm [32].

Similar compartments sizes (230 nm) has also been seen for diffusion of individual phospholipids in normal rat kidney fibroblast [33]. The phospholipid 1,2-dioleoyl-sn-glycerol-3-phosphoethanolamine (DOPE) was tagged with either the fluorescent dye Cy-3 or 40 nm gold particles and followed by SPT. The diffusion coefficient was found to be 20 times slower than diffusion in large unilamellar vesicles (LUV). The trajectories of DOPE showed diffusion confined within compartments of 230 nm placed within larger compartments of 750 nm. The authors believe that the compartmentalization is caused by the proteins anchoring the membrane skeleton, in the membrane, hindering a free motion of the phospholipids. The compartmentalization in the normal rat kidney cells have been further elucidated using electron microscopy tomography [32]. The membrane skeleton structure was found, it was composed mainly of actin. Analyzing the three dimensional structure just beneath the eukaryotic membrane showed compartments of 200 nm compartments.

4.4 Diffusion in prokaryotes

Although single molecules diffusion studies in eukaryotic cell is well studied, experiments within prokaryotic cells have not until recently been performed. The first experiments performed on single molecule mobility in the outer membrane of bacteria were performed in our group [5]. In the experiments performed, the mobility of an outer membrane protein in

E. coli, the λ -receptor, was recorded with optical tweezers and single particle tracking. The λ -receptor showed confined diffusion in the membrane. The λ -receptor is an 18 stranded β -barrel, which transports maltodextrins (sugar) across the outer membrane.

The mobility of other β -barrels in the outer membrane of bacteria have been recorded as ensemble studies. The mobility of the β -barrel IcsA has been investigated [34]. It was shown that the protein is inserted into one or both poles in the outer membrane. The protein, IcsA, then diffuses out into the membrane; this diffusion depends on the lipopolysaccharides (LPS) and the fluidity of the membrane. IcsA belongs to a class of proteins called autotransporters. The localization and mobility of several other autotransporters have been investigated [35]. The common feature that was conserved within different species of rod-shaped bacteria was that the autotransporters were mainly localized at the poles, if an intact LPS was present (which is not the case in *E. coli* K12). In the presence of a truncated LPS as in *E. coli* K12 the proteins diffused more, moving away from the poles. The influence of LPS on outer membrane diffusion have also been investigated by [36]. Two classes of protein mobility was seen; a class of mobile protein seen all over the cell even at the poles and a group of immobile proteins. The immobile proteins were found both at the poles and in patterns along the bacteria. LPS was also seen in a similar pattern along the bacteria, it was however not mobile.

Using fluorescence, the mobility and localization of non specified outer membrane proteins have been studied. It was found that proteins are more stable at the poles of the cell [37], which is also the case for the peptidoglycan layer. The influence of the peptidoglycan layer was further elucidated by poisoning the cells with amdinocillin, a penicillin which specifically inhibits the penicillin binding protein 2 (PBP2). Amdonocillin hence blocks the same step of the peptidoglycan synthesis as ampicillin used in this study (see chapter 6). Cells exposed to amdinocillin showed stable proteins in other areas of the outer membrane than the poles after amdonocillin exposure. However, amdonocillin also caused a large morphological change.

Bacterial *in vivo* single molecules studies of the mobility of the actin homolog PleC has been performed [38], [39], [40]. PleC is an inner membrane protein. Two different types of mobility were seen, the slow moving associated with the filament form of the molecule and the freely diffusing single proteins. *In vivo* measurements of single molecules of the diffusion of the bacterial tubulin homolog FtsZ was recently achieved [41]. Two types of motion were seen here, the almost stationary proteins found at the Z band at the center of the cell, and proteins diffusing by subdiffusion. By stacking of several images it was shown that the diffusing molecules moved in a helical pattern within the cell.

Besides the work done in our research group the only other work done on *in vivo* measurements of single particles in the outer membrane was done by Gibbs et al. [20]. They used two different techniques for visualization of the mobility and distribution of the λ -receptors. The overall distribution of the receptor was found using fluorescent tails of bacteriophage λ , a bacterial virus, see chapter 10. Here they saw an uneven distribution of infected λ -receptors. To follow the mobility of individual λ -receptors, a gold recognition site was introduced in all λ -receptors. They attached 20 nm gold beads to the receptors. The mobility was followed by single particle tracking (SPT). In the mobility of the gold

beads two kinds of behavior was reported, a confined bead that moved within an range of 20-50 nm (similar to our results), and a larger range up to 300 nm. Gold nano particles allowed the use of smaller particles than by using polystyrene beads. The point spread function of a 20 nm gold particle is approximately 300 nm, two particles closer than 300 nm imaged in a light microscope will therefore appear as one point. The picture from the microscope can be used by a centroid tracking routine to reliably track the centroid of one particle down to a resolution of 10 nm, however, it is not able to track the centroid of a particle if the point spread function of the particle overlaps that of other particles. The gold recognition site does not require the cells own biotinylation system, and the number of receptors on the surface able to bind gold is higher than the number of receptors in our experiments able to bind to the streptavidin coated beads, even with the same bacterial strain. It is therefore possible that the sub-population of λ -receptors observed by Gibbs et al. [20] postulated to move distanced of 300 nm could be caused by two or more gold nanoparticles located within the point spread function of each other. We visualized the mobility of the λ -receptor by attaching streptavidin coated quantum (size) dots, and we still only saw λ -receptors moving within a 50 nm range, hence, size does not matter (these experiments were performed by Lei Xu).

Previously, bacteria have been thought of as small containers of DNA; this picture however seems to be too simple. There seems both to be a structure within the cell and a structure in the outer membrane. Here we focus on the mobility and the fluidity, of the outer membrane. Studies on the diffusion of single particles in prokaryotic cells have been done, but still only in very limited numbers. Compared to eukaryotic cells, bacteria have the disadvantage that they are small thus making the detection more difficult.

Chapter 5

The effect of energy metabolism on the λ -receptor motility

5.1 Introduction

Protein motility plays a key role in the function of many biological processes e.g. nutrient uptake or the regulatory mechanisms of the cell. Several studies have been made on single protein motility in the membrane on eukaryotic cells. The movement of, and within a membrane depends on the environment of the membrane such as temperature, but also the energy present. Theoretically it has been shown that there is a dependence between the compartmentalization of a lipid membrane and the activation of membrane proteins [3]. Experimentally the protein bacteriorhodopsin embedded in artificial membranes undergo oligomerization upon photoactivation [4]. However, only few studies have been performed on single molecule diffusion in prokaryotic cells. The first single molecule protein diffusion experiment in prokaryotic cells was done in our research group by Oddershede et al. [5]. Here the mobility of single λ -receptors in the outer membrane of *E. coli* was first measured. It was reported that in the absence of glucose, receptor mobility was barely observed. We therefore wanted to further investigate if the λ -receptor mobility is energy dependent. This was done by arsenate and azide poisoning, which blocks the energy metabolism of the cell.

5.2 Biology

The main energy source of the cell is ATP. ATP is synthesized from ADP and a phosphate group. One way of synthesizing ATP is by glycolysis where sugar is digested. A large part of the production of ATP is done in the respiratory chain.

Arsenate has the formula AsO_3^- , and it closely resembles the phosphate group PO_3^- that is used during ATP synthesis. Arsenate blocks the first energy producing step in glycolysis. Here glyceraldehyde 3-phosphate is transferred into 1,3-bisphosphoglycerate under the production of NADH, this step is catalyzed by the enzyme glyceraldehyde 3-phosphate dehydrogenase. Arsenate binds the enzyme instead of the phosphate group, forming the

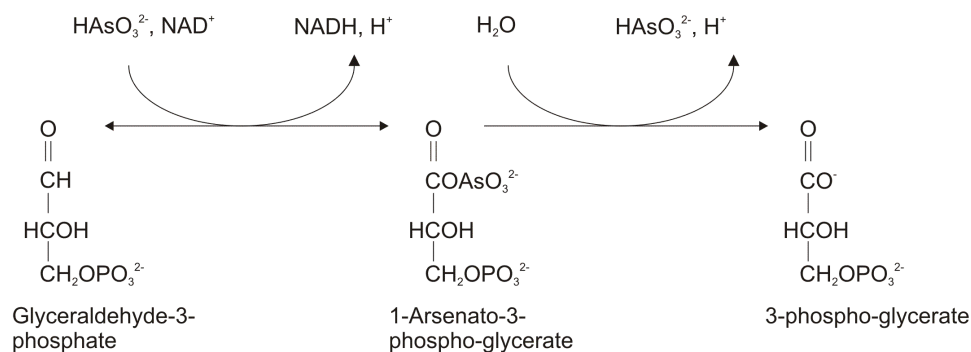


Figure 5.1: Arsenate binds the enzyme glyceraldehyde-3-phosphate dehydrogenase. This complex is unstable and undergoes a spontaneous reaction releasing arsenate and 3-phosphoglycerate. As 3-phosphoglycerate can not be used in the glycolysis, the glycolysis is hence stopped.

unstable complex 1-Arseno-3-phosphoglycerate, which under the release of a protons and arsenate becomes 3-phosphoglycerate [42], see figure 5.1. As arsenate works by resembling the phosphate group, the experiments were performed in phosphate free media, see appendix 5.

The working mechanism of azide is more complex as it attacks several steps in the respiratory system of the cell and in the protein translocation process. During the synthesis of energy from carbon sources (e.i. the glycolysis), material which can donate high energy electrons is produced. If these electrons would react directly with protons to form water, a large amount of their energy would be transformed into heat. This is prevented by letting the electrons go into a chain of reactions where the process is done more gradually. This way the cell stores nearly half of the released energy. The reaction chain of the electrons is used to pump protons out of the cell, creating a proton gradient across the membrane. When the protons are allowed to flow back over the membrane, the energy gradient can be used for energy synthesis or for driving the motion of the flagella.

The respiration system of *E. coli* resembles the electron transport system of the mitochondria in eukaryotic cells. It consists of an electron donor (the primary dehydrogenase) that is linked by an electron transporter (quinones, ubiquinone, menaquinone and demethylmenaquinone) to the electron acceptor (terminal reductase or oxidase). *E. coli* has 15 primary dehydrogenases and 10 terminal reductases, which is more than eukaryotic cells. Under aerobic conditions O_2 is the preferred electron acceptor in the terminal reductase; O_2 also represses anaerobic respiration. Under anaerobic respiration nitrate is the preferred terminal reductase and it represses other terminal reductases. The whole respirational system will not be explained here, but it is well explained in [21] or [43]. The primary scope here is to explain the main parts of the respiratory system and the parts that are influenced by azide (N_3^-). The first step in the electron transport is the NADH dehydrogenase (equivalent to complex I in eukaryotic cells), which is a primary dehydrogenase. NADH releases two

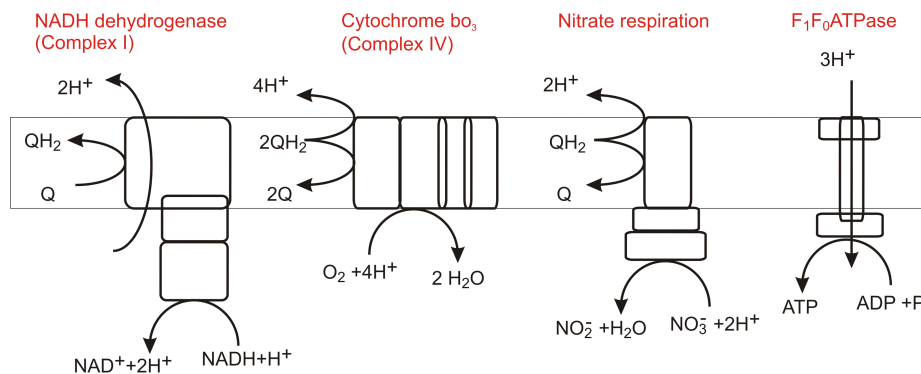


Figure 5.2: To the left a schematic drawing of the NADH dehydrogenase is shown. The NADH dehydrogenase is equivalent to complex I in the electron transport chain in eukaryotic cells. NADH donates two electrons to quinones, which then transport two protons across the membrane. The second drawing from the left is a schematic drawing of the cytochrome bo_3 complex (equivalent to complex IV in the eukaryotic electron transport chain). Here oxygen takes up an electron under the production of water, while the quinones transport protons across the membrane. The cytochrome bo_3 complex is inhibited by azide. The third drawing from the left is the nitrate respiration (used as an electron transporter under anaerobic growth). Here nitrate is the electron donor, producing nitrite and water, while the quinones transport protons across the membrane. The nitrate respiration is inhibited by azide. The electron transport steps described above is used to create a proton gradient across the membrane. When the protons are allowed to flow back into the cell they can be used by the F_1 -ATPase to produce ATP as shown to the right. The F_1 -ATPase is blocked by azide.

electrons which are donated to quinones together with two protons, under the transport of two protons to the periplasm of the cell.

In a later step the electrons are transported from the quinones to cytochrome bo_3 (termed complex IV in eukaryotic cells). At the cytochrome bo_3 complex, oxygen takes up the electrons under the production of water. The cytochrome bo_3 complex is inhibited by azide [44] [21]. Under anaerobic conditions the electrons can be donated to the nitrate respiration system. Here nitrate is used as a electron acceptor, it takes up two protons and two electrons and is reduced to nitrite. Azide is here a competitor inhibitor of this complex, binding more strongly than nitrate does [45] [46].

The protons that are pumped out of the cell, create a proton gradient across the membrane. This proton gradient can be used to synthesize ATP from ADP and a phosphate group by the enzyme F_1 -ATPase. The F_1 -ATPase is also blocked by azide [47]. An overview of the electron transport and the F_1 -ATPase can be found in figure 5.2.

Besides, azide goes in and hinders the sec pathway. The sec pathway is very important for the transport of most outer membrane and periplasmic proteins, and some inner membrane proteins. Azide blocks protein transport by blocking SecA [48].

5.3 Model

We have followed the mobility of a bead attached to a single λ -receptor with the optical tweezers. To extract the pure motion of the receptor, a model was made [49]. The model as well as the extension of the model to include the effect of energy depletion is described briefly in the following. The model is largely proposed by Kirstine Berg-Sørensen. The motion of the λ -receptor occur within small confined area [5] in the bacterial membrane. We do only measure the motion of a bead place on top of the bacteria. The effects of the curvature of the bacteria is therefore neglected. The experimentally obtained data is a projection of the bead's position onto the (x,y)-plan parallel to the outer bacterial membrane. The curvature of the bacterial membrane is not taken into account and to minimize its influence measurements were only conducted on bacteria where the bead was placed right on top of the bacterium. The position of the bead is recorded as a function of time. The motility of the receptor is described by a simple model in [5] [49]. The attachment between the biotin-streptavidin is tight, but even so the position of the center of the bead might differ from the position of the protein, as the bead can twist around the protein. This freedom of movement of the bead compared to the position of the protein might even be larger if the protein and/or the membrane itself can yield. The nature of the forces and the degree of freedom between the position of the bead and the protein is not known. The simplest model to describe the forces is a Hookean spring, and the attachment between the biotinylated protein and the streptavidin coated bead is hence treated as a Hookean spring with spring constant κ_{bs} . Similar arguments leads to treat the attachment of the protein to the bacterial membrane as a Hookean spring with spring constant κ_{cw} . The coupling of the bead in the optical trap is treated as an Hookean spring with spring constant κ (see 2.2.1). The motion of the protein in the membrane is modelled as a heavily overdamped frictional motion with friction coefficient γ_{prot} . This lead to the following equations of motion:

$$M_{bead}\ddot{x}_{bead} = -\kappa(x_{bead} - x_{trap}) + \kappa_{bs}(x_{prot} - x_{bead}) - \gamma_{bead}\dot{x}_{bead} + F_{bead} \quad (5.1)$$

$$M_{prot}\ddot{x}_{prot} = -\kappa_{cw}(x_{prot} - x_{cw}) - \kappa_{bs}(x_{prot} - x_{bead}) - \gamma_{prot}\dot{x}_{prot} + F_{prot} \quad (5.2)$$

M_{bead} and M_{prot} denote the masses of the bead and the protein. x_{trap} is the equilibrium position of the bead in the optical trap. x_{cw} is the equilibrium position of the protein in the membrane. F_{bead} and F_{prot} are the stochastic forces which are assumed to have properties of "white noise", i.e. vanishing expectation value and delta-funtion auto-correlations.

When this model is used for data analysis it turns out that the total spring constant felt by the bead is given by $\kappa_{total} = \kappa + \kappa_{cw}$ [5]. From the individual optical tweezers measurements one obtains a time series of positions visited by the bead. The corresponding position histogram is well described by a Gaussian distribution with the standard deviation σ given by:

$$\sigma^2 = \frac{k_B T}{\kappa + \kappa_{cw}} \quad (5.3)$$

We can find κ from the power spectrum calibration (2.2.1), and using 5.3 we can find κ_{cw} . From this, the standard deviation of the position visited by the protein can be found as:

$$\sigma_\lambda^2 = \frac{k_B T}{\kappa_{cw}} \quad (5.4)$$

The description above explains the system when the bacteria are kept in a metabolically competent state. By adding poison to the bacteria we introduce changes in the system; the bacteria are energy depleted. We proposed two different models to describe this change.

- **Model A :** The motility of the λ -receptor is described not as purely thermal, but it is enhanced due to energy available from the life processes. The simplest way to incorporate this into the model is to assume that the enhanced motility can be expressed by the white-noise forces with a different "temperature". The time-series data from the motility of the bead on metabolically competent λ -receptor is still described by κ_{bs} , γ_{prot} , and κ_{cw} but the the white noise term is characterized by the "bacterial temperature" T_{bac} . The time-series obtained from the energy depleted bacteria is assumed to be described by κ_{bs} , γ_{prot} , and κ_{cw} , but now the white noise is described by the ambient temperature T . If the motion is active $T_{bac} > T$. The effect of the two phases is illustrated to the left in figure 5.3, here the active motion of the protein is illustrated by the protein being dragged by a pickup truck. After poisoning, the motion of the protein decreases and it is no longer an active motion.
- **Model B :** A change in λ -receptor motility after poisoning is described as a change in the membrane structure of the bacteria, giving a change in the spring constant of the protein in the bacterial membrane, κ_{cw} . The parameters κ_{bs} , γ_{prot} , and κ_{cw} are estimated from the time-series obtained from the bacteria kept in normal growth medium. The white noise is assumed to be characterized by a "normal" ambient temperature T . The motility of the bead from the time-series in the media with poison is assumed to be characterized by κ_{bs} , γ_{prot} , an $\kappa_{cw,p}$, and the white noise is still described by the ambient temperature T . The effect of the two phases is illustrated right in figure 5.3. Here the protein moves more freely before poisoning. After poisoning a change in the membrane occurs (a change in κ_{cw}) leading to a decrease in the protein mobility, this change is illustrated as aggregation of other membrane proteins and a stronger attachment between the peptidoglycan layer and the protein. A decrease in protein motility upon poisoning will give rise to an increase in $\kappa_{cw,p}$.

The left side in the equations 5.1 and 5.2 can be neglected due to the small Reynolds number. The equations are then Fourier transformed and the power spectrum of the position of the bead is derived. The general result is:

$$P_{bead}(f) = \frac{D_{bead}}{2\pi^2} \cdot \frac{(b+c)^2 + r^2(f/f_c) + 2 + trb^2}{D} \quad (5.5)$$

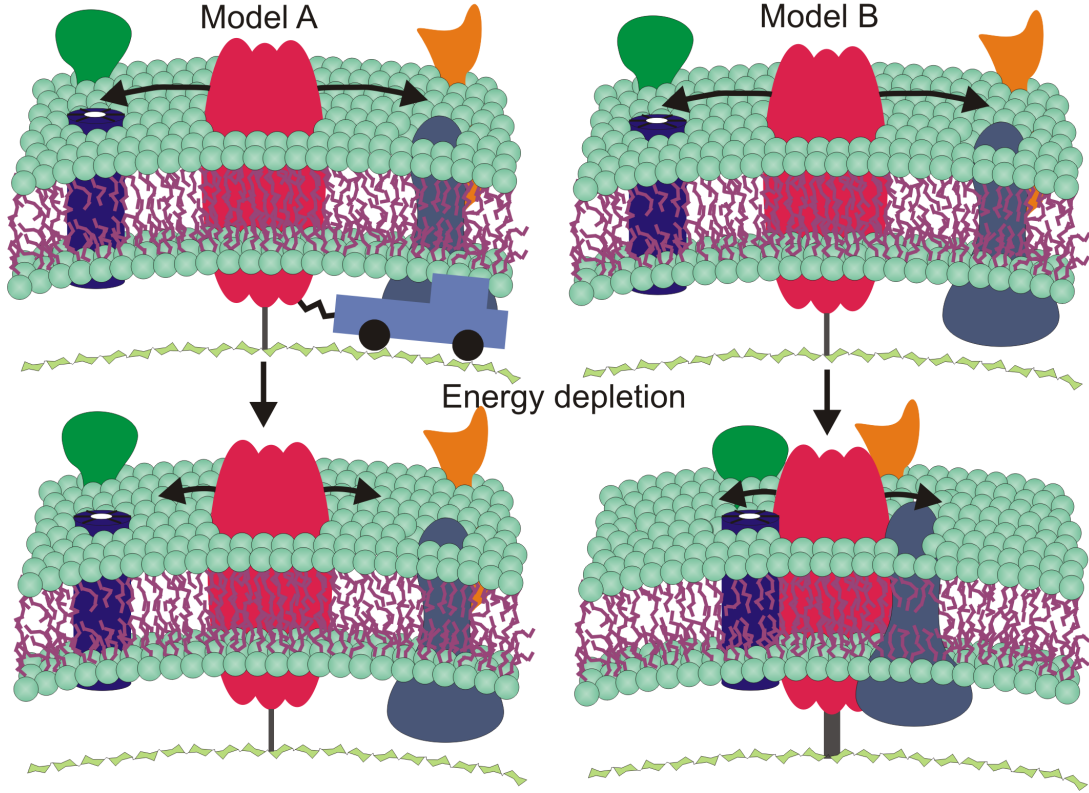


Figure 5.3: Model A is shown to the left, here the active motion of the protein is illustrated by the protein being dragged by a pickup. After poisoning (hence energy depletion) the motion of the protein decreases and it is no longer an active motion. To the right model B is illustrated. Here the protein moves more freely before poisoning. After poisoning a change in the membrane occur (a change in κ_{cw}) leading to a decrease in the protein mobility, this change is illustrated as aggregation of other membrane proteins and a stronger attachment between the peptidoglycan layer and the protein.

with

$$D = f_c^2 [r^2 (f/f_c)^4 + ((b+c)^2 + 2br^2 + r^2b(2+b^2))(f/f_c)^2 + 2bc(b+c) + (b+c)^2 + b^2c^2] \quad (5.6)$$

and the following ratios

$$r = \frac{D_{bead}}{D_{prot}}; \quad b = \frac{\kappa_{bs}}{\kappa}; \quad c = \frac{\kappa_{cw}}{\kappa}; \quad f_c = \frac{\kappa}{2\pi\gamma_{bead}}; \quad t = \frac{T_{bac}}{T} \quad (5.7)$$

Model A: The time-series from the bacteria taken under normal growth conditions is fitted by 5.5 with $t = \frac{T_{bac}}{T}$ as a variable. The time-series from the bacteria in media with

poison is fitted to 5.5 but with $t = 1$. The fitting are made as a simultaneous fit where the data obtained from the normal growth conditions and the media with poison is fitted at the same time. The values of b and r obtained correspond to the best fit for both data sets.

Model B: The time-series of the data taken under normal conditions is fitted with 5.5 with $t = 1$. The time-series obtained in media containing poison is also fitted by 5.5 but with c replaced by $c_p = \frac{\kappa_{cw,p}}{\kappa}$ and $t = 1$. The fit is here also done simultaneously.

5.4 Experimental procedures

The bacteria strains used in these experiments were S2188 with the plasmid pLO16. For a full description of the strains and plasmid see [27], [5] or section 3.2.

The growth of the bacteria was done in the following way:

- Single bacteria colonies were grown overnight at 37 °C on YT-agar plates [50] supplemented with 25 $\mu\text{g}/\text{ml}$ chloramphenicol.
- A single colony was transferred sterile into M63 media [50] containing 1 $\mu\text{g}/\text{ml}$ B1, 25 $\mu\text{g}/\text{ml}$ Chloramphenicol, 0.1% casein hydrolysate, and 0.2% glycerol, and grown in shaking water bath overnight at 37 °C.
- 0.1 ml of the overnight culture was diluted into 3 ml of MOPS or M63 media and grown at 37 °C until log-phase.
- To induce the expression of the λ -receptor 3 ml of MOPS or M63 media supplemented with 0.2mM IPTG (giving a final concentration of 0.1 mM IPTG) was added and the bacteria were grown for an additional 1/2 hour.
- 1 ml cell culture was spun down at $1673 \times g$ for 5 minutes and the cells resuspended in 100 μl buffer. The buffer used throughout the experiments was 10 mM potassium phosphate, 0.1 M KCl, pH 7.

The mobility of the biotinylated λ -receptor is followed with the optical tweezers by attaching a streptavidin coated bead. The beads used were streptavidin-coated polystyrene beads from Bang Laboratories, Inc (Fishers, In) with a diameter of $\sim 0.5 \mu\text{m}$. These beads are washed before use in the following way:

- The beads are suspended in millipore water and thereafter centrifuged $1673 \times g$ for 5-10 min.
- The supernatant was discarded and the beads resuspended in buffer.
- The beads were sonicated for at least 15 min to remove aggregates.

At the microscope the bacteria were kept in a perfusion chamber when studied. The perfusion chamber was made in the following way:

- At least 5 μl poly-l-lysine was spread in a line on a coverslip (0.17 mm) and left to dry.
- Two pieces of double layer of scotch double sticky tape was placed on the coverslip surrounding the dried poly-l-lysine.
- Another coverslip (0.17 mm) was placed on top as a lid. The final volume was 5-10 μl .

The preparation of the bacteria in the perfusion chambers was done over water bath in the following way:

- The chamber was washed twice with Millipore water.
- 10 μl of the bacteria were perfused into the chamber, and left 15-25 minutes to adhere.
- Ten microliters of 12.5 mg/ml heparin was flushed into the samples and left for 15 minutes. Heparin decreases the attraction between the surface and the streptavidin-coated beads.
- To remove dust, the samples were rinsed by perfusing the chambers four times with buffer.
- 10 μl washed streptavidin coated polystyrene beads were perfused into the chamber and left there 15 minutes to attach.
- Excess beads were removed by flushing the chamber 3-5 times with MOPS glucose media. MOPS was chosen as medium as it can be made phosphate free and therefore well suited for arsenate poisoning. Glucose was used as a carbon source inside the perfusion chambers to support anaerobic growth.
- The bacteria were stored in the refrigerator until use.

After the samples were prepared they were visualized in the microscope. A bacterium was found which had a wiggling bead placed on top. The optical tweezers were then used to check if the bead was specifically attached to the bacterium, by pulling on the bead. The motion of the bead-receptor complex was then recorded with the optical tweezers. The motion of a freely moving bead held in the same height as the attached bead was recorded for calibration to the spring constant of the trap κ . The motion of the bead-receptor complex was then studied in the following way.

- A freely diffusing bead was found and held close by the bacteria in the same height as the attached bead. A powerspectrum of the Brownian motion of the bead was recorded. The power spectrum of the bead was used for calibration to find the conversion factor between the voltage output of the diode and the nanometer displacement of the bead.

- The motility of a single bead-receptor complex was recorded with the optical tweezers.
- The bacteria were poisoned with $2 \times 100 \mu\text{l}$ solution of arsenate and azide ($20 \mu\text{M}$ NaN_3 , and $1 \mu\text{M}$ KH_2AsO_4). For technical reasons the poisoning was done by flushing in $5 \times 20 \mu\text{l}$, then a break of 5-10 min was held, and the poisoning step was then repeated.
- The motility of the exact same bead-receptor complex was then measured again with the optical tweezers.

5.5 Results

We have investigated the effect of energy metabolism on the mobility of a single λ -receptor by poisoning the cells with arsenate and azide. The motility of the exact same receptor was measured *in vivo* before and after arsenate and azide exposure with the optical tweezers. The recorded data are visualized as a time series in figure 5.4, here the motility of the bead-receptor complex in a metabolic competent cell (blue) and the motility of the exact same receptor complex after arsenate and azide exposure (red) are shown. The break on the axis indicate the break in time where the media was exchanged, i.e. arsenate and azide was flushed in. The distribution of positions visited by the bead-receptor complex is well fitted with a Gaussian and shown as an insert in the left corner. The insert to the right shows the scatter plot of the positions visited before poisoning (blue) and after poisoning (red). In total the motility of the receptor-bead complex was measured on 29 data sets. A clear decrease was seen in the motility of the λ -receptor upon arsenate and azide exposure. The effect was rapid within minutes. A data set is used for the time series recorded with the optical tweezers for either the x or the y channel, which are treated collectively. The individual bacteria used for measuring the receptor motility is orientated randomly with respect to the x and the y channel. We did not experience any difference between the recorded time series of the x and the y channel. Due to experimental difficulties it was not always possible to record both the x and the y signal on a bacterium. The motility of the λ -receptor was quantified by the standard deviation of the position histogram of the bead-receptor complex (as shown in the left insert in figure 5.4). The effect of energy metabolism on the motility of the λ -receptor was quantified by comparing the standard deviation of the motility of the bead-receptor complex before σ_{before} and after σ_{after} arsenate and azide exposure. On average the standard deviation before was $\sigma_{before} = (7.17 \pm 0.56)$ nm (mean \pm SEM) in the metabolic competent cells and $\sigma_{after} = (2.98 \pm 0.36)$ nm (mean \pm SEM) after arsenate and azide exposure. To test whether the standard deviation before and after arsenate and azide poisoning is significantly different a student's t-test was used. Here the probability that two populations are accidentally different is found (the p-value). A low p-value support the hypothesis that change is significant. This analysis gave a p-value of $p = 3.6 \times 10^{-7}$. There is hence a significant difference between the motility of the λ -receptor in metabolic competent cells and in cells treated with arsenate and azide.

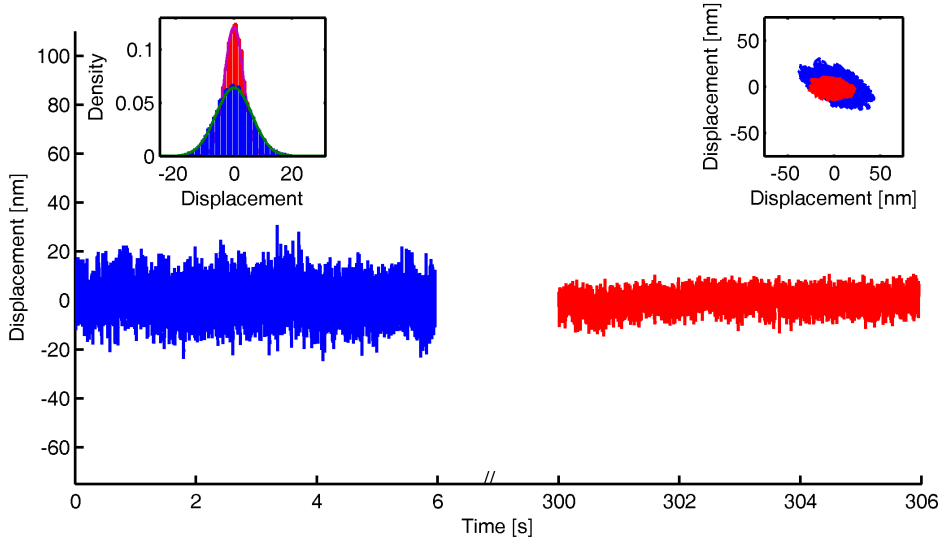


Figure 5.4: *The motility of the bead-receptor complex in a metabolic competent cell is shown in blue and the motility of the exact same receptor complex after arsenate and azide exposure is shown in red. The break on the axis indicate the break in time where the media was exchanged, i.e. arsenate and azide was flushed in. The lower part of the figure shows the time trace recorded with the optical tweezers, in the left corner the same data are visualized as a histogram, in the right corner the data for both the x and the y directions are plotted in scatter plot.*

The measured motility of the bead-receptor complex provides an indirect information on the pure motility of the receptor. The standard deviation of the motility of the receptor can be found from the position histograms using equation 5.4 when κ and κ_{cw} are known. From the standard deviation of the pure λ -receptor, σ_λ , was found from the position histograms (using equation 5.4) as $\sigma_{\lambda,before} = (10.3 \pm 1.6)$ nm (mean \pm SEM) in metabolic competent cells and $\sigma_{\lambda,after} = (4.4 \pm 0.4)$ nm (mean \pm SEM) for the energy depleted cells. A student's t-test gave a probability of $p = 3.5 \times 10^{-4}$, and the probability that the difference seen between the two populations is random is therefore very low. Depleting the cells of energy hence causes a significant change in the motility of the λ -receptor.

We have investigated if the exchange in media could cause the change in the receptor motility described above. The experimental procedure was the same as in the experiments above but with arsenate and azide exchanged with growth media. There was no significant difference between the motility before and after exchanging the media.

During data acquisition two different types of diodes were used; a quadrant photodiode and a position sensitive diode. The diodes each suffer from different artifacts. The quadrant photodiode has a pronounced high frequency filtering [11]. The position sensitive diode suffers less from frequency filtering but it is slightly more noisy in the low frequency regime. The results described above were obtained from analyzing data taken from both

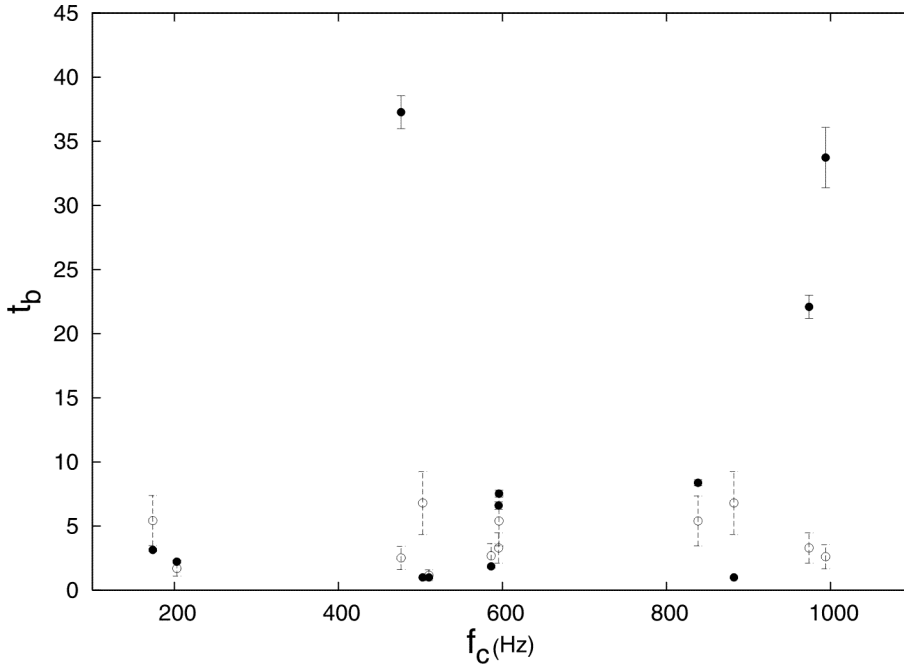


Figure 5.5: Here the ratio between the normal ambient temperature in and the artificial temperature is shown as function of the corner frequency.

photodiodes. However, in power spectral based data analysis where the high frequency regime is important only data obtained with the position sensitive diode was used.

The models A and B were now used to analyze the data. In model A, the energy dependence is taken into account as an artificial temperature (T_{bac}) in the living cells. If there is an energy dependence on the motility of the receptor, the artificial temperature would be higher than the surrounding temperature ($T_{bac} > T$). The ratio $t_b = \frac{T_{bac}}{T}$ between the artificial temperature and the normal temperature is shown as a function of the corner frequency in figure 5.5. This gives an average ratio between artificial temperature and the ambient temperature as $t_b = 10.5 \pm 3.8$ (SEM). The artificial temperature is independent of the corner frequency and hence the laser power used.

In model B, the energy dependence of the motility of the receptor is taken into account by a change in the cell wall stiffness, described by $\kappa_{cw,bac}$ and $\kappa_{cw,poi}$. An energy dependence gives a stiffer membrane upon poisoning ($\kappa_{cw,poi} > \kappa_{cw,bac}$). In average the ratio between $\frac{\kappa_{cw,poi}}{\kappa_{cw,bac}}$ is 27.6 ± 12.4 (std.err). The outcome of the power spectral analysis was that model A is favored with a higher χ^2 in 10 out of 12 data set.

5.6 Summary

The energy dependence on the motility of a single protein in the outer membrane of *E. coli*, the λ -receptor, has been investigated. The energy synthesis of the cells was stopped by

poisoning the cells with arsenate and azide. The motility of the exact same λ -receptor was measured with optical tweezers before and after poisoning. In living cells the λ -receptor performs a wiggling motion. We saw a significant decrease in the λ -receptor motility upon poisoning the cells. There hence seems to be a energy dependence in the motility of the λ -receptor, the motion appears to be active. To analyze the motility of the λ -receptor two models have been made. In model A, the difference in motility between energy depleted cells and metabolic active cells is modelled as an artificial temperature, giving a ratio between the temperature in the metabolic active cells and the energy depleted cells of roughly 10. In model B, the change in receptor motility is modelled as an change in the membrane stiffness. The membrane becomes roughly 28 times stiffer in the energy depleted cells. A χ^2 test favors model A, but the truth should probably be found somewhere in between. It is however not possible to fit for both models simultaneously. The origin of this wiggling motion is further elucidated in chapter 6 and 7. The wiggling motion of the receptor might be to help the transport of the maltodextrin chains through the channel. As the motion of the receptor seems to depends on energy, one has to take this into account in studies on protein diffusion in artificial membranes.

Chapter 6

The effect of the peptidoglycan layer, using ampicillin

6.1 Introduction

In the previous chapter we saw that the wiggling motion performed by the λ -receptor decreased upon arsenate and azide poisoning. We have hence established that the motility of the λ -receptor is energy dependent. The λ -receptor is thought to be anchored in the peptidoglycan layer [1]. In this chapter, we have investigated if the peptidoglycan layer influenced the mobility of the λ -receptor. By exposing the cells to ampicillin, a penicillin, we can stop the synthesis of new peptidoglycan layer. As a result of this treatment, we saw a significant decrease in the receptor mobility.

6.2 Biology

E. coli is a gram negative bacterium with three layers of membrane, an inner membrane, the peptidoglycan layer and the outer membrane. The peptidoglycan layer is a mesh-like network which stabilizes the cell and gives it rigidity. A cell with no peptidoglycan layer can not resist differences in the osmotic pressure, and the cell will hence rupture under normal conditions. All experiments are therefore done in the presence of sucrose, which prevents the cells from rupturing by creating an osmotic pressure outside the cell similar to the osmotic pressure inside the cell. Ampicillin or any penicillin hinders the peptidoglycan synthesis by resembling a specific structure of the peptidoglycan layer. The target for ampicillin is the enzyme that cross-links different strands together, illustrated in figure 6.1. If ampicillin is present, the enzyme forms an inactive complex together with ampicillin. This stops the connection of newly synthesized peptidoglycan strands to the existing peptidoglycan layer. It therefore takes some time for ampicillin to work and the cells need to be growing.

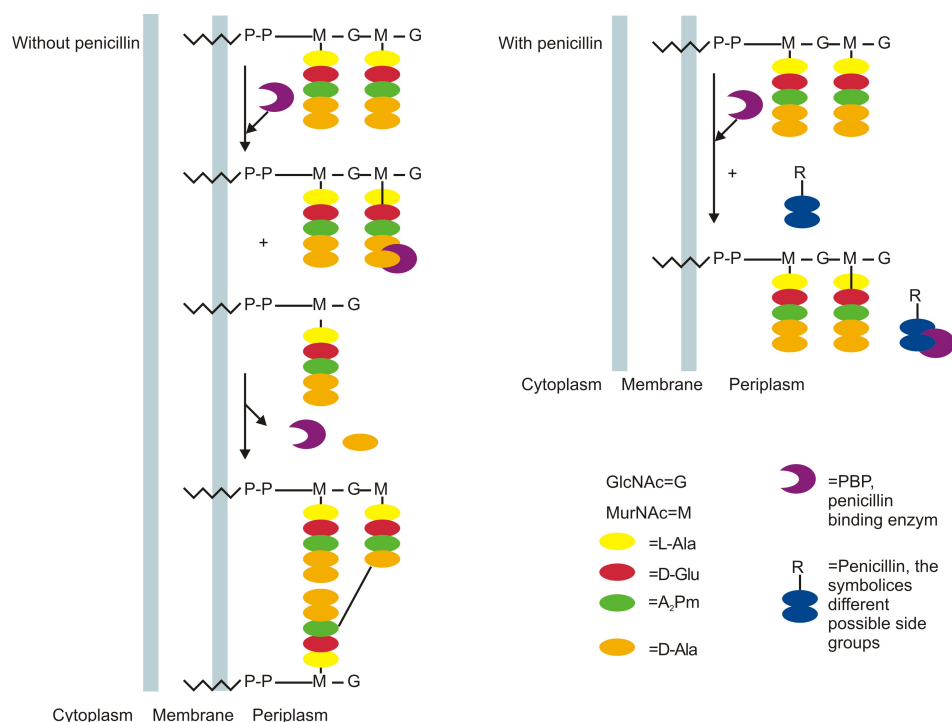


Figure 6.1: A schematic overview of the working mechanism of the cross-linking of two peptidoglycan strands (left) and the the working mechanism of ampicillin (right, for a detailed description see [21], [51]). Ampicillin resembles the two last amino acids in the peptidoglycan strands (D-Ala-D-Ala). The penicillin binding enzyme therefore binds covalently to ampicillin, this binding is irreversible. Cross linking of new peptidoglycan strands is thereby stopped. The short handed notation in the figure is the following: N-acetylglucosamine (GlcNAc)=G, N-acetylmuramic acid (MurNAc)=M, PEP=phosphoenolpyruvate, Ala=alanine, Glu=glucose, A₂M= meso-diaminopimelic acid, P=phosphogroup, UDP=uridine diphosphate, UMP=uridine monophosphate, PBP=penicillin binding protein.

6.3 Experimental procedures

The bacteria strains used in these experiments were S2188 with the plasmid pLO16, for a full description of the strains and plasmid see [27], [5] or section 3.2.

The growth of the bacteria was done in the following way:

- Single bacteria colonies were grown overnight at 37 °C on YT-agar plates [50] supplemented with 25 µg/ml chloramphenicol.
- A single colony was transferred sterile into M63 media [50] containing 1 µg/ml B1, 25 µg/ml Chloramphenicol, 0.1% casein hydrolysate, and 0.2% glycerol, and grown in shaking water bath overnight at 37 °C.

- 0.1 ml of the overnight culture was then diluted into 3 ml of fresh media supplemented with 12 % sucrose and grown at 37 °C until log-phase.
- To induce the expression of the λ -receptor, 3 ml of fresh M63 media supplemented with 1mM IPTG (the final concentration IPTG was 0.5mM) and 12 % sucrose was added, and the bacteria were grown for an additional 1/2 hour.
- In the ampicillin experiments, ampicillin was added to give a final concentration of 100 $\mu\text{g}/\text{ml}$ and the bacteria were grown for another hour.
- 1 ml cell culture was spun down at $1673 \times g$ for 5 minutes and the cells resuspended in 100 μl buffer supplemented with 12 % sucrose. The buffer used throughout the experiments was 10 mM potassium phosphate, 0.1 M KCl, pH 7.

The mobility of the λ -receptor was followed with the optical tweezers by attaching a streptavidin coated bead to the biotinylated receptor. The beads used were streptavidin-coated polystyrene beads from Bang Laboratories, Inc (Fishers, In) with a diameter of $\sim 0.5 \mu\text{m}$. These beads are washed before use in the following way:

- The beads are suspended in millipore water and thereafter centrifuged at $1673 \times g$ for 5-10 min.
- The supernatant was discarded and the beads resuspended in buffer supplemented with 12 % sucrose.
- The beads were sonicated for at least 15 min to remove aggregates.

At the microscope the bacteria were kept in a perfusion chamber when studied. The perfusion chamber was made in the following way:

- At least 5 μl poly-l-lysine was spread in a line on a coverslip (0.17 mm) and left to dry.
- Two pieces of double layer of scotch double sticky tape was placed on the coverslip surrounding the dried poly-l-lysine.
- Another coverslip (0.17 mm) was placed on top as a lid. The final volume was 5-10 μl .

The preparation of the bacteria in the perfusion chambers was done over water bath in the following way:

- 10 μl of the bacteria were perfused into the chamber, this step was repeated. The bacteria were left for 15-25 minutes to adhere to the surface.
- Ten microliters of 12.5 mg/ml heparin supplemented with 12 % sucrose was flushed into the samples and left for 15 minutes. Heparin decreases the attraction between the surface and the streptavidin-coated beads.

- To remove dust, the samples were rinsed by perfusing the chambers four times with buffer supplemented with 12 % sucrose.
- 10 μl washed streptavidin coated polystyrene beads were perfused into the chamber and left there 15 minutes to attach.
- Excess of beads were removed by flushing the chamber 3-5 times with M63 glucose media, supplemented with 12% sucrose and 100 $\mu\text{g}/\text{ml}$ ampicillin. Ampicillin was left out in the control experiments. Glucose was used as a carbon source inside the perfusion chambers to support anaerobic growth.
- The bacteria were stored in the refrigerator until use.

After the samples were prepared they were visualized in the microscope. A bacterium was found which had a wiggling bead placed on top. The optical tweezers were then used to check if the bead was specifically attached to the bacterium, by pulling on the bead. The motion of the bead-receptor complex was then recorded with the optical tweezers. The motion of a freely moving bead held in the same height as the attached bead was recorded for calibration to the spring constant of the trap κ . The experiment was either performed on bacteria suspended in an ampicillin solution or on a bacteria in normal growth media.

6.4 Results

We have investigated the effect of ampicillin poisoning on the motility of an outer membrane protein, the λ -receptor. Ampicillin works by hindering crosslinking of newly synthesized peptidoglycan strands. The cells therefore have to be grown in ampicillin to be effected. For this reason, it was not possible to measure the motility of the same bead-receptor complex before and after poisoning. Instead the motility of bead-receptor complexes were measured in different populations (as described in 6.3). In population I the cells were kept in ampicillin, present both during growth and during experiments. In population II the cells were grown with ampicillin, but the experiments were carried out in healthy growth media. The third population III was the control: here the cells had been kept in healthy growth media at all times. The three different populations are shown in table 6.1.

In figure 6.2 the recorded time series from a control experiment (population III) is shown in blue, afterwards a recorded time series taken from a cell kept in ampicillin under the experiment (population I), in red. The break on the axis is inserted between the recorded time series from a control experiment (population III) and the recorded time series of a ampicillin exposed bacterium (population I). The distribution of the positions visited by the bead-receptor complex is well fitted by a Gaussian as shown in the left insert corner. In the right corner is an insert of the data shown as a scatter plot. In total 38 data sets were measured on different days on bacteria exposed to ampicillin at all times (population I). The standard deviation of the position histogram visited by the bead-receptor complex was $\sigma_{ampicillin, population I} = (3.43 \pm 0.32)$ nm (mean \pm SEM). In the

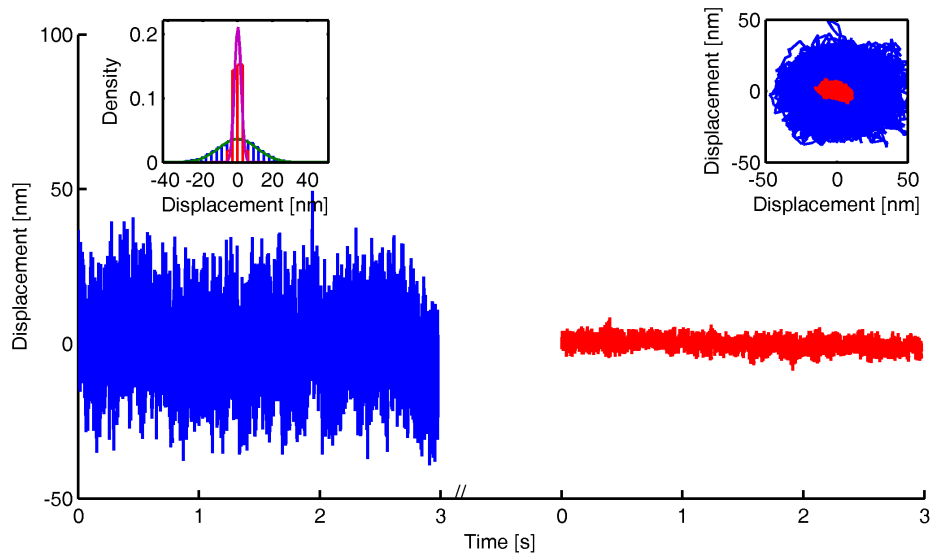


Figure 6.2: The recorded time-series from a control experiment (population III) is shown in blue. In red is shown a recorded time series taken from a cell kept in ampicillin during the experiment (population I). The break on the axis is inserted between the recorded time series from a control experiment (population III) and the recorded time series of a ampicillin exposed bacterium (population I). In the left corner the same data are shown as an histogram. In the right corner the insertion shows data from the x and the y channel plotted as a scatter plot.

Presence of ampicillin			
	Population I	Population II	Population III
Growth	+ Ampicillin	+ Ampicillin	No Ampicillin
Experiment	+ Ampicillin	No Ampicillin	No Ampicillin
‡ data sets	38	28	24
$(\sigma(x+y) \pm \text{SEM})/\text{nm}$	3.43 ± 0.32	10.25 ± 0.70	11.32 ± 0.89

Table 6.1: The table shows an overview of the three different types of ampicillin experiments: Ampicillin exposed cells (population I), cells where ampicillin had been removed at least 1 hour before conducting the experiment (population II) or in an untreated control group (population III). The number of data sets for each experiment is stated, as well as the standard deviation of the bead-receptor complex.

experiment on bacteria grown in ampicillin but where the experiments had been performed in growth media (population II), 28 data sets were conducted. The standard deviation of the bead-receptor complex was $\sigma_{\text{ampicillin, population II}} = (10.25 \pm 0.70)$ nm (mean \pm SEM). In the control experiment with no ampicillin (population III), 24 data sets were conducted. The standard deviation of the bead-receptor complex was $\sigma_{\text{control, population III}} = (11.3 \pm$

0.89) nm (mean \pm SEM). The results are summarized in table 6.1.

To evaluate if the observed differences was accidental a student's t-test was used. Using a student's t-test we showed that there is a significant difference ($p = 2.1 \times 10^{-14}$) between ampicillin exposed cells (population I) and our control group (population III). In the same way we tested the difference between the control group (population III) and the cells where ampicillin was removed (population II), here no significant difference was seen ($p = 0.11$). Removing ampicillin from the solution seems to restore receptor motility. Finally we investigated if there was a significant difference between the ampicillin exposed cells (population I) and the cells where ampicillin had been removed (population II) ($p = 5.7 \times 10^{-15}$). The results are summarized in table 6.2. Hence, the motility of the λ -receptor hence seems to be dependent on a growing peptidoglycan layer. The influence of ampicillin was reversible, and λ -receptor motility was restored if ampicillin was removed.

p-value found by student's t-test		
	Population I	Population II
Population II	5.7×10^{-15}	-
Population III	2.1×10^{-14}	0.11

Table 6.2: *The p-value obtained using a student's t-test giving the probability that the observed differences between the populations are accidental.*

6.5 Summary

We investigated the effect of ampicillin on the motility of single λ -receptors. Ampicillin hinders the formation of peptide bonds in the peptidoglycan layer and it thereby stop the dynamic remodelling of the peptidoglycan layer. We see a significant decrease in the receptor motility in cells exposed to ampicillin. However, if ampicillin treated cells are transferred to growth media, protein motility seems to be restored assuming the same motility as untreated cells. The decrease in receptor motility upon ampicillin treatment is in agreement with [1], where the λ -receptor was postulated to be firmly attach to peptidoglycan layer. The fact that the decrease in λ -receptor motility is reversible indicate that the motion is closely connected to the dynamic reconstruction of the peptidoglycan layer. This is in good agreement with our previous finding where we showed that the "wiggling" motion of the receptor was energy dependent, see chapter 5. The wiggling motion performed by the receptor therefore seems to be both energy dependent and relying on the dynamical reconstruction of peptidoglycan layer.

Chapter 7

The effect of the peptidoglycan layer, using vancomycin

7.1 Introduction

In the chapter 5 we have seen that the mobility of the λ -receptor depends on energy. The λ -receptor is thought to be firmly attached to the peptidoglycan layer [1]. The effect of a destroyed peptidoglycan layer on the λ -receptor mobility was investigated by ampicillin poisoning (see chapter 6). We saw a decrease in the λ -receptor mobility upon ampicillin poisoning. We also saw that the motility of individual λ -receptors was regained if ampicillin was removed after poisoning. Vancomycin is another antibiotic that hinders peptidoglycan synthesis. We therefore wanted to investigate the effect of vancomycin on the motility of the λ -receptor.

Vancomycin is normally used against gram positive bacteria, which lacks the outer membrane. Vancomycin is a large molecule that cannot pass the outer membrane of normal gram negative bacteria. However, if the cells have the mutation of increased (outer) membrane permeability, they are susceptible to larger molecules as vancomycin or bile salts. Increased (outer) membrane permeability (*imp*) in *E. coli* was found in 1989 [52], but not until recently was it established that this was due to the absence of either one of two outer membrane proteins [53], [54].

In this chapter I first describe how we made an *E. coli* strain with increased outer membrane permeability suitable for our experiments. Secondly, I show the results from experiments performed on the *imp* strain.

7.2 Biology

Vancomycin works by binding to the D-ala-D-ala residue of the peptidoglycan strands and hereby blocking further synthesis of the peptidoglycan layer. For a review on the binding of vancomycin and other peptidoglycan inhibitors see [55] or [56]. The binding of vancomycin to the peptidoglycan strand can be seen in figure 7.1

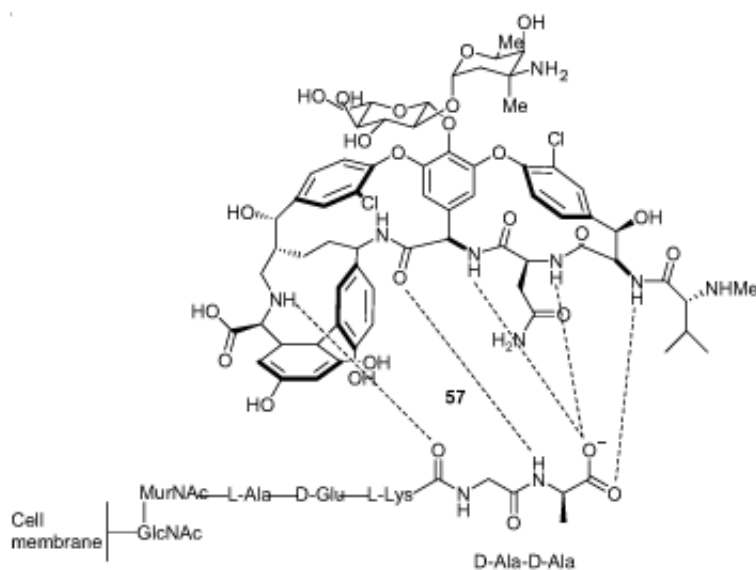


Figure 7.1: The binding between vancomycin (upper structure) and an individual peptidoglycan strand (lower structure) is here shown [57].

In 2005 the genes responsible for increased membrane permeability, which makes *E. coli* tolerant to vancomycin, were found [53], [54]. Thomas Silhavy and Natividad Ruiz kindly provided the strain NR701 having increased outer membrane permeability. The strains are all based on MC4100 (a commonly used strain of *E. coli*). The strains used in this project are MCR106 = MC4100 $\Delta lamB106$ and NR701 = MC4100 *imp4213 yfhS::Tn10*. The goal was to get a strain that had increased outer membrane permeability, no λ -receptor (LamB), and no pili: the strain needs to be without *lamB*, as we want only to have *lamB* present on a plasmid; this way we are able to control the expression of λ -receptors on the surface. The strain has to have increased membrane permeability as our goal is to see the influence of vancomycin. The strain has to be without pili to insure that the mobility of our bead is not hindered by their presence.

We had access to cells that were without pili and without LamB or strains with increased membrane permeability, but unfortunately not everything in the same strain. We therefore needed to make a new strain to fulfil our needs. We did this by using bacteriophage P1 (a bacterial virus). When P1 infects the bacteria it makes a long strand of multiple copies of its own DNA. Afterwards it cuts the phage DNA into sizes containing on full phage DNA, and finally it packs it each DNA piece into a new phage capsid. In 1 %, of the cutting procedure enzymes cut the *E. coli* genome instead of the phage DNA. A P1 containing *E. coli* DNA will transfer this instead. P1 can therefore be used to transfer one or more genes into another *E. coli* strain (termed a P1 transduction). It is only possible to move

more than one gene at the time if the genes are in close proximity of each other at the genome. The gene of increased membrane permeability (*imp*) is close to the gene coding for arabinose (*ara*). When *ara* is transferred from one *E. coli* to another, (*imp*) will sometimes be transferred together with it. Arabinose was therefore used as a marker for the targeted gene, increased membrane permeability. The plan was then to take the NR701 which is *ara*⁻ and transfer *ara*⁺ into NR701 from another strain, and make sure that the *imp4213* (a specific increased membrane permeability mutation) was still preserved. Thereafter we should transfer *imp4213* and *ara*⁺ together into a new cell, which did not produce LamB or pili. For a graphical illustration see figure 7.2.

7.3 P1 transduction protocol

There are three basic steps in the process of transferring DNA from one cell to another with P1 (a P1 transduction). The first step is to make a phage solution from a single plaque. The second step is to use this P1 to take up the wanted DNA from a selected bacterial strain (the donor). The third step is to transfer this DNA into the targeted bacteria (the recipient). In the third step I had some problems with the choice of bacterial strains, so this step was done twice.

The recipes of all media used in this chapter can be found in appendix A.2

7.3.1 Getting a single phage colony

The starting step is to get a genetically identical P1 phage solution. This is done as described below.

A single colony of S971 [58] was transferred into 5 ml of YT-broth, where it was grown for 3 hours. Then 0.03 ml 1M CaCl₂ was added and it was grown for additional ½-1 hour. A dilution series of P1_{vir} was made by transferring 0.05 ml into 5 ml YT-broth supplemented with 10 mM CaCl₂. The solution was mixed. Then 0.05 ml into 5 ml YT-broth supplemented with 10 mM CaCl₂ to a dilution of 10⁴; this was repeated until a dilution of 10⁸. Now 0.1 ml of each concentration was transferred to a small wasserman tube. A control was made by transferring the same amount of pure YT 10 mM CaCl₂. To each tube 0.1 ml of the bacterial culture was now added. The tubes were incubated at 37 °C for 10 min. Now 0.1 ml 1M CaCl₂ was added plus 0.2 ml 20% glucose (w/V). 3 ml of H-top (6 g agar) was added and immediately poured onto a YT-plate. The plates were left in the warm room at 37 °C overnight.

The plaques were counted the following day to establish the number of plaque forming units (pfu) in the original solution. The result was 345 plaques in the 10³ dilution, which means I had 3*10⁵ pfu per ml in the original P1_{vir} solution. A single plaque was cored out with a sterile disposable glass pipette. It is important to check that the whole plaque is cored out. It was transferred into 1 ml YT broth where 0.1 ml of 1M CaCl₂ was added.

We now had a solution of genetically identical phages.

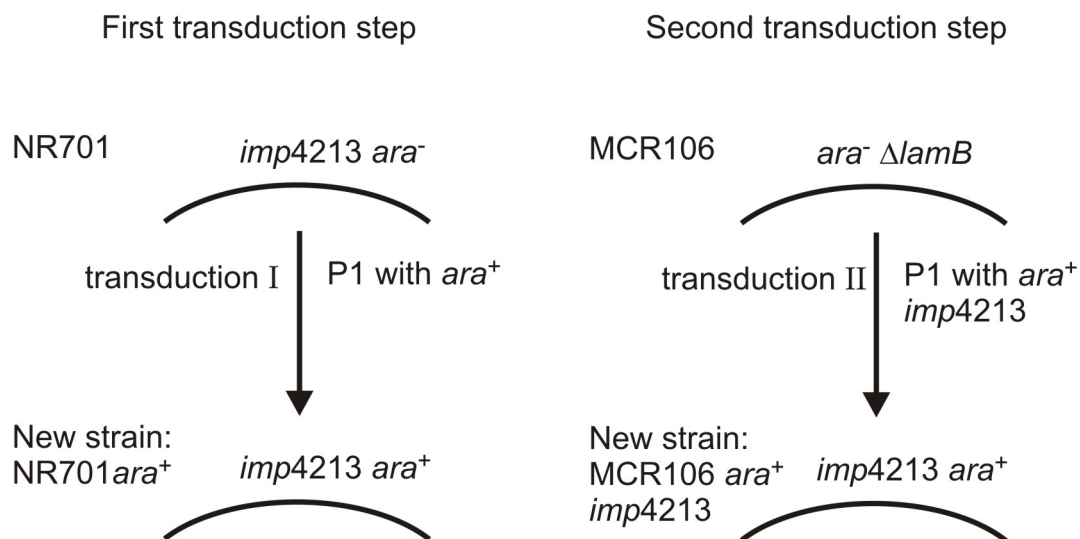


Figure 7.2: A graphical illustration of the intended P1 transduction procedure. To the left the gene for arabinose (*ara*⁺) is transferred into NR701. The genes from our new strand are then transferred into MCR106, illustrated to the right.

7.3.2 Getting a P1 transduction solution

Here we wanted to get a P1 phage that could transfer the gene *ara*⁺. This was done as described below.

0.5 ml of an overnight culture of MG1655 [59] was transferred into 5 ml YT-broth+ 10 mM CaCl₂ after which it was grown for 45 min. To the YT-broth CaCl₂ solution with the single plaque described above, 0.1 ml of the bacterial culture was added. Then 3 ml of sloppy H-top (3 g agar) agar was added and it was poured onto plates immediately. The plates were placed with the lid upwards. The sloppy agar is used as it makes it simpler to extract the phages from the plate.

When the plates looked sponge-like the phages should be scraped of. After 7 hours, the plate looked like a sponge. 3 ml of YT-broth was added and the H-top was scraped of. It was transferred to centrifuge tubes where 0.3 ml 1M MgSO₄ and 1 drop of CHCl₃ was added. The flasks were vortexed vigorously. It was spun down at 6000 rpm for 5 min. The supernatant was taken and filter sterilized (0.45 μm).

We now had phages that could transfer *ara*⁺ into chosen bacterial strains.

7.3.3 P1 transduction NR701

We wanted to transfer *ara*⁺ into the strain NR701, which is *ara*⁻ and has the desired gene *imp4213*. NR701 can not live of arabinose as a carbon source, unless *ara*⁺ is inserted. By growing the bacteria on minimal media plates with arabinose as only carbon source we selected only bacteria which had genetic material inserted. The goal is to get a strain that

is *imp4213 ara*⁺.

5 ml of NR701 overnight culture was spun down at 4000 rpm for 5 min. The cells were resuspended in 5 ml of transduction salts. This solution was transferred to a 37°C water bath, and kept there for 10 min. This exposes the cells to a short period of starvation, which should make them take up the phage DNA better. 3 small wasserman glasses were prepared with 0.1 ml of P1 transduction in the following dilution 0, 10 and 10². To each glass there was added 0.1 ml of the bacteria solution. As control, we made a tube where the phage solution was exchanged with YT broth (no phage control) and a tube where the bacteria were exchanged with transduction salts (no bacteria control). The solutions were now put in a water bath of 37°C for 10 min. 0.1 ml of each tube was spread together with 0.2 ml Na-citrate onto M63 $\frac{1}{2}$ -ara plates. The plates were put in the 37°C room overnight. The result was:

dilution of phages	# bacteria
0	894
10	291
10 ²	151
No phage control	101
No bacteria control	0

We now had a bacteria that in some cases would have the wanted genetic combination *imp4213 ara*⁺.

7.3.4 Purification and testing of the bacteria

The cloned bacteria from the section above were now ready for purification and testing. The purification is done to remove all phages left. The testing is done to check if the bacteria have both the *imp4213* and *ara*⁺. The first step was to remove excess phages. 24 single colonies of the bacteria from the 0 dilution plates were transferred with a sterile toothpick and spread out on a M63 $\frac{1}{2}$ -ara plate.

The testing was done by transferring a single colony from each of the 24 chosen bacteria colonies to first YT-, then MacConkey-, and then a M63 $\frac{1}{2}$ -ara plates. MacConkey plates contain bile salts that are toxic to strains with increased membrane permeability (hence having the *imp4213*) but non toxic to normal cells. It is done by sticking a sterile toothpick through the colony which is selected for transfer and then sticking it into the targeting plates. From the point where the bacteria were placed on the YT plate a line is drawn with a sterile flat toothpick. A SDS disk is placed on the center of each bacteria line made on the YT plate. This is a second indirect way to check for *imp4213*, as SDS kills *E. coli* with increased membrane permeability, but does not harm a normal *E. coli*. The SDS disk is made in the following way: Take your tweezers and dip it into alcohol, put it into a flame to light on the alcohol (do not keep it inside the flame), add 7.5 μ l 100 mg/ml SDS to the sterile cotton disk, this gives 750 μ g SDS pr disk.

The result was that of the 24 bacteria colonies, 5 had both the *imp4213* and *ara*⁺ genes.

To store the bacteria, frozen stocks were made of each of these 5 bacterial strains that were *imp4213* and *ara*⁺. The stored *imp4213* and *ara*⁺ bacteria were termed TM3-TM6.

7.3.5 Getting a P1 transduction solution

Here we wanted to get a phage that could transfer *imp4213 ara*⁺ into a bacterial strain of choice. The whole process is described below.

0.5 ml of an overnight culture of TM4 and TM5 were transferred into 5 ml YT-broth + 0.03 ml 1 M CaCl₂, after which it was grown for 1 hour. In small wasserman tubes 0.1 ml phage (from the purified P1's I made) was added in the following dilutions 10³, 10⁴, and 10⁵, and a control without any phages. To each tube 0.2 ml bacteria were added. The cells were now moved to 37 °C for 10 min. To each tube, 0.1 ml 1 M CaCl₂ and 0.2 ml 20 % w/V glucose and 3 ml of sloppy H-top (3 g agar) agar was added and it was poured onto plates immediately. The plates were placed with the lid upwards. After 6 hours the 10⁴ dilution was harvested by adding 3 ml of YT-broth, and the H-top was scraped of. It was transferred to centrifuge tubes, where 0.3 ml 1 M MgSO₄ and 1 drop of CHCl₃ was added. The flasks were vortexed vigorously. It was spun down at 6000 rpm in 5 min. The supernatant was taken and filter sterilized (0.45 μm). After 10 hours, the 10⁵ solution was harvested in the same way.

I now had phages that could transfer *imp4213* and *ara*⁺ into other bacterial strains.

7.3.6 P1 transduction MCR106

We wanted to move *imp4213* and *ara*⁺ into the bacterial strain MCR106 which is without pili and has no λ-receptor. MCR106 is *ara*⁻, and hence unable to live of arabinose as a carbon source. Minimal plates with arabinose as only carbon source can again be used to select for bacteria with genetic material inserted. The transferring of the genes is described below.

5 ml of MCR106 overnight culture was spun down at 4000 rpm in 5 min. The cells were resuspended in 5 ml of transduction salts. This solution was transferred to a 37 °C water bath, and kept there for 10 min. 3 small wasserman tubes were prepared with 0.1 ml of P1 made on TM4 and TM5 in the following dilution 0, 10 and 10². To each tube 0.1 ml of the bacteria solution was added. As control we made a tube where the phage solution was exchanged with YT broth (no phage control) and a tube where the bacteria were exchanged with transduction salts (no bacteria control). The solutions were now put in a water bath of 37 °C for 10 min. 0.1 ml of each tube was spread together with 0.2 ml Na-citrate on M63 ½-ara plates. The plates were put in the 37 °C overnight.

The result was devastating, because there were several bacteria growing on the bacteria control. This indicated that there were many spontaneous revertant bacteria, meaning bacteria that without insertion of the new gene had adapted to the new environment and regained their ability to live of arabinose as a carbon source.

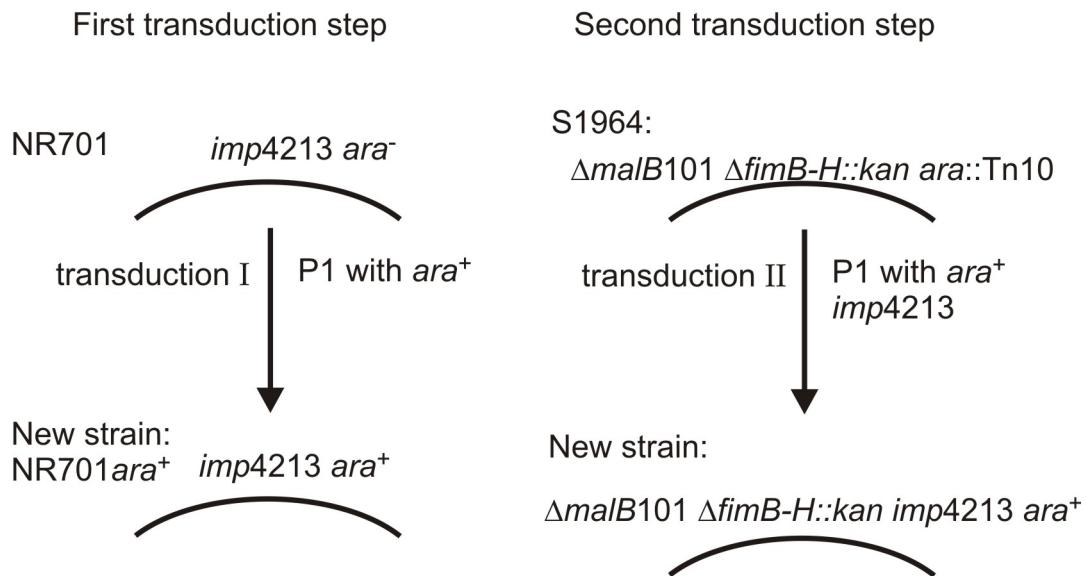


Figure 7.3: A graphical illustration of the P1 transduction procedure. To the left the gene for arabinose (*ara⁺*) is transferred into NR701. The genes from our new strand is then transferred into MCR106, illustrated to the right

7.3.7 P1 transduction into S1964

MCR106 turned out to be unsuitable for creating a strain that had both *imp4213* and *ara⁺* as too many bacteria spontaneously regained their ability to live of arabinose as a carbon, as described above. To avoid this problem of revertants, a strain of *E. coli* with a more serious change in the arabinose gene was chosen. The selected strain was S1964 [60], which most important genes for this study is $\Delta malB101 \Delta fimB-H::kan ara::Tn10$ mini-tet. This strain is without λ -receptor, has no pili and cannot live of arabinose. Here a whole transposon carrying tetracyclin resistance is inserted into the arabinose gene. This makes it very hard for the *E. coli* to regain its ability to live on arabinose.

5 ml of S1964 overnight culture was spun down at 4000 rpm for 5 min. The cells were resuspended in 5 ml of transduction salts. This solution was transferred to a 37 °C water bath, and kept there for 10 min. 3 small wasserman tubes were prepared with 0.1 ml of P1 made on TM4 and TM5 in the following dilution 0, 10 and 10². To each glass, 0.1 ml of the bacteria solution was added. As control we made a tube where the phage solution was exchanged with YT broth (no phage control) and a tube where the bacteria were exchanged with transduction salts (no bacteria control). The solutions were now put in a water bath of 37 °C for 10 min. 0.1 ml of each tube was spread together with 0.2 ml Na-citrate on M63 $\frac{1}{2}$ -ara plates. The plates were put in the 37 °C overnight. The result was:

dilution of phages	# bacteria P1 from TM4	# bacteria P1 from TM5
0	19	12
10	4	2
10 ²	1	0
No phage control	0	0
No bacteria control	0	0

We now had bacteria that might have both the gene *imp4213* and *ara*⁺, besides that the strain had no pili and no λ -receptor, as we wanted.

7.3.8 Testing and purification

We here first purified the bacteria from excess phages and then tested if the strains were *imp4213 ara*⁺.

From the 0 times dilution, 12 bacteria colonies were transferred to M63 $\frac{1}{2}$ -ara plates, where 0.1 ml Na-citrate was added; this is done to remove excess phages. The 24 chosen bacteria candidates, TM4, TM5, NR701 and S1964 were tested for the *imp* gene in the following way. A single colony of each bacteria was transferred, first to a empty flask for making a frozen stock, then to MacConkey agar plate, then M63 ara plates supplemented with tetracycline, and finally for a positive control to a YT plate. The bacteria were spread normally on the MacConkey and the M63 disk. On the YT plate, a line was drawn on the plate with a flat toothpick. A SDS disk (750 μ g) was placed on the center of this line (see 7.3.4 above for a description). To store the bacteria, I froze down 8 candidates which are termed TM8-TM15. TM9 and TM15 are *imp*⁺, the rest are *imp4213*.

The result was that I had succeeded in transferring *imp4213* and *ara*⁺ into a bacteria lacking both pili and the λ -receptor.

7.3.9 Inserting of the plasmid

To be able to use the bacteria for measuring the mobility of the λ -receptor with the optical tweezers, the plasmid pLO16 [5] had to be inserted into the bacteria, this work was done by Dr. Stanley Brown at Department of Biology, University of Copenhagen.

The plasmid pLO16 and the control plasmid pSB2267 was purified. The purified plasmids were checked for changes in genetic code. The plasmid was inserted into the bacterial strains TM14 and TM9. It was checked that the bacteria had regained their ability to live of maltose.

We therefore now had bacteria that were suitable for optical tweezers experiments and were sensitive to vancomycin.

7.4 Experimental procedures

As describes we succeeded in making a strain that could be used for optical tweezers measurement on vancomycin poisoning. The following part of the chapter will contain the

preparation for the optical tweezers measurements and the results obtained. The bacteria strains used in these experiments were TM14 with the plasmid pLO16 inserted, for a full description of the strains and plasmid see [60], [5] and section 3.2.

The growth of the bacteria was done in the following way:

- Single bacteria colonies were grown overnight at 37 °C on YT-agar plates [50] supplemented with 25 $\mu\text{g}/\text{ml}$ chloramphenicol.
- A single colony was transferred sterile into M63 media [50] containing 1 $\mu\text{g}/\text{ml}$ B1, 25 $\mu\text{g}/\text{ml}$ Chloramphenicol, 0.1% casein hydrolysate, and 0.2% glycerol, and grown in shaking water bath overnight at 37 °C.
- 0.1 ml of the overnight culture was then diluted into 3 ml of fresh media and grown at 37 °C until log-phase.
- To induce the expression of the λ -receptor 3 ml of fresh M63 media supplemented with 1mM IPTG (the final concentration IPTG was 0.5 mM and the bacteria were grown for an additional $\frac{1}{2}$ hour) was added and the bacteria were grown for an additional $\frac{1}{2}$ hour.
- 1 ml cell culture was spun down at $1673 \times g$ for 5 minutes and the cells resuspended in 100 μl buffer. The buffer used throughout the experiments was 10 mM potassium phosphate, 0.1 M KCl, pH 7.

The mobility of the biotinylated λ -receptor was followed with the optical tweezers by attaching a streptavidin coated bead. The beads used were streptavidin-coated polystyrene beads from Spherotech, with a diameter of 0.44 μm . These beads are washed before use in the following way:

- Washing the beads were done by suspending the beads in millipore water and thereafter centrifuged at $1673 \times g$ for 10 min.
- The supernatant was discarded and the beads resuspended in buffer and sonicated for at least 15 min to remove aggregates.

At the microscope, the bacteria were kept in a perfusion chamber when studied. The perfusion chamber was made in the following way:

- At least 5 μl poly-l-lysine was spread in a line on a coverslip (0.17 mm) and left to dry.
- Two pieces of double layer of scotch double sticky tape were placed on the coverslip surrounding the dried poly-l-lysine.
- Another coverslip (0.17 mm) was placed on top as a lid. The final volume was 10-15 μl .

The preparation of the bacteria in the perfusion chambers was done over water bath in the following way:

- The chamber was washed twice with Millipore water.
- 15 μ l of the bacteria was perfused into the chamber, and left 15-25 minutes to adhere.
- 15 μ l of 12.5 mg/ml heparin was flushed into the samples and left for 15 minutes. Heparin decreases the attraction between the surface and the streptavidin-coated beads.
- To remove dust, the samples were rinsed by perfusing the chambers four times with buffer.
- 15 μ l washed streptavidin coated polystyrene beads were perfused into the chamber and left there 20 minutes to attach.
- Excess of beads was removed by flushing the chamber 3-5 times with M63 glucose media. Glucose was used as a carbon source inside the perfusion chambers to support anaerobic growth.
- The bacteria were stored in the refrigerator until use.

After the samples were prepared they were visualized in the microscope. A bacterium was found which had a wiggling bead placed on top. The optical tweezers were then used to check if the bead was specifically attached to the bacterium, by pulling on the bead. The motion of the bead-receptor complex was then recorded with the optical tweezers. The motion of a freely moving bead held in the same height as the attached bead was recorded for calibration to the spring constant of the trap κ . The motion of the bead-receptor complex was then measured in the following way.

- A freely diffusing bead was found and held close by the bacteria in the same height as the attached bead. A powerspectrum of the Brownian motion of the free bead was recorded. The power spectrum of the bead is used for calibration, to find the conversion factor between the voltage output of the diode and the nanometer displacement of the bead.
- The motility of a single bead-receptor complex was recorded with the optical tweezers.
- The cells were poisoned with vancomycin. The poisoning was done in the following way: 20 μ l of 0.08 mg/ml vancomycin (this is $100 \times$ the known MIC [61]) was flushed into the chamber, this was repeated 5 times. Then a break of roughly 3 min was held. The previous step was repeated.
- The motility of the exact same bead-receptor complex was then measured again with the optical tweezers.

7.5 Results

The influence of vancomycin on the λ -receptor mobility was investigated. The motility of the exact same λ -receptor was measured *in vivo* before and after poisoning. The cells were poisoned with a solution of vancomycin $100 \times$ the known MIC concentration. Two types of vancomycin experiments were conducted. In the first set of experiments the bacteria were grown at 37°C , but the measurement of the motility was done at room temperature (22°C). The motility of an individual bead-receptor complex was measured with the optical tweezers. A time series of the motility of the bead-receptor complex is shown in figure 7.4, the motility before vancomycin exposure in blue and the motility of the exact same receptor immediately after vancomycin exposure (0-3 min) in red. The break on the axis indicate the break in time where the media was exchanged, i.e. vancomycin was flushed in. The data are well fitted to a Gaussian function as visualized in the insertion in the left corner. In the right corner is an insertion of a scatter plot. The result shows a decrease in the mobility of the λ -receptor. Before vancomycin exposure the width of the position histogram visited by the receptor-bead complex is $\sigma_{\text{before}, 22^\circ\text{C}} = (9.6 \pm 0.97)$ nm (std \pm SEM). Immediately after vancomycin exposure (0-3 min) the width of the position histogram decreases to $\sigma_{0-3\text{min}, 22^\circ\text{C}} = (3.4 \pm 0.44)$ nm (std \pm SEM). Ten data sets are measured. The development in the λ -receptor motility upon vancomycin treatment was measured as a function of time and the results are presented in table 7.1.

Vancomycin	$(\sigma_{(22)^\circ\text{C}} \pm \text{SEM})/\text{nm}$	# data sets
Prior to vancomycin	9.6 ± 0.97	10
0-3 min of vancomycin	3.4 ± 0.44	10
15 min of vancomycin	5.3 ± 1.89	8
30 min of vancomycin	2.8 ± 0.33	8

Table 7.1: The table shows the amount of vancomycin exposure versus the average motility of the bead-receptor complex at room temperature.

The second set of experiments were performed in the same way, but by using a stage heater the samples were kept at 37°C at the microscope before, during, and after poisoning. A decrease is seen in the receptor mobility upon vancomycin exposure. An individual data set is shown in figure 7.5. Here the motility of the bead-receptor complex measured before vancomycin exposure is shown in blue. The motility of the exact same receptor immediately after vancomycin exposure (0-3 min) is shown in red. The break on the axis indicate the break in time where the media was exchanged, i.e. vancomycin was flushed in. The data are well fitted to a Gaussian function shown as an insertion in the left corner. In the right corner the data are shown as a scatter plot. The standard deviation of the bead-receptor complex with no vancomycin present was found to be $\sigma_{\text{before}, 37^\circ\text{C}} = (7.3 \pm 1.26)$ nm (std \pm SEM). Immediately after vancomycin exposure (0-3 min) it is $\sigma_{0-3\text{min}, 37^\circ\text{C}} = (4.5 \pm 0.81)$ nm (std \pm SEM). Ten data sets are measured. The development in the λ -receptor

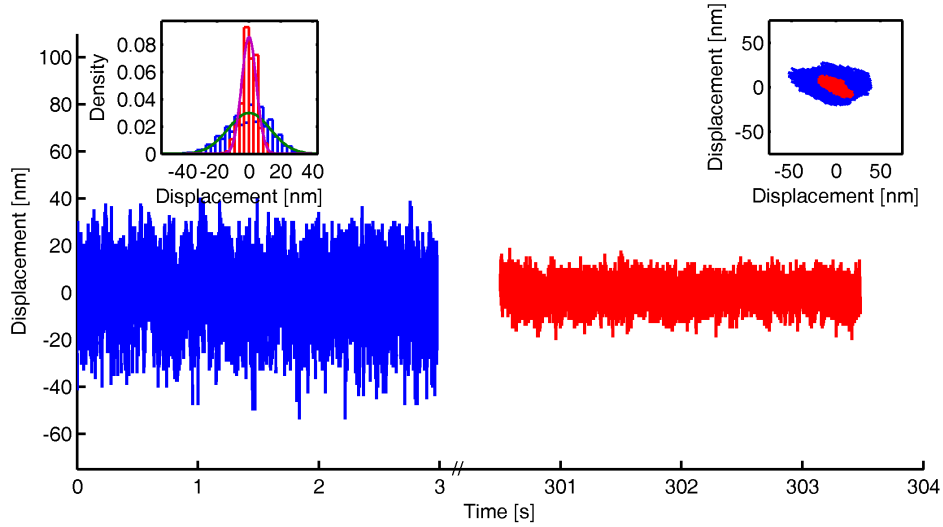


Figure 7.4: The motility of the bead-receptor complex at 22°C in a healthy cell is shown in blue and the motility of the exact same receptor complex immediately after vancomycin treatment (0-3 min) is shown in red. The break on the axis indicates the break in time where the media was exchanged, i.e. vancomycin was flushed in. The lower part of the figure shows the time trace recorded with the optical tweezers, in the left corner the same data are visualized as a histogram, in the right corner the data for x and the y directions are plotted in scatter plot.

motility upon vancomycin treatment was measured as a function of time and the results are presented in table 7.2. Technically the experiments performed at 37°C were much harder to conduct as the fluctuations in the chamber also increased.

Vancomycin	$(\sigma_{(37)^\circ C} \pm \text{SEM})/\text{nm}$	# data sets
Prior to vancomycin	7.3 ± 1.26	10
0-3 min of vancomycin	4.5 ± 0.81	10
15 min of vancomycin	4.8 ± 0.92	8
30 min of vancomycin	2.4 ± 0.53	6

Table 7.2: The table shows the amount of vancomycin exposure versus the average motility of the bead-receptor complex.

Using a student's t-test we showed that there was no significant difference between the data recorded at room temperature and the data recorded at 37°C see table 7.3; and the data will therefore in the following be treated together.

We investigated how the motility of the λ -receptor changes with time. The standard deviation of the receptor motility was $\sigma_{\text{Before}, (22+37)^\circ C} = (9.13 \pm 0.72)$ nm (20 data sets). Right after vancomycin exposure motility decreases $\sigma_{0-3\text{min}, (22+37)^\circ C} = (3.95 \pm 0.48)$ nm

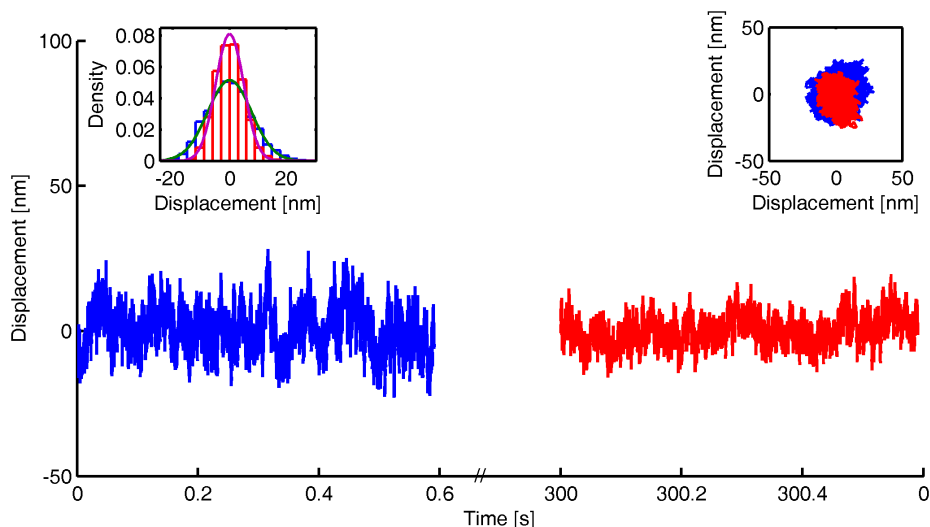


Figure 7.5: The motility of the bead-receptor complex at 37°C in a healthy cell is shown in blue and the motility of the exact same receptor complex immediately after vancomycin treatment (0-3 min) is shown in red. The break on the axis indicate the break in time where the media was exchanged, i.e. vancomycin was flushed in. The lower part of the figure shows the time trace recorded with the optical tweezers, in the left corner the same data are visualized as a histogram, in the right corner the data for x and the y directions are plotted in a scatter plot.

	$\sigma_{\text{Before}, 22^\circ\text{C}}$	$\sigma_{0-3\text{min}, 22^\circ\text{C}}$	$\sigma_{15\text{min}, 22^\circ\text{C}}$	$\sigma_{30\text{min}, 22^\circ\text{C}}$
$\sigma_{\text{Before}, 37^\circ\text{C}}$	0.16	-	-	-
$\sigma_{0-3\text{min}, 37^\circ\text{C}}$	-	0.24	-	-
$\sigma_{15\text{min}, 37^\circ\text{C}}$	-	-	0.58	-
$\sigma_{30\text{min}, 37^\circ\text{C}}$	-	-	-	0.37

Table 7.3: The table give the p -values found from a student t -test between the results obtained at 22°C and the results obtained at 37 °C. No significant difference is seen between the λ -receptor motility at 22°C and 37 °C neither before or after vancomycin exposure.

(20 data sets). This decrease in the motility of the receptor could be caused by a stiffening of the peptidoglycan layer due to the interaction with vancomycin. After 15 minutes of vancomycin exposure a slight increase and a larger fluctuation within the measured motilities is seen. The standard deviation measured was $\sigma_{15\text{min}, (22+37)^\circ\text{C}} = (5.04 \pm 1.05)$ nm (16 data sets). It is possible that the slight increase in the motility is due to the peptidoglycan layer regaining some of its flexibility. After 30 minutes of vancomycin exposure the standard deviation of the bead-receptor motility decreases to a lower value than seen right after exposure, and the variation within the measured motilities also decreases $\sigma_{30\text{min}, (22+37)^\circ\text{C}} = (2.67 \pm 0.30)$ nm (14 data sets). It is possible that the decrease in the motility here is

due to growth of the peptidoglycan layer being stopped. All the data are summarized in table 7.4.

Vancomycin	$(\sigma_{(22+37)^{\circ}C} \pm \text{SEM})/\text{nm}$	# data sets
Prior to vancomycin	9.13 ± 0.72	20
0-3 min of vancomycin	3.95 ± 0.48	20
15 min of vancomycin	5.04 ± 1.05	16
30 min of vancomycin	2.67 ± 0.30	14

Table 7.4: *The table shows the amount of vancomycin exposure versus the average motility of the bead-receptor complex.*

$(22+37)^{\circ}C$	$\sigma_{0-3min, (22+37)^{\circ}C}$	$\sigma_{15min, (22+37)^{\circ}C}$	$\sigma_{30min, (22+37)^{\circ}C}$
$\sigma_{Before, (22+37)^{\circ}C}$	5.3×10^{-6}	0.000097	1.7×10^{-7}
$\sigma_{0-3min, (22+37)^{\circ}C}$	-	0.14	0.021
$\sigma_{15min, (22+37)^{\circ}C}$	-	-	0.024

Table 7.5: *The table shows the amount of vancomycin exposure versus the average motility of the bead-receptor complex.*

To ensure that the imp strain had a normal division cycle we visualized the cell division within the perfusion chambers. The sample was prepared as for the vancomycin experiments but the cells were kept in growth media at all times. The sample was visualized at the microscope at $37^{\circ}C$. Every 30 minutes an image was taken of the sample. Within 90 minutes several cell division were seen, see figure 7.6.

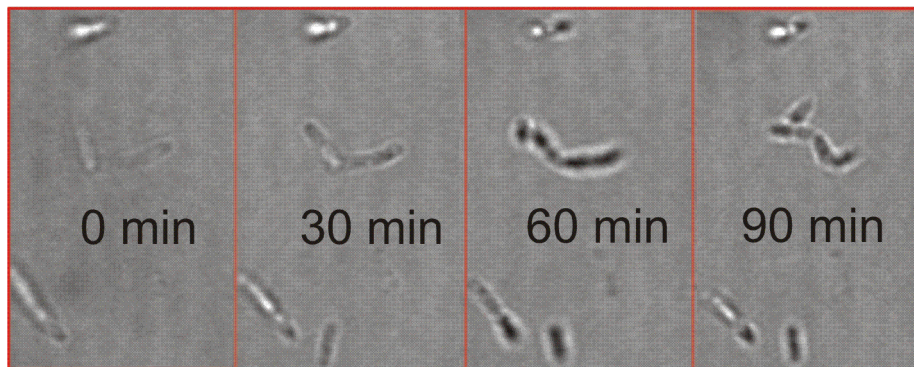


Figure 7.6: *The pictures show cell division of our bacteria within the perfusion chamber. The sample was maintained at 37°C. An image was taken every 30 min. Within 90 minutes several cell divisions were seen.*

7.6 Summary and conclusion

In order to further study the influence of the peptidoglycan layer on the λ -receptor motility, we wanted to see the effect of vancomycin, an antibiotic which hinders peptidoglycan synthesis. Vancomycin is a large molecule which cannot pass the outer membrane of normal gram negative bacteria. Therefore, we made a bacterial strain of *E. coli* which had increased membrane permeability, no pili and no λ -receptor. Insertion of the plasmid pLO16 [5] harboring the λ -receptor with a biotinylation sequence made it perfect for our optical tweezers experiments. We investigated the influence of vancomycin on the mobility of the λ -receptor. Vancomycin poisoning decreased the mobility of the λ -receptor even after short exposure time. The results were independent on if the experiments were performed at room temperature or at 37°C. The decrease in the motility of the receptor after short exposure to vancomycin might be caused by a stiffening of the peptidoglycan layer. After 30 minutes of exposure, the protein motility decreased further. It is possible that what we see here is the blocking of the peptidoglycan growth. By arsenate and azide poisoning we have showed that the motility of the λ -receptor is energy dependent, chapter 5. Ampicillin exposure, which blocks transpeptidase action, decreased the motility of the λ -receptor. This effect was seen to be reversible, chapter 6. The motility of the λ -receptor seems to be dependent on the dynamic reconstruction of the peptidoglycan layer. This finding is further supported by the fact that vancomycin poisoning significantly decreases the motility of the receptor. The motility of the λ -receptor does not seem to be influenced by changes in the outer membrane.

Chapter 8

The influence of antimicrobial peptides on the λ -receptor motility

8.1 Introduction

Previously, we have shown that the mobility of the λ -receptor is energy dependent (see chapter 5). We have also shown that there is a decrease in the mobility of the λ -receptor in cells exposed to ampicillin and vancomycin see chapters (6 or 7).

Antimicrobial peptides (AMPs) can be used as an alternative to conventional antibiotics. Here we have investigated the effect of the toxic antimicrobial peptide polymyxin B (PMB), on the motility of the λ -receptor. PMB creates holes in the outer membrane that are large enough to allow the protein to pass (self promoted uptake). PMB then attacks the inner membrane making it more permeable, destroying the electro chemical gradient leading to cell death. As the inner membrane is more permeable, energy rich molecules within the cell are free to diffuse out and the experiments are hence somewhat equivalent to the energy depletion experiments performed by arsenate and azide poisoning see chapter 5.

We also investigated the effect of the non toxic antimicrobial peptide polymyxin B nonapeptide (PMBN). PMBN alters the outer membrane and increases the outer membrane permeability [62] [63], making the cells more susceptible to larger molecules, but without killing the bacteria.

8.2 Biology

Antimicrobial peptides have gained renewed interest due to the increasing amount of bacterial resistance. Polymyxins are very interesting, as they binds to the lipopolysachharides (LPS), the compound that give rise to toxic shock. Polymyxins are derived from *Bacillus polymyxa*. PMB is a mixture of polymyxins B₁ and B₂. It consists of a heptapeptide ring attached to a peptide side chain, which terminates in a fatty acid residue, see figure 8.1. It has a molecular weight of 1200 Da and a diameter of roughly 1.2 nm. The molecule is

twice the maximal size for nonspecific diffusion through the outer membrane [64]. PMBN is a truncated derivate of PMB, it lacks the fatty acid tail; see figure 8.1.

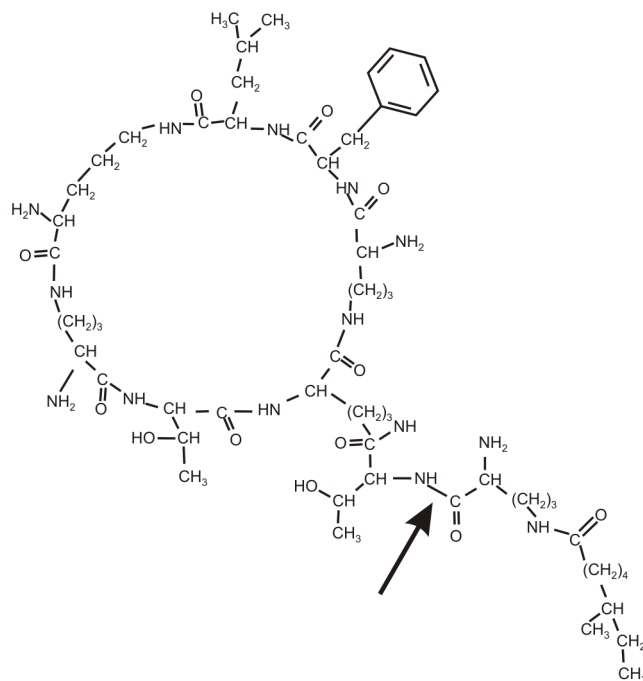


Figure 8.1: Here the structure of PMB can be seen. If the tail of the molecule is removed as indicated by the arrow we have the structure of PMBN.

The effect of PMB and PMBN on the outer membrane of gram negative bacteria is dramatic. This is illustrated very nicely in the electron microscope picture of change in the outer membrane in *Salmonella typhimurim* treated for 10 minutes 30 μg of either PMB or PMBN, see figure 8.2.

An increased outer membrane permeability can be measured by measuring the release of one or more periplasmic proteins. An increased inner membrane permeability can be measured by the release of one or more cytoplasmic proteins. Using β -lactamase as a periplasmic marker and β -galactosidase as a cytoplasmic marker it was shown that PMB and PMBN work within minutes [65] and only small concentrations is needed (5 $\mu\text{g}/\text{ml}$). PMB induced a release of both the periplasmic and the cytoplasmic marker, it hence increases both the outer and the inner membrane permeability. It is the increased inner membrane permeability that is toxic to the cells as the electrostatic gradient across the membrane is destroyed. Using PMBN only a release of the periplasmic marker was seen, PMBN hence increases only the outer membrane permeability. However, cells treated with PMBN become sensitive to large molecules as vancomycin, which is normally blocked by the outer membrane, but the cells are not killed by PMBN alone.

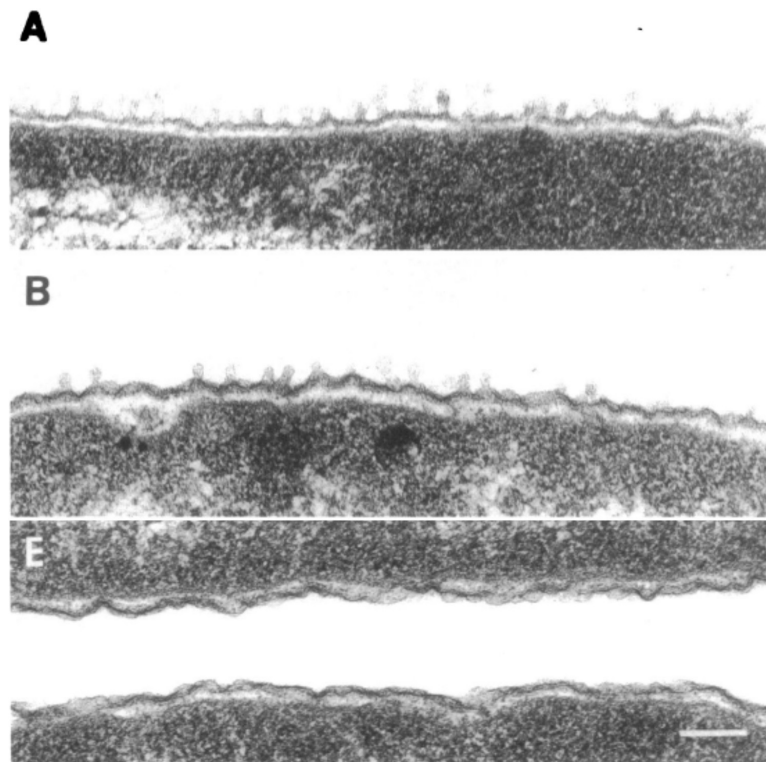


Figure 8.2: *The effect of polycations on the cell envelope of Salmonella typhimurium SL696. The cells were treated for 10 min with 30 μg of A: PMB, B: PMBN and E: control bacteria. The cells exposed to either PMB or PMBN have fingers of membrane material. It hence seems that there is more membrane material present in the cells exposed to PMB or PMBN than to the control cell. The bar is 0.1 μm [62]*

8.3 Experimental procedures

The bacteria strains used in these experiments were S2188 with the plasmid pLO16, for a full description of the strains and plasmid see [27], [5] or section 3.2.

The growth of the bacteria was done in the following way:

- Single bacteria colonies were grown overnight at 37°C on YT-agar plates [50] supplemented with 25 $\mu\text{g}/\text{ml}$ chloramphenicol.
- A single colony was transferred sterile into M63 media [50] containing 1 $\mu\text{g}/\text{ml}$ B1, 25 $\mu\text{g}/\text{ml}$ Chloramphenicol, 0.1% casein hydrolysate, and 0.2% glycerol, and grown in shaking water bath overnight at 37°C.
- 0.1 ml of the overnight culture was then diluted into 3 ml of fresh M63 media and grown at 37°C until log-phase.
- To induce the expression of the λ -receptor, 3 ml of fresh M63 media supplemented with 1mM IPTG (the final concentration IPTG was 0.5mM) was added and the bacteria were grown for an additional $\frac{1}{2}$ hour.
- 1 ml cell culture was spun down at $1673 \times g$ for 5 minutes and the cells resuspended in 100 μl buffer. The buffer used throughout the experiments was 10 mM potassium phosphate, 0.1 M KCl, pH 7.

The mobility of the biotinylated λ -receptor was followed with the optical tweezers by attaching a streptavidin coated bead. The beads used were streptavidin-coated polystyrene beads from Bang Laboratories, Inc (Fishers, In) with a diameter of $\sim 0.5 \mu\text{m}$. These beads are washed before use in the following way:

- The beads are suspended in millipore water and thereafter centrifuged $1673 \times g$ for 5-10 min.
- The supernatant was discarded and the beads resuspended in buffer.
- The beads were sonicated for at least 15 min to remove aggregates.

At the microscope, the bacteria were kept in a perfusion chamber when studied. The perfusion chamber was made in the following way:

- At least 5 μl poly-l-lysine was spread in a line on a coverslip (0.17 mm) and left to dry.
- Two pieces of double layer of scotch double sticky tape was placed on the coverslip surrounding the dried poly-l-lysine.
- Another coverslip (0.17 mm) was placed on top as a lid. The final volume was 5-10 μl .

The preparation of the bacteria in the perfusion chambers was done over water bath in the following way:

- The chamber was washed twice with millipore water.
- 10 μl of the bacteria was perfused into the chamber, and left 15-25 minutes to adhere.
- This step was omitted in the experiments with PMB. To times 10 μl PMBN (10 or 125 μM) was flushed in and left to adhere for 30 min. The PMBN is flushed in before the heparin, to prevent any effect of the heparin on the PMBN.
- 10 μl of 12.5 mg/ml heparin was flushed into the samples and left for 15 minutes. Heparin decreases the attraction between the surface and the streptavidin-coated beads.
- To remove dust, the samples were rinsed by perfusing the chambers four times with buffer.
- 10 μl washed streptavidin coated polystyrene beads were perfused into the chamber and left there 15 minutes to attach.
- Excess beads were removed by flushing the chamber 3-5 times with M63 glucose media. Glucose was used as a carbon source inside the perfusion chambers to support anaerobic growth.
- The bacteria were stored in the refrigerator until use.

After the samples were prepared they were visualized in the microscope. A bacterium was found which had a wiggling bead placed on top. The optical tweezers were then used to check if the bead was specifically attached to the bacterium, by pulling on the bead. The motion of the bead-receptor complex was then recorded with the optical tweezers. The motion of a freely moving bead held in the same height as the attached bead was recorded for calibration to the spring constant of the trap κ . The motion of the bead-receptor complex was then studied in the following way.

- A freely diffusing bead was found and held close by the bacteria in the same height as the attached bead. A powerspectrum of the Brownian motion of the free bead was recorded. The power spectrum of the bead was used for calibration to find the conversion factor between the voltage output of the diode and the nanometer displacement of the bead.
- The motility of a single bead-receptor complex was recorded with the optical tweezers.
- In the experiments with PMB, the bacteria were now poisoned by perfusing the chamber with 5×10^{-10} μl PMB 100 $\mu\text{g}/\text{ml}$ in buffer. PMBN treated cells were kept in M63-glu during the experiment. The motility of the exact same bead-receptor complex was then measured again with the optical tweezers.

8.4 Results

8.4.1 PMB results

The influence of the antimicrobial peptide polymyxin B (PMB) on the motility on a λ -receptor has been measured. Here the mobility of a λ -receptor was first measured in a healthy bacterium. The bacteria were then poisoned, and the mobility of the exact same receptor was then measured again. A recorded time series of the motility of a bead-receptor complex can be seen in figure 8.3. Here the motility of the bead-receptor complex before PMB treatment is shown in blue and the motility of the exact same receptor after PMB treatment in red. The break on the axis indicate the break in time where the media was exchanged, i.e. PMB was flushed in. The data are well fitted to a Gaussian function as shown in the insertion left. To the right corner of the picture is an insertion of the data as a scatter plot. The motility of the bead-receptor complex was measured on 12 data sets

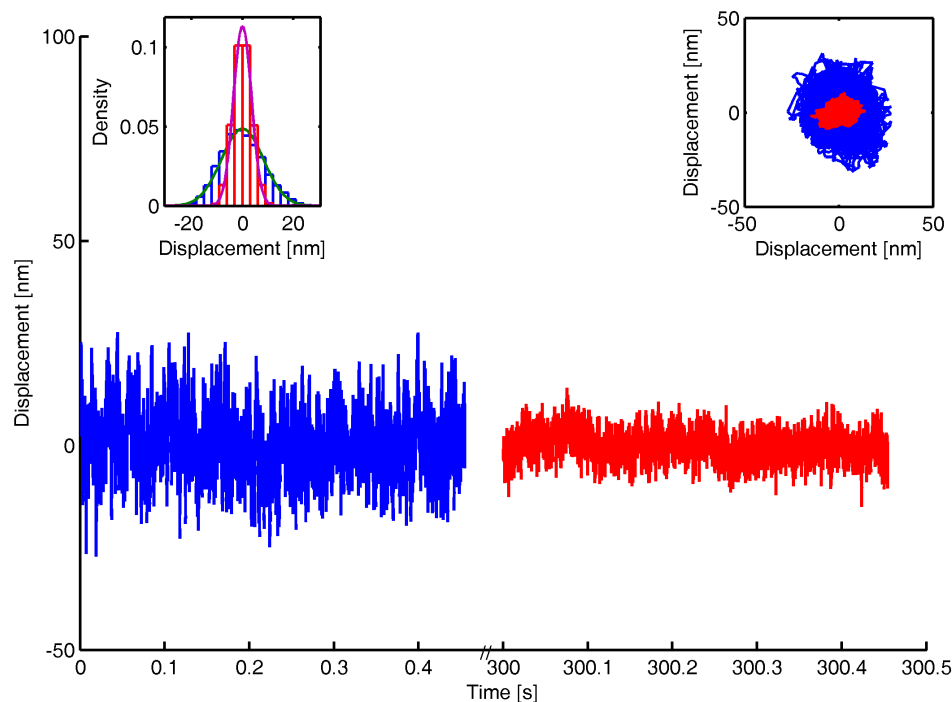


Figure 8.3: *The motility of the bead-receptor complex in a healthy cell is shown in blue and the motility of the exact same receptor complex after PMB treatment is shown in red. The break on the axis indicate the break in time where the media was exchanged, i.e. PMB was flushed in. The lower part of the figure shows the time trace recorded with the optical tweezers, in the left corner the same data are visualized as a histogram, in the right corner the data for both the x and the y direction are plotted in scatter plot.*

before poisoning and the standard deviation found as $\sigma_{before} = (9.13 \pm 0.59)$ nm (std \pm SEM), and $\sigma_{after} = (3.32 \text{ nm} \pm 0.67)$ nm (std \pm SEM) after PMB exposure, the results are summarized in table 8.1. To investigate if the decrease seen in receptor mobility upon PMB exposure was significantly different from the motility in healthy cells a student's t-test was made. There is a significant difference between motility in healthy cells and in cells exposed to PMB ($p = 0.000034$). PMB was dissolved in buffer, the measurement was performed within minutes after PMB exposure. The decrease seen in receptor motility should therefore be caused by PMB. If the experiment had taken place over longer time, one would need to take the use of buffer instead of growth media into account.

Poison used	# data sets	$(\sigma \pm \text{SEM})/\text{nm}$
Prior to PMB	12	9.13 ± 0.59
After PMB	12	3.32 ± 0.67

Table 8.1: *The average mobility of the exact same λ -receptor before and after PMB poisoning displacement is shown in the table. The mobility was measured on 12 data sets.*

8.4.2 PMBN results

By PMBN exposure we have investigated the influence of a change in the outer membrane on the λ -receptor mobility. PMBN increases the outer membrane permeability without killing the cells. The bacteria were exposed to PMBN prior to the experiments for 30 min. The exposure of PMBN was done before heparin was flushed into the perfusion chambers. The reason for this particular procedure is that PMBN is known to bind electrostatically to the outer membrane and heparin might thus shield this binding [66]. The motility of the λ -receptor was measured on 34 data sets treated with PMBN. The distribution of positions visited by the bead-receptor complex is well fitted with a Gaussian function. To quantify the influence of PMBN on the motility of the λ -receptor the standard deviation of the position histogram was found to be $\sigma_{PMBN} = (9.53 \pm 0.41)$ nm (std \pm SEM). The motility of the receptor was measured, 18 data sets of untreated cells but else prepared in the same way; the standard deviation found $\sigma_{Control} = (9.68 \pm 0.53)$ nm (std \pm SEM). Hence the treatment of PMBN did not give rise to a change in the λ -receptor motility. PMBN has a strong electrostatic interaction with the outer membrane, and it is assumed to be firmly attached to the bacteria while performing the experiments. A small risk exists that the bacteria resumed to "normal" protein motility when the drug was not abundantly present.

8.5 Summary

The cells were exposed to the toxic antimicrobial peptide PMB. PMB increases the permeability of both the inner and outer membrane. The mobility of the exact same protein was measured before and after exposure to PMB; a significant decrease in protein mobility

upon exposure to PMB was observed. In PMB treated cells both the inner and the outer membrane gets permeable, the cell is therefore depleted of energy. The decrease seen in the receptor motility is hence in good agreement with our previous findings of a decrease in protein motility upon arsenate and azide treatment, see chapter 5.

There was seen no change in the motility of the λ -receptor upon treatment with PMBN. It is therefore likely that PMBN does not influence the motion of the receptor. PMBN was added prior to the experiments and was not present during the measurements but as its interaction is strong and electrostatic, it is assumed to be firmly attached to the membrane during the experiments. The risk exists however that the bacteria had resumed normal mobility as the drug was not abundantly present.

This supports our overall hypothesis that the λ -receptor is linked to the peptidoglycan layer. The energy dependent dynamic reconstruction of the peptidoglycan layer is needed for the motility of the λ -receptor. A treatment of the outer membrane has no effect on the motility of the receptor.

Chapter 9

Motility of the inner membrane protein, DsbB

9.1 Introduction

In the previous chapters we have studied the mobility of the outer membrane protein the λ -receptor. We have shown that the wiggling motion performed by the λ -receptor is energy dependent (chapter 5 and 8) and that this motion depends on a growing peptidoglycan layer (chapter 6 and 7). We have however not investigated the motility of inner membrane proteins, and we were wondering whether similar effects were true for inner membrane proteins. Therefore we initiated a study on the mobility of the inner membrane protein, DsbB, in *E. coli*. The work was a collaboration with Daniel Otzen and Uffe Westergaard. The plan was to introduce a biotin acceptor site in the periplasmic site of DsbB (pointing outwards of the inner membrane). We wanted to use the biotinylation system present in *E. coli* to attach biotin to DsbB. By removing the outer membrane and attaching a streptavidin coated bead to DsbB, the mobility of the protein could then be followed by optical tweezers (as in the experiments performed on the λ -receptor). A spheroplast is here used as a term for a gram negative bacterium in which the outer membrane has been removed.

The inner bacterial membrane resembles the eukaryotic lipid lipid membrane, which has been studied for decades. The diffusion in the inner bacterial membrane is however barely studied with the exception of diffusion of the inner membrane PleC which has recently been reported [38], [39], [40]. For PleC two different types of mobility were seen: a slow movement, associated with the filament form of the molecule, and free diffusion of single proteins.

Unfortunately, the experimental protocol for observing the movement of DsbB was more challenging than expected. In the following, I will briefly describe the problems that occurred. The exact experimental protocol can be found in appendix A.3.

9.2 Biology

Dsb stands for disulfide bond. Many proteins need disulfide bonds to stabilize their tertiary structure. These disulfide bonds are in *E. coli* mainly made by the protein pair DsbA and DsbB. When a protein is made in the cytoplasm it is transported into the periplasm. In the periplasm, DsbA can transfer its disulfide bond to another protein. DsbA is then left in its reduced state. To regain catalytic activity DsbA must be reoxidized. This reoxidation of DsbA is done by DsbB, see figure 9.1. DsbB is an inner membrane protein, which is predicted to span the inner membrane four times. It has two cystine pairs on the extracellular site one between Cys41 and Cys44 and one between Cys104 and Cys130. The structure of DsbB is, however, not known. For more information about the disulfide bond formation pathway in *E. coli* see [67]

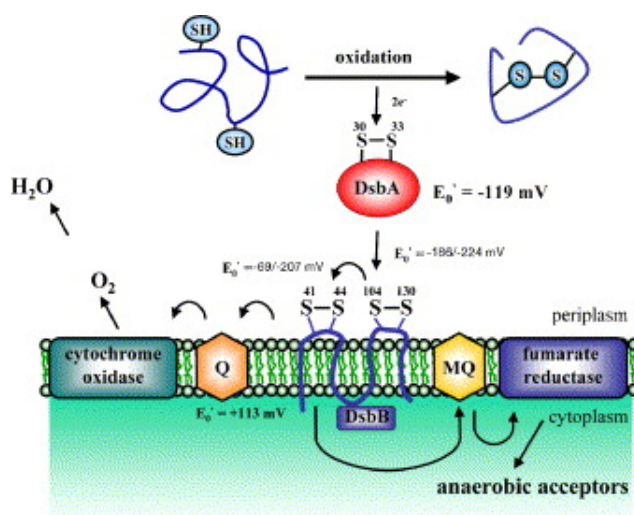


Figure 9.1: A figure of the disulfide bond formation in *E. coli* [67]. In the pictures the electrons flow is in the direction of the arrows. The disulfide bond of a protein is created by DsbA. The reduced DsbA is then reoxidized by DsbB.

9.3 Problems and current status of the project

The progress of the insertion of the biotin acceptor site in DsbB was performed by Uffe Westergaard and it was delayed due to experimental difficulties. It was not clear if there was a working *in vivo* biotinylation. However, for single molecule diffusion studies it is important to have only one receptor per bead. Though it was difficult to prove *in vivo* biotinylation it might have been sufficient for single molecule studies.

A lot of work needed to be done to insure that the biotinylation procedure had been successful and that the amount of biotinylated proteins on average was less than one per cell. This is a very time consuming step.

Working with inner membrane proteins is different than working with the λ -receptor. The number of λ -receptors in a single cell can be up to thousands without harming the cell. This is not the case for the DsbB. We induced the λ -receptor once the cells are dividing exponentially and let them grow for roughly $\frac{1}{2}$ hour with IPTG. After private correspondence with Daniel Otzen, we learned that this is not the most optimal procedure for inner protein expression. The addition of IPTG should arrest bacterial for a period of time and besides this a large number of inner membrane biotinylated DsbB's should destabilize the inner membrane. It should therefore be better to add IPTG to a late log-phase or saturated bacterial culture. So we needed to find a new protocol for growing the bacteria.

The last problem was the stability of the spheroplasts: can they be centrifuged, pipetted, perfused into the perfusion chambers without harm? Another problem concerned how to attach the spheroplasts to the surface. Can poly-L-lysine be used, to make a spheroplast stick, does it change their shape, rigidity or the phase of the lipid membrane in any way? If a uniform population of spheroplasts could be attached to the surface of a coverslip, is it then possible to wash the perfusion chamber without harming them?

To solve these problems I tried to vary several parameters to obtain a dense population of spheroplasts without aggregates in the perfusion chambers. However, I never managed to find a good protocol.

Due to the limited time and the number of problems encountered we decided to stop working on the DsbB project before obtaining any results. However, if the technical difficulties could have been solved it would have been very interesting to compare diffusion in spheroplasts to the *in vivo* experiments on the λ -receptor motility, and if possible to the motion of an inner membrane protein in metabolic competent bacteria.

Chapter 10

Ejection of the DNA of bacteriophage λ

10.1 Introduction

The vast majority of the work presented in this thesis deals with the λ -receptor, its motility, function and attachment to the membrane structure. However, a small fraction of my thesis is also devoted to the virus bacteriophage λ , which infects *E. coli* and exactly targets the λ -receptor.

This part of the work was done in the group of Professor Rob Phillips at Caltech. The *in vitro* work was primarily carried out by Paul Grayson.

Using fluorescently stained DNA we were able to follow the *in vivo* ejection process of individual phages. The phages attach to the *E. coli* bacteria. The phages were visualized using fluorescence at a frame rate of 4 frames per second. This not fast enough to detect the wiggling motion of the λ -receptor reported in the previous chapter. However, a larger diffusion of several hundred nanometers would have been detected. No mobility of the phage was observed upon attachment. This agrees well with our previous findings of the motility of the λ -receptor. Upon attachment of the bacteriophage λ to the bacteria an apparent random waiting time is seen, before the *in vivo* ejection occurred. The full ejection occurred within seconds and no pause was seen in the *in vivo* ejection process.

Recently (2005) it was shown using fluorescent microscopy that the *in vitro* ejection of bacteriophage T5 was a stepwise process[68]. We investigated individual ejections of the DNA from bacteriophage λ . Except for a pause at the end of the ejection, the whole DNA is ejected without pauses. The ejection occurs as fast as 1.5 s, giving a speed of 60 kbp/s. The effect of the DNA length on ejection speed has been investigated using different λ phages containing the shortest and the longest DNA sequences that is still infectious. Here, a shorter piece of DNA gives a slower ejection speed with a shorter total ejection time. The pressure of the DNA within the capsid also effects the ejection time. The effect of different pressure within the phage capsid has been investigated using either divalent (magnesium) or monovalent (sodium) ions.

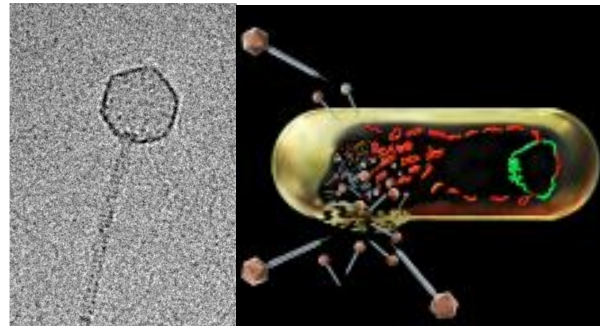


Figure 10.1: To the left is shown an electron microscope picture of the bacteriophage λ (the image is taken from [69]). To the right is an illustration of the phage cycle of bacteriophage λ (the image was taken from [70]). The phage DNA (red) is either copied and inserted into new phage capsids lysing the bacteria (bursting the bacteria), or the phage DNA is inserted into the bacterial genome (green).

10.2 Biology

The bacterial virus bacteriophage λ was first found in 1959 in a study on the effect of UV-light on bacteria. The infection of bacteriophage λ can take two different paths: either the phages insert its DNA into the bacterial DNA, or the phage produces progeny. If the phage is replicated, the bacterium finally bursts and is hence killed. The phage can live silently within the bacterium until the bacterium gets stressed, as in the case of UV exposure, upon which the phage switches to replication. Both phage cycles are illustrated in figure 10.1 right.

The bacteriophage λ has a some resemblance to the Greek letter when visualized in an electron microscope as seen in figure 10.1 left. It consists of a long cylindrical tail and a round protein capsid. The capsid is 30 nm in diameter and it is hence smaller than the persistence length of DNA. Within the capsid, the phage carries a 48.6×10^3 bp tightly packed DNA. The DNA sequence is much longer (roughly 400 times) than the diameter of the capsid. The reason for this very tightly packing of DNA might be found in the function of the phage. The bacteriophage λ s bind to the outer membrane protein, the λ -receptor, of *E. coli*. The binding to the λ -receptor creates a conformational change in the tail of the phage, opening the tail so that the DNA is ejected into the bacterium, through the λ -receptor. The ejection of bacteriophage λ is suppressed in the presence of a large external pressure (≈ 20 atm) [71].

10.3 Experimental procedures for *in vitro* investigations

The *in vitro* ejection experiments were performed in the following way. The purified phages (A.3.1) were visualized at the microscope in a perfusion chamber. The perfusion chamber was made in the following way:

- Two holes were drilled in a cover glass
- Tygon tubing (inner diameter of 0.02) was attached in the holes by epoxy.
- A 5 mm wide, 120 μ thick channel was constructed from an adhesive sheet (Grace Biolabs). The channel was made by laser cutting (Popolu Corporation)
- A coverslip was cleaned by heating to 95 °C in 0.5 %alconox detergent for 30-60 min. Rinsed twice in water and dried in an air stream.
- The chambers were assembled and heated on a hot plate for several seconds.

The preparation of the phages was done over water bath in the following way:

- To remove premature released DNA from the phages solution, a phage solution of 10^{10} pfu/ml (pfu = plaque forming units) were incubated with 4 μ g/ml DNase I at 37 °C for 15 min
- 0.1 μ m fluorescent beads were added to the phages to a dilution of $\approx 10^7$. The fluorescent bead were added to help focussing at the surface at the microscope.
- The solution was left for at least 15 min at room temperature to adhere to the surface.

The prepared samples were taken to the microscope. The tubing of the fluidity chamber was in one end connected to a syringe pump and the other to a reservoir. The syringe allowed controlled flow through the chamber. The flow was used for stretching the DNA. A sample was mounted at the microscope and the the microscope was focussed at the bottom of the coverslip using the fluorescent beads. The sample was then rinsed in the following way:

- To remove unbound particles the sample was rinsed with 800 μ l Mg or Na buffer.
- The dye solution was now flushed in; 40 μ l of the same buffer as in the previous step containing 1 % oPOE, 10^{-5} dilution of SYBR gold. To prevent photodamage the following oxygen reducing mixture was added: 1 % gloxy A.3.1, 0.4 % glucose and 1% 2-mercaptoethanol.
- The last step was to flush in solution as above but with 2.5 ug/ml LamB added. Adding LamB makes the bacteriophage ejects its DNA. No ejections are seen prior to adding LamB.

- The ejection was observed on a inverted Nikon microscope using a 100×1.4 NA oil immersion objective. The samples were illuminated with a 100-W mercury lamp. Images were acquired with a Photometric Coolsnap FX camera at a frame rate of 4 frames per second.

10.4 *In vitro* results

To reduce photodamage, the phages were during the experiments kept in an oxygen reducing environment, which enabled a frame rate of 4 frames per second. The ejection speed of two different λ phages have been measured. One with a genome length of 38 kbp (λ b221), the shortest possible DNA length of the phage, and one with 48.5 kbp (λ cI60), the longest possible DNA length of the phage. The dependence of divalent ion concentration on the ejection speed was investigated by comparing the ejection speed of the phages kept in a buffer containing 10 mM either Mg^{2+} or Na^+ . There are 81 ejection events measured. The ejection is fastest in the beginning and slows down towards the end of ejection, as seen in figure 10.2.

Once the DNA was fully extended it spent an apparent random amount of time before the final release. This waiting time before final release was often longer than the destruction time by photodamage. The reason for this long waiting time before the final release could be because of the 12 bp overhang of the phage DNA.

Prior to ejection a waiting time was seen, which appeared random. This effect was also seen in the *in vivo* measurements.

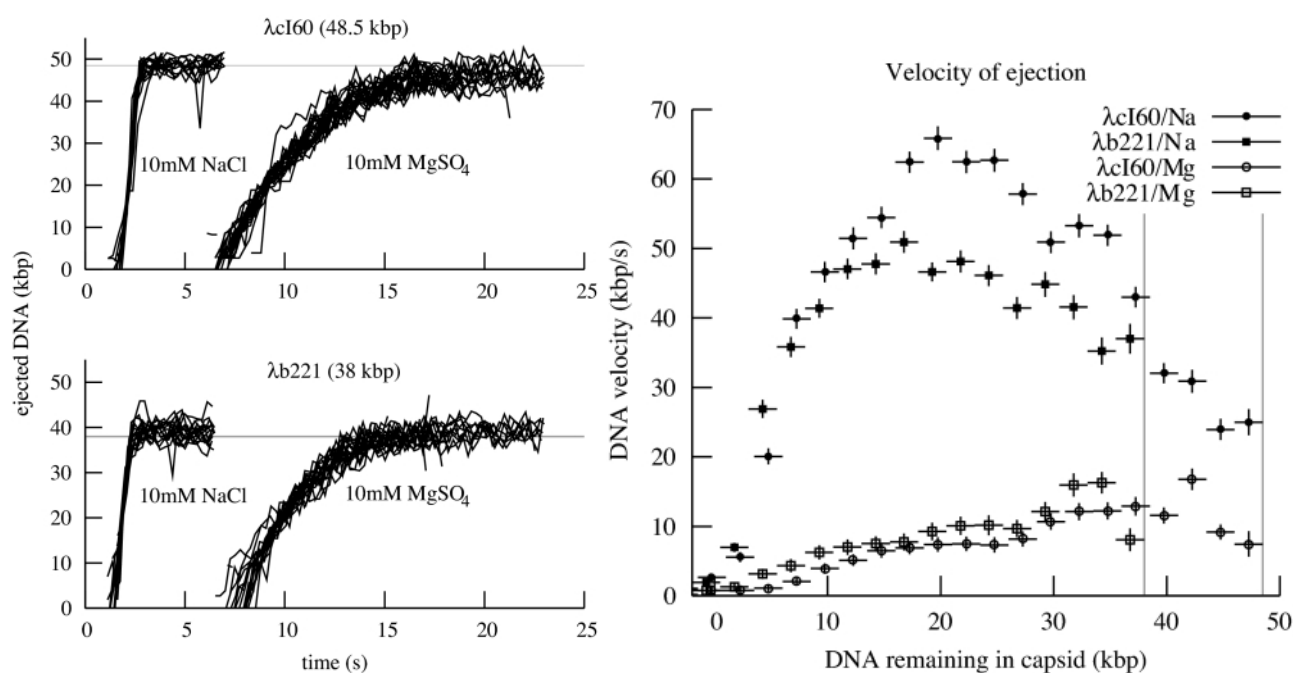


Figure 10.2: To the left is shown the graph of individual ejection trajectories of $\lambda cI60$ and $\lambda b221$ as function of time and the amount of divalent ions. The ejection trajectories are shown for ejection occurring in 10 mM either NaCl or $MgSO_4$. To the right is seen the velocity of the ejection events as function of the DNA remaining within in the capsid. The ejection velocity is shown for $\lambda cI60$ and $\lambda b221$ and for 10 mM either NaCl or $MgSO_4$. The gray lines in the image illustrate the full DNA length of $\lambda b221$ and $\lambda cI60$ [72].

10.5 *In vivo* results

The *in vivo* ejection of individual phages have been investigated using fluorescence. By fluorescently staining the DNA of bacteriophage λ we were able to follow the *in vivo* ejection process of individual phages. The DNA was stained with SYBR gold.

The first step that needed to be answered was if phages stained with SYBR gold were still able to infect bacteria. A dilution of bacteria poured onto an agar plate forms a bacterial lawn. Adding a dilute solution of phages to the bacteria, immediately before spreading the bacteria on a agar plate, visualizes individual phage infection as "holes" (plaques) in the lawn. How well a solution of phages infects bacteria is measured as the number of plaque forming units per ml (pfu/ml). The number of infections of SYBR gold stained phages was compared to the number of infections of not stained phages. SYBR gold staining did not influence the number of infection of the bacteriophage.

Phages stained with SYBR were visualized in the microscope by fluorescent illumination. A picture of phages attached to a bacteria is shown in arbitrary colours in figure 10.4, here the phages are shown in green and the bacteria appear black while the background

is red. The *in vivo* ejection of single phages was followed as a decrease in the relative fluorescent intensity signal 10.3. Two individual ejection events are shown in figure 10.4. The decrease in signal intensity is much more abrupt than by photobleaching.

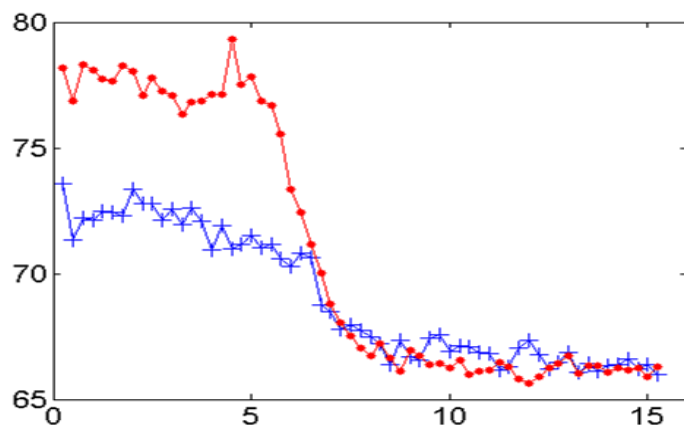


Figure 10.3: The graph shows the relative intensity of the DNA within two individual phages as function of time. The y-axis is the relative intensity and the x-axis is the time in seconds.

A random waiting time is seen prior to ejection, similar to the one reported for the *in vitro* experiments. The reason for this waiting time is not known. No long term motion of the attached λ phages was detected (with a frame rate of 4 pictures per second, possible fast movement was not recorded). This finding is in accordance with the results presented in this thesis (chapter 5, 6, 7, and 8) on the λ -receptor motility. The *in vivo* ejection appeared to be completed within seconds. It is possible that the wiggling motion of the receptor helps the final release of the phage DNA from the capsid.

By staining both capsid and DNA of the phages simultaneously we investigated if stained DNA was only seen in the presence of a capsid. This way we checked that we did not have stained artifacts. The protein of the capsid of the phage is stained by NHS-Rhodamine, shown in red and the DNA is stained with SYBR gold, shown in green, see figure 10.5. The images were taken at the same place in the setup but with different filter cubes. It is possible to stain both capsid and DNA simultaneously. No DNA was seen without a capsid. However empty capsids were seen. Hence we do not suffer from artificial staining.

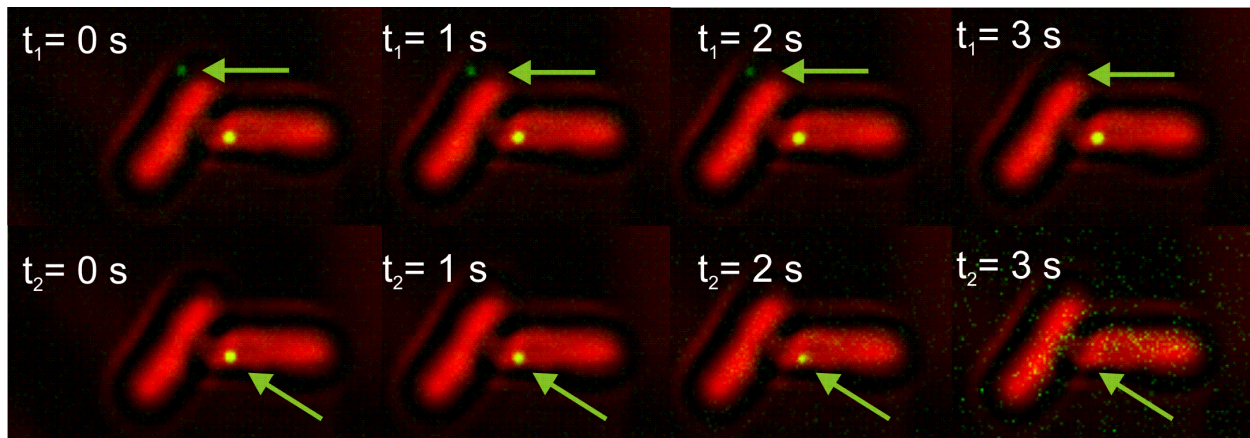


Figure 10.4: This is a picture series of two individual λ phage (shown in greenish) ejections in two *E. coli* cells.

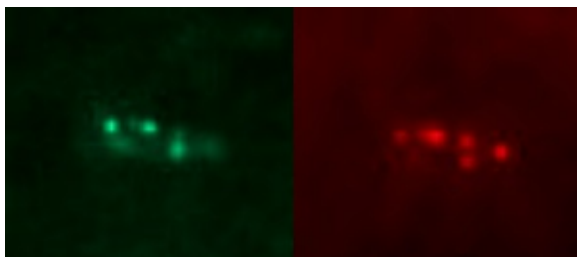


Figure 10.5: The picture shows the capsid of bacteriophage λ in red. And the DNA of bacteriophage λ is shown in green. The phages are attached to a hardly visible bacterium. The colours are arbitrary.

10.6 Summary

The ejection of individual λ phages was followed *in vitro*. Investigating the ejection speed in either magnesium or sodium buffer, showed that the ejection speed depends on the pressure within the capsid. The ejection speed occurred much faster in the sodium buffer, which gives the highest pressure within the capsid. In the sodium buffer the whole genome length was injected within ≈ 1.5 s, giving an ejection speed of 60 kbp/s. In the magnesium buffer the ejection speed was 8-11 s. The DNA length of the phage also played an important role for the ejection speed. This was investigated using two different phages with the shortest and the longest possible DNA length. The ejection speed of the phage with respectively the short DNA is slower, however the total time of ejection is shorter. After the DNA had ejected the full length of DNA an apparent random waiting time was seen before the release of the DNA. It is possible that this waiting time is created by the 12 bp overhang at the end of the DNA sequence. Prior to ejection there also seemed to be an apparent

random waiting time.

We also succeeded in following the ejection process of individual phages *in vivo*. The ejection time was fast, within seconds. *In vivo* there was seen no pause before the final release of the DNA. It is possible that the wiggling motion of the λ -receptor as measured in this thesis (chapter 5, 6, 7, and 8) helps the final release of the phage DNA *in vivo*. No long term motility was seen of individual phages attached to bacteria. Phages attached to bacteria had an apparent random waiting time before ejection. We do not know the reason for this waiting.

Chapter 11

Discussion and conclusion

In this phd thesis I have investigated the *in vivo* motility of the λ -receptor under the influence of energy depletion, antibiotics and antimicrobial peptides.

Using the *in vivo* biotinylation system of *E. coli* ensures a low number of biotinylated λ -receptors in the outer membrane, on average less than one per cell [5]. The biotinylation of the λ -receptors was used to attach either streptavidin coated polystyrene beads of roughly $0.5 \mu\text{m}$ in size or streptavidin coated quantum dots with a diameter of 15 nm. This way the motility of the bead-receptor complex was followed by the optical tweezers. The receptor performed an area confined diffusional "wiggling" motion.

We investigated if the "wiggling" motion of the λ -receptor is energy dependent or purely thermal. This was studied by poisoning the cells with arsenate and azide which block the energy metabolism of the cell. The motility of the exact same λ -receptor was measured *in vivo* before and after energy depletion. Upon energy depletion, a significant decrease was seen in the width of the distribution of positions visited by the receptor. The response was fast, within minutes and of constant magnitude. The timescale is so fast that it excluded an explanation including transcription of regulatory protein. There is hence a difference in the membrane protein movement between physiologically healthy cells and bacteria without functioning metabolism. Theoretical predictions have previously shown a correlation between protein motility and the energetic state of the membrane, e.g. [3], [73], but to our knowledge this connection has not been established experimentally before. The movement of the λ -receptor depends on energy; one possible reason for this active motion could be that it assists the transport of maltose through the pore. The observation of energy dependence on protein diffusion is important for interpretation of diffusion constants, especially while comparing results obtained from living organisms to artificial membranes.

The biological mechanism of this motion was investigated by poisoning the cells with the common antibiotic ampicillin. Ampicillin hinders the crosslinking of peptide bonds in the peptidoglycan layer, hence inhibiting the dynamic remodelling of the peptidoglycan layer. The motion of single proteins in the outer membrane was then measured in the presence and absence of ampicillin. The movement of the receptor decreased significantly upon ampicillin treatment. The decrease in receptor motility upon ampicillin treatment is in agreement with previous findings where it was shown that the λ -receptor was attached

firmly enough to withstand SDS treatment [1]. The receptor motility was also measured in cells that had time to revive after ampicillin treatment where protein motility was restored. The restoring of the λ -receptor motility in cells where ampicillin had been removed suggests that the motility is closely connected to the dynamic re-construction of the peptidoglycan layer.

Single molecule experiments can be used to study effects hidden in ensemble measurements. We have followed the evolution in time of vancomycin exposure on the λ -receptor motility. Vancomycin is another antibiotic interacting with the peptidoglycan synthesis. The λ -receptor motility decreased within minutes after vancomycin treatment; the motility however decreased further after 30 minutes treatment. This could give detailed information of the working mechanism of vancomycin, whether the first part of the binding is to intermediates of the peptidoglycan synthesis [74]. The first reaction of vancomycin might cause structural changes, whereas longer effects of vancomycin is hindering the peptidoglycan synthesis.

Vancomycin is a large molecule which cannot diffuse across the outer membrane and therefore a bacterial strain with increased membrane permeability was used. The motility of the λ -receptor in strains with increased membrane permeability did not differ from the motility of the receptor in strains without this genetic change.

The influence of the toxic antimicrobial peptide polymyxin B (PMB) was investigated. PMB increases the permeability of both inner and outer membrane; this destroys the electrostatic gradient across the inner membrane leading to cell death. The motility of the exact same λ -receptor was measured before and after PMB exposure. The λ -receptor motility decreased significantly after PMB exposure, the response was fast within minutes.

The effect of PMB exposure, energy depletion, ampicillin or vancomycin treatment decreases the motility of the λ -receptor. This observation supports our hypothesis that the motility of the λ -receptor is mediated through a firm connection to the peptidoglycan layer. The dynamic remodelling of the peptidoglycan layer seems to give rise to the observed motility of the λ -receptor. Crystallographically it has been shown that the λ -receptor has a so-called "greasy slide" consisting of 6 contingent aromatic residues; maltose is bound here during its guided transport into the cell [17], [75]. It is therefore possible that the cell facilitates the active movement of the λ -receptor to assist the guided diffusion of maltodextrins into the cell. Structural changes in the outer membrane do not seem to influence the receptor motility.

We have shown that the motility of the outer membrane protein the λ -receptor depends on energy metabolism. The motility of the receptor displayed a confined diffusional motion, with a typical area of 50 nm, using either 15 nm quantum dots or 0.5 μm polystyrene beads. We stopped the energy metabolism of the cells by poisoning the cells with arsenate and azide, and showed that this had a rapid and significant effect on the receptor motility. The biological basis of the motility was further elucidated by ampicillin treatment. Ampicillin targets the peptidoglycan layer hindering the transpeptidase action. Ampicillin treatment effectively stopped the motility of the λ -receptor, but this process was observed to be reversible. The treatment with vancomycin showed a significant decrease in the λ -receptor motility. This effect was seen both at 22 °C and 37 °C. We were

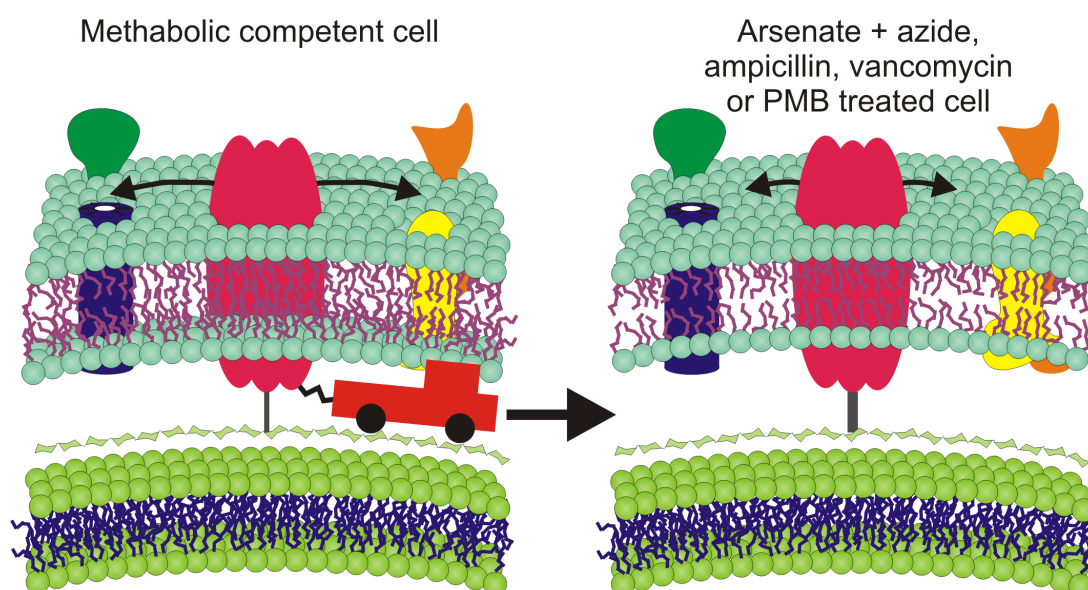


Figure 11.1: *The left side illustrates the motility of the λ -receptor in a metabolic competent cell, illustrated by a pickup truck dragging the protein. Upon treatment with either arsenate plus azide, ampicillin, vancomycin or PMB the movement of the receptor decreases to a minimum, shown as a stronger attachment to the peptidoglycan layer, illustrating that the remodelling of the peptidoglycan layer is hindered.*

able to follow the development in time of vancomycin exposure on the motility of individual λ -receptors. The receptor motility decreased rapidly upon vancomycin exposure, but a further decrease was seen after 30 min. Exposure to the toxic antimicrobial peptide PMB decreases the λ -receptor motility. This all support our hypothesis that the motility of the λ -receptor is directly linked to the reconstruction of the peptidoglycan layer. This is illustrated in 11.1 where the motility of the metabolic active cell is shown as by a pickup truck dragging the λ -receptor. Upon treatment with either arsenate plus azide, ampicillin vancomycin or PMB the movement of the receptor decreases to a minimum shown, as a stronger attachment to the peptidoglycan layer, illustrating that the remodelling of the peptidoglycan layer is hindered.

In summary, we have shown that the motility of the λ -receptor in *E. coli*: Depends on energy, and on a growing peptidoglycan layer.

11.1 Outlook

Since we have shown that a growing peptidoglycan layer is necessary for the motility of the λ -receptor, it would be interesting to study the influence of cell division and cell growth on the λ -receptor. This could be done using a stage sample heater maintaining the samples at 37°C. During the whole experiment, the λ -receptor movement could be recorded for single

particle tracking and optical tweezers measurements.

Another exciting control experiment would be to compare the movement of a mutant λ -receptor, which is not attached to the peptidoglycan layer, to the results obtained with ampicillin. How much would such a receptor diffuse in the outer membrane? Or similar to insert the λ -receptor into an artificial membrane or a bacteria without the peptidoglycan layer. However, it could also be very interesting to study the motility of another outer membrane protein, known *not* to be attached to the peptidoglycan layer. Would a *not* anchored protein "wobble", would it be influenced by energy depletion or would it diffuse freely?

In previous studies of the λ -receptor movement, pauses were seen in the motion of the λ -receptor. The pauses were normally short, which ultimately might be due to changes in the energy level inside the cells. It would be interesting to study this effect by single particle tracking, in which the movement of the λ -receptor is tracked over a longer period of time.

Appendix A

Appendix

A.1 Biological dictionary

Bacteriophage (or phage): is a bacterial virus. Some of these can incorporate themselves into the genome, while others can only multiply themselves and kill the bacteria.

pfu: plaque forming unit, a number of the density of the plaque forming phages in the solution. See also plaque.

Phage: see Bacteriophage.

Plaque: Is the hole made by a bacteriophage in a bacteria lawn. On a petri dish covered with a thin layer of bacteria a plaque looks like a clear round spot in the bacteria surface. If your density of phages are not too high, each plaque will correspond to one phage in the original solution.

A.2 Stock solutions Media

20% w/V Glucose:

20 g glucose

Add millipore water to 100 ml

filter sterilize the solution.

20% w/V arabinose:

20 g arabinose

Add millipore water to 100 ml

filter sterilize the solution.

20 mM FeSO₄, 20 mM Na-Citrate, autoclave and store in refrigerator in dark bottle.

1 mg/ml Thiamine, autoclave and store in refrigerator

1 M MgSO₄, autoclave

5 × M63: dissolve and bring to a volume of 1 l with millipore water

15g anhydrous KH₂PO₄

35g anhydrous K₂HPO₄

10g (NH₄)₂SO₄

2.5 ml 20 mM FeSO₄, 20 mM Na-Citrate

autoclave the solution.

A.2.1 Frozen stocks

50% w/V Glycerol:

30 g glycerol

Add millipore water up to 60 ml.

autoclave the solution.

To make a frozen stock:

Sterile transfer 1 ml of saturated bacterial culture to a Nunc tube.

Add 0.8 ml 50 % w/V Glycerol.

Vortex the solution.

Freeze immediately at -80 °C.

A.2.2 Vancomycin P1 transduction

MacConkey Agar base plate:

Fill 500 ml millipore water in a large bottle

Add 20 g MacConkey powder.

autoclave the solution.

Pour onto plates.

H-top:

Take 100 ml millipore water

Add:

1 g tryptone

0.6 g agar

0.8 g NaCl₂

Sloppy H-top:

Take 100 ml millipore water

Add:

1 g tryptone

0.3 g agar

0.8 g NaCl₂

YT-broth:

Fill 500 ml millipore water in a large bottle

Add:

2.5 g NaCl₂ 4 g tryptone

2.5 g yeast extract

autoclave the solution.

YT-Plates:

Fill 1l millipore water in a large bottle

Add:

5 g NaCl₂

8 g tryptone

5 g yeast extract

12 g agar

autoclave the solution.

Pour onto plates.

M63 glu plates:

autoclave separately

800 ml millipore water + 15 mg agar

200 ml 5 × M63

after autoclaving, 1) immediately mix water-agar to fully distribute the agar 2) let water-agar cool to 60 °C 3) add to the following to the water-agar solution and mix:

1 ml 1 mg/ml Thiamine

1ml 1M 1 M MgSO₄

10 ml 20 % w/V glucose

M63 ara plates:

autoclave separately

800 ml millipore water + 15 mg agar

200 ml 5 × M63

after autoclaving, 1) immediately mix water-agar to fully distribute the agar 2) let water-agar cool to 60 °C 3) add to the following to the water-agar solution and mix:

1 ml 1 mg/ml Thiamine

1ml 1M 1 M MgSO₄

10 ml 20 % w/V arabinose

M63 $\frac{1}{2}$ -ara plates:

autoclave separately

800 ml millipore water + 15 mg agar

200 ml 5 × M63

after autoclaving, 1) immediately mix water-agar to fully distribute the agar 2) let water-agar cool to 60 °C 3) add to the following to the water-agar solution and mix:

1 ml 1 mg/ml Thiamine
1ml 1M 1 M MgSO₄
5 ml 20 % w/V arabinose

1 M Na-citrate:

Fill roughly 50 ml milliporre water into a autoclave bottle.
Add 29.4 g Na-Citrate.
Add water until 100 ml.
autoclave the solution.

1 M CaCl₂:

Fill roughly 50 ml milliporre water into a autoclave bottle.
Add 14.7 g CaCl₂.
Add water until 100 ml.
autoclave the solution.

Transduction salts:

Fill roughly 50 ml milliporre water into a autoclave bottle.
Add 0.294 g CaCl₂ to give a final concentration of 20 mM.
Add 2 ml 1M MgCl₂ to give a final concentration of 10 mM.
Add water until 100 ml.
autoclave the solution.

A.2.3 Arsenate and azide experiments

MOPS-media:

To 88 ml of autoclaved milliporre water add 10 ml 10 × MOPS (the recipe can be found in [76]), 1 ml 20% glycerol (or glucose), 0.5 ml 20% CAA (casein amino acids) 0.1 ml 1mg/ml B1 MIX, 0.1 CAM 25 mg/ml, and 1 ml 0.132 M K₂HPO₄. The solution is filter-sterilized into sterile containers.

MOPS-phosphate free:

To 45 ml of autoclaved milliporre water add 5 ml 10 × MOPS (the recipe can be found in [76], without ammonia), 0.5 ml 20% glucose, and 0.05 CAM 25 mg/ml. The solution is filter-sterilized into sterile containers.

arsenate and azide poison Mix 970 μl MOPS-phosphate free add 20 μl 64 mg/ml azide, and 10 μl 18 mg/ml arsenate.

A.2.4 DsbB experiments

The commercial available strain of *E. coli* BL21 gold was used. The vector with DsbB was then inserted. The vector with "normal" DsbB gene is termed WM76. The vector with

DsbB with a biotinylation sequence (GLNDIFEAQKIEWH) inserted after Cys44 and it is termed C44btn. For further information please contact professor Daniel Otzen at Århus University.

LB-Media:

In 475 ml of H₂O add:

5 g Bacto-Tryptone

2.5 g Yest extract

5 g NaCl

Mix until the salts are dissolved.

Adjust the pH to 7.0 by adding 5 N NaOH (~ 0.2 ml)

Adjust volume to 500 ml with H₂O.

Sterilize by autoclaving and store at room temperature.

Stock solutions:

1 M Tris-HCl, pH=8

5 M NaCl

0.5 M EDTA filtersteril

Buffers:

Tris/sucrose:

500 μ l 1M Tris-HCl, pH=8

12.8 g sucrose

Dissolved in 50 ml to a final concentration of 10 mM Tris-HCl, 0.75 M sucrose.

EDTA/Tris:

150 μ l 0.5 M EDTA

500 μ l 1M Tris-HCl, pH=8

Dissolved in 50 ml to a final concentration of 1.5 mM EDTA, 10 mM Tris-HCl.

Wash buffer:

4.27 g sucrose 1.5 ml 5 M NaCl 500 μ l 1M Tris-HCl, pH=8

Dissolved in 50 ml to a final concentration of 0.25 M sucrose, 150 mM NaCl, and 10 mM Tris-HCl.

A.3 DsbB experimental procedures

All media and a description of the strains can be found in appendix A.2.4

In this experiment I simply tried to make spheroplasts.

0.1 ml overnight culture of BL21 gold with vector WM76 was transferred to 3 ml of

LB media. It was grown in here for 1 hour. Additional 3 ml of LB -media supplemented with 2 mM IPTG was added (this gives a final concentration of 1 mM IPTG), the bacteria were grown for an additional hour. 2 ml bacteria culture was spun down at 5000 rpm for 5 min and resuspended in 500 μ l wash buffer. The bacteria were spun down again and resuspended in 500 μ l Tris/sucrose. 25 μ l (2 mg/ml) lysozyme was added. Then 1000 μ l EDTA/Tris is added gently down the side of the eppendorf tube. The bacteria were left on ice for 25 min. The bacteria were visualized in the microscope, see figure A.1

There were few spheroplasts, see figure A.1. Perhaps some of the spheroplasts were ruptured. I decided to give them shorter time with the lysozyme in the following experiments.



Figure A.1: *This is a picture of the few spheroplasts obtained.*

As I had very few bacteria in the last experiment, I used a smaller amount of lysozyme to investigate the effect of this. The bacteria were further more visualized at different times after lysozyme exposure.

0.1 ml overnight culture of BL21 gold with vector C44-btn was transferred to 3 ml of LB media. It was grown in here for 1 hour. Additional 3 ml of LB -media supplemented with 2 mM IPTG was added (this gives a final concentration of 1 mM IPTG), the bacteria were grown for an additional hour. 3 ml bacteria culture was spun down at 5000 rpm for 5 min and resuspended in 500 μ l wash buffer. The bacteria were spun down again and resuspended in 250 μ l Tris/sucrose. 12.5 μ l (2 mg/ml) lysozyme was added. Then 500 μ l EDTA/Tris was added gently down the side of the eppendorf tube. The bacteria solution was put on ice until use. Images were taken of the bacteria without lysozyme, after 20 min of lysozyme exposure, and after 34 min of lysozyme exposure, this picture was taken after the solution in the chamber had been exchanged with Tris/sucrose buffer.

There was here indications of spheroplasts, but only in limited number see figure A.2.

Since the previous experiments I had learned that the amount of expression of DsbB influences the stability of the spheroplasts. I therefore tried to lower the concentration of IPTG, since I did not know how it influences the spheroplasts to be pipetted or flushed into a perfusion chamber. I investigated if it would be more gently to flush lysozyme exposed bacteria into the perfusion chambers right after exposure. The lysozymes were

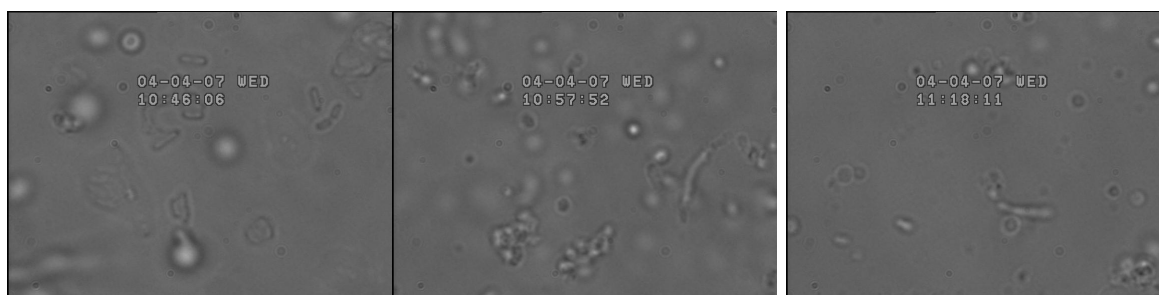


Figure A.2: *To the left a picture of the bacteria. In the middle a picture after 20 min of lysozyme treatment. To the right a picture after 34 minutes of lysozyme treatment, but after the solution was exchanged with a Tris/sucrose buffer.*

removed this time before visualization. I also tried to flush in beads this time.

0.1 ml overnight culture of BL21 gold with vector C44-btn was transferred to 3 ml of LB media. It was grown in here for 0.5 hour. Additional 3 ml of LB -media supplemented with 1 mM IPTG was added (this gives a final concentration of 0.5 mM IPTG), the bacteria were grown for 0.5 hour. 4 times, 1 ml bacteria culture was spun down at 5000 rpm for 5 min and resuspended in 500 μ l wash buffer. The bacteria were spun down again and resuspended in 250 μ l Tris/sucrose. 12.5 μ l (2 mg/ml) lysozyme was added. Then 500 μ l EDTA/Tris was added gently down the site of the eppendorf tube. I stirred very gently with the tip of a pipette. A line of poly-l-lysine was drawn on a clean coverslip and it was left to dry. Two pieces of double sticky tape was placed with spacing of a couple of millimeters. Another coverslip was placed on top as a lid. The bacteria with lysozyme were perfused into the chambers and left on ice for 20 min. The chambers were flushed with 60 μ l of Tris-sucrose solution. An image was taken. 25 μ l beads plus 975 μ l water was spun down at 5000 rpm for 5 min and resuspended in 150 μ l Tris-sucrose buffer. Beads were flushed into the chambers and left 15 min to adhere. The chambers were then flushed with 60 μ l Tris-sucrose buffer. I observed the chambers.

I could not detect any mobility of any beads. It was very hard to distinguish deformed spheroplast from beads. There was a lot of deformed aggregates, see figure A.3.

Then lysozyme again was removed before visualization but I also added sucrose in the final media in the same concentration as used in the buffers to try and stabilize the spheroplasts.

0.1 ml overnight culture of BL21 gold with vector C44-btn was transferred to 3 ml of LB media. It was grown in here for 45 min. Additional 3 ml of LB -media supplemented with 1 mM IPTG was added (this gives a final concentration of 0.5 mM IPTG), the bacteria were grown for 0.5 hour. 1 ml bacteria culture was spun down at 4000 rpm for 4 min and resuspended in 500 μ l wash buffer. The bacteria were spun down again and resuspended in 250 μ l Tris/sucrose. 12.5 μ l (2 mg/ml) lysozyme was added. Then 500 μ l EDTA/Tris was

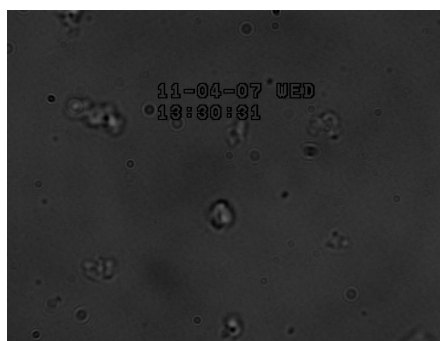


Figure A.3: *This is a picture of the few spheroplasts that I had.*

added gently down the site of the eppendorf tube. I stirred very gently with the tip of a pipette. The eppendorf tube was turned gently upside down once. The bacteria were put on ice for 20 min. A line of poly-l-lysine was drawn on a clean coverslip and it was left to dry. Two pieces of double sticky tape was placed with spacing of a couple of millimeters. Another coverslip was placed on top as a lid. 100 μ l bacteria were flushed into the chamber. The chamber was then washed with 50 μ l LB + 8.5% sucrose. The chamber was then left for 20 min to let the cells adhere.

The result was that I had too many aggregates and too few spheroplast, see figure A.4.

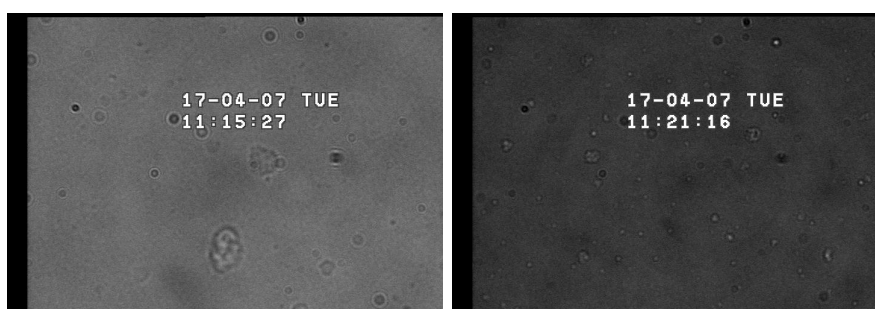


Figure A.4: *To the left is a picture of a small area with the spheroplasts that were obtained. To the right is a picture of a larger area of the spheroplasts obtained that day*

Then I investigated the effect of a larger spacing between the two coverslips leading to a larger perfusion chamber. The hope was that this would decrease the amounts of aggregates.

0.1 ml overnight culture of BL21 gold with vector C44-btn was transferred to 3 ml of LB media. It was grown in here for 0.5 hour. 1 ml bacteria culture was spun down at 4000 rpm for 4 min and resuspended in 500 μ l wash buffer. The bacteria were spun down again and resuspended in 250 μ l Tris/sucrose. 12.5 μ l (2 mg/ml) lysozyme was added. Then 500 μ l EDTA/Tris was added gently down the site of the eppendorf tube. I stirred very

gently with the tip of a pipette. The cells were left at ice for 20 min. **Four** pieces of double sticky tape were placed with spacing of 5-6 millimeters. Another coverslip was placed on top as a lid. Poly-l-lysine was flushed in and left for 15 min. The chambers were flushed with washbuffer. The spheroplast were flushed in and left for 20 min.

There were still a lot of aggregates and dust, see figure A.5.

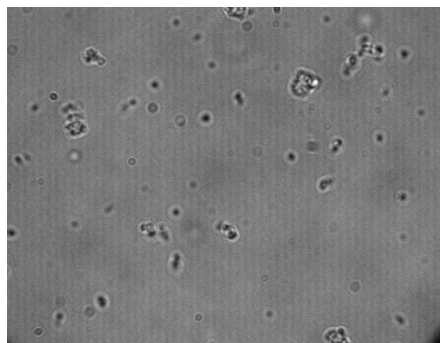


Figure A.5: *This is a picture of the few spheroplasts obtained.*

A.3.1 Phage ejection experiments

gloxy: 17 mg glucose oxidase (Sigma G2133-10KU) and 60 μ l catalase (Roche 10681325), in 140 μ l Mg buffer.

In vitro ejection experiments

Na buffer: 10 mM Tris, 10 mM NaCl, pH=7.8.

Mg buffer: 10 mM Tris, 10 mM MgSO₄, pH=7.8.

TM buffer: 50 mM Tris, 10 mM MgSO₄, pH=7.4.

Preparation of a crude Lambda lysate

Media: Large Tryptone plates: 10 g tryptone 5 g NaCl 2.5 g MgSO₄ (which corresponds to a final concentration of roughly 10 mM) 20 mg FeSO₄ (which corresponds to a final concentration of roughly 4 μ M) 13 mg CaCl₂ (which corresponds to a final concentration of roughly 75 μ M) 20 g agar Fill water to 1 l. Autoclave. Add 2 mg thiamine. Let cool down and pour 15 cm plates half full (one liter should give around 10-14 plates).

Soft LB-agar (LB-top): To one liter of water. Add 10 g tryptone 5 g NaCl 2.5 g MgSO₄ 7H₂O (which corresponds to a final concentration of roughly 10 mM) 10 g agar (7 g of agar works as well). Autoclave.

10 times TM buffer: 60.6 g Tris 24.6 g MgSO₄ 7H₂O Add 900 ml water and adjust pH to between 7.4-7.6 with HCl. Fill to one liter.

TM cleaning buffer: 50 ml TM 10 times. 1 mg DNaseI (2 mg/l). Does not have to be that accurate just add enough. 2.5 mg lysozyme (5 mg/l). Does not have to be that accurate just add enough.

Day one: Grow 1 ml of overnight culture in LB.

Day two: Melt the soft LB-agar in microwave and keep molten in water bath at 42-46 degrees until use. Dilute 20 μ l off the overnight culture into 5 ml of fresh LB. Let grow in shaker at 37 degree for 2 hours, until it gets just visible cloudy. Mix 5 times 10^4 phages with 1 ml of bacteria. Let the phage bind to the bacteria for 30 min at room temperature. Add 10 ml of soft LB-agar. Wait 6-10 hours. Put 500 μ l CHCl₃ (chloroform) on top of the plates and pour on 20 ml TM cleaning buffer. Let it sit for 2 hours for room temperature. Pipette the buffer out. Spin down 5000 times g for 10 minutes. Save supernatant. Titer the phages diluting and counting plaques.

Purification of LamB

The strains used are *E. coli* pop154, these strains express the *lamB* gene from *S. sonnei*.

Start an overnight culture of bacteria in 5 ml LB+0.2% maltose (Remember that all sugars, except glycerol has to be filter sterilized and not autoclaved).

Put this overnight culture into 2L of LB+0.2% maltose and grow it overnight.

Take the 2L of overnight culture and spin it down for 30 min at 5000 rpm (5,500 G) at 4 °C. Keep pellet, discard supernatant.

For each gram of pellet add 10 ml of breaking buffer (8 times 40 ml is properly suitable). The pellet is resuspended in the liquid by vortexing.

Put the solution through the French press twice; this breaks the membranes.

Prespin: Spin down the solution at $2500 \times g$ (a higher g force may be used here but Falcon tubes can not take more) for 10 minutes. This spin is done to remove broken membranes.

Ultracentrifuge spin: The supernatant is then moved into ultra centrifuge tubes (remember that they should at least be half full and extremely well balanced $\pm 0.02g$) and spun down for 40 min at 30000 rpm (in a Ti60 rotor).

Homogenizing: 20 ml 20 mM Na-phosphate buffer is added to each tube of pellet and it is scraped out of the tubes and into a homogenizer. Use the homogenizer until the pellet is fully resuspended (this takes 3-4 times).

Add oPOE so that the final concentration becomes 0.3% v/v. Incubate the solution for 50

minutes at 40 °C

Repeat the following three steps: Prespin, Ultracentrifuge spin, and Homogenizing.

Add oPOE so that the final concentration becomes 0.5% v/v. Incubate the solution for 50 minutes at 40 °C

Repeat the following three steps: Prespin, Ultracentrifuge spin, and Homogenizing.

Add oPOE so that the final concentration becomes 3% v/v. Incubate the solution for 40-60 minutes at 37 °C.

Repeat the following three steps: Prespin, Ultracentrifuge spin, and Homogenizing. Keep the supernatant!!!! Dilute the solution 3 times to get the oPOE concentration down to 1%.

Amylase Column: The column is washed (by letting the solution drip through) 1 with ethanol, 2 with Millipore water, and 2 with 20mM Na-Phosphate. Let the LamB solution drip through and measure the absorption of the solution. Let 25 ml of 20 mM Na-Phosphate+1% v/v oPOE drip through the column. Check the absorption at 280 nm. If the absorption is less than 0.05 mg/ml then continue, else let some more 20 mM Na-Phosphate+1% v/v oPOE. Let 10 ml of 20mM Na-Phosphate+1% v/v oPOE+ 20% w/v Maltose drip through the column. The maltose brings the LamB out of the column. Collect what is dripping through in 1.5 ml (sterilized) eppendorf tubes. Measure the absorption in all the tubes. Tubes with an absorption higher than 0.1 mg/ml at 280 nm contains the protein.

Concentration of protein: If there is more than 2 ml of liquid that contains the protein, then protein should be concentrated. This is done by spinning the liquid down through a 4 ml filter tube.

Dialysis: The liquid is now dialyzed to remove the maltose. Wash out a dialysis tube with water. Put the solution containing your protein into it. Put the dialysis tube in 50 ml Na-Phosphate+1% v/v oPOE, and let it stand for 1 hour (it helps to stir the solution around with a stirrer). Repeat this last step.

Products used:

For dialysis: Firm: Spectrum Name of product: Float-A-Lyzer MWCO: 15000 Diameter: 5mm Volume: 00 ul Reorder No: 235020

Amylose gradient: Firm: Pierce Name of product: Disposable Columns Sample Kit Product #: 29925

Purification of phage

Spin phages in ultra centrifuge 30000 rpm (remember to balance to about 0.02) for 2.5 hours with the break turned down very low, to get spin down very slowly. Take out immediately after it stops, save pellet and discard supernatant. Add 1 ml of TM buffer to pellet and let it stay for at least 2 hours or overnight in refrigerator. Make sure that it is all suspended, it can be shaken gently.

Spin to clean $2500 \times g$ for 10 minutes and put supernatant in amicon ultra 15 filter (falcon tube with filter). Spin down at $4000 \times g$ to 1.5 ml it takes between 5-20 min. (Remove the phage from the tube with a pipette). Add phages to a 3 ml centrifuge tube on the balance, add TM buffer to a total of 1.675 grams. Add 1.325 g of CsCl. Make a balance out of the same material. Spinn down at 30000 rpm (TLS100) overnight (at least 10). Use with mouth tip to suck out the band in the middle, which contains the phages. Use a amicon filter to desalts.

In vivo experiments

Experimental procedure for 271106:

Buffer= 10mM potassium phosphate, 0.1M KCl, pH=7

Phages: Mix 1 μ l I60 with 1 μ l SYBR (10^3 dilution, properly in buffer), leave at room temperature for an hour. Spinfiltered down twice in 500 μ l buffer. Resuspended into 300 μ l buffer with 3 μ l β ME and 3 μ l gloxy.

Bacteria: 20 μ l overnight culture (C600) was put into 2 ml of LB and grown for 1 hour. The bacteria were then spun down $4000 \times g$ for 5 min, and resuspended in 300 μ l of buffer.

Perfusion chambers: Two pieces of double sticky tape was put on a coverslip with a spacing of roughly 2-3 mm. A small coverslip was put on top as a lid. In this way a chamber of roughly 10 μ l is formed. Poly-l-lysine is flushed into the chamber. Bacteria is then flushed into the chamber and left for 15-25 min. 100 μ l of the phage solution is flushed through immediately before the chambers are used.

Bibliography

- [1] Joëlle Gabay and Kakuko Yasunaka. Interaction of the *lamB* protein with the Peptidoglycan Layer in *Escherichia coli* K12. *European Journal of Biochemistry*, 104:13–18, 1979.
- [2] Ken Ritchie, Jeff Spector. Single Molecule Studies of Molecular Diffusion in Cellular Membranes: Determining Membrane Structure. *Biopolymers*, 87:95–101, 2007.
- [3] Mads C. Sabra and Ole G. Mouritsen. Steady-State Compartmentalization of Lipid Membranes by Active Proteins. *Biophysical Journal*, 74:745–52, 1998.
- [4] Kahay Nicoletta, Douwe A. Wiersma, Bert Poolman, and Dick Hoekstra. Spatial Organization of Bacteriorhodopsin in Model Membranes. *The Journal of Biological Chemistry*, 277:39304–11, 2002.
- [5] Lene Oddershede, Jakob Kisbye Dreyer, Sonia Grego, Stanley Brown, and Kirstine Berg-Sørensen. The Motion of a Single Molecule, the λ -Receptor in the Bacterial Outer Membrane. *Biophysical Journal*, 83:3152–61, 2002.
- [6] Michelle D. Wang, Mark J. Schnitzer, Hong Yin, Robert Landick, Jeff Gelles, Steven M. Block. Force and Velocity Measured for Single Molecules of RNA polymerase. *Science*, 282:902–7, 1998.
- [7] Athur Ashkin. Acceleration and trapping of particles by radiation pressure. *Physical review letters*, 24:156–9, 1970.
- [8] Mette Bredmose Rasmussen, Lene Oddershede, and Henrik Siegumfeldt . Optical Tweezers Cause Physiological Damage to *Escherichia coli* and *Listeria* Bacteria. *Applied and Enviromental Microbiology*, 74:2441–2446, 2008.
- [9] Karel Svoboda, Steven M. Block. Biological applications of optical forces. *Annu. Rev. Biophys. Biomol. Struct.*, 23:247–85, 1994.
- [10] Lene Oddershede, Sonia Grego, Simon F. Nørrelykke and Kirstine Berg-Sørensen. Optical Tweezers: Probing Biological Surfaces. *Probe Microscopy*, 2:129–37, 2001.

- [11] Kirstine Berg-Sørensen, Lene Oddershede, Ernst-Ludwig Florin and Henrik Flyvbjerg. Unintended filtering in a typical photodiode detection system for optical tweezers. *Journal of applied physics*, March 2003.
- [12] Poul Martin Hansen, Iva Marija Tolic-Nørrelykke, Henrik Flyvbjerg, and Kirstine Berg-Sørensen, . Tweezercalib 2.0: Faster version of a MatLab package for precision calibration of optical tweezers. *Computer Phys. Comm.*, 2006.
- [13] Keir C. Neuman, Steven M. Block. Optical trapping. *Review of Scientific Instruments*, 75:2787–2809, 2004.
- [14] dtu. Electron microscope picture of *E. coli*.
- [15] tpsd. Schematic drawing of a gram negative bacterium.
- [16] Yan-Fei Wang, Raimund Dutzler, Pierre J. Rizkallah, Jurg P. Rosenbusch, and Tilman Schirmer. Channel Specificity: Structural Basis for Sugar Discrimination and Differential Flux Rates in Maltoporin. *Journal of Molecular Biology*, 272:56–63, 1997.
- [17] Tilman Schirmer, Thomas A. Keller, Yan-Fei Wang, and Jurg P. Rosenbusch. Structural Basis for Sugar Translocation Through Maltoporin Channels at 3.1 Å Resolution. *Science, New Series*, 267:512–514, 1995.
- [18] Antoinette Ryter, Howard Shuman and Maxime Schwartz. Integration of the Receptor for Bacteriophage Lambda in the Outer Membrane of *Escherichia coli*: Coupling with Cell Division. *Journal of Bacteriology*, 122:295–301, 1975.
- [19] G. H. Vos-Scheperkeuter, E. Pas, G. J. Brakenhoff, N. Nanninga, and B. Witholt. Topography of the Insertion of LamB Protein into the Outer Membrane of *Escherichia coli* Wild-Type and *lac-lamB* Cells. *Journal of Bacteriology*, 159:440–7, 1984.
- [20] Karine A. Gibbs, Daniel D. Isaac, Jun Xu, Roger W. Hendrix, Thomas J. Silhavy and Julie A. Theriot. Complex spatial distribution and dynamics of an abundant *Escherichia coli* outer membrane protein, LamB. *Molecular Microbiology*, 53:1771–83, 2004.
- [21] Frederick Carl Neidhardt. *Escherichia coli and Salmonella: Cellular and molecular biology*. ASM Press, American Society for Microbiology, 1996.
- [22] Jean Van Heijenoort. Formation of the glycan chains in the synthesis of bacterial peptidoglycan. *Glycobiology*, 11:25R–36R, 2001.
- [23] Jean Van Heijenoort. Recent advances in the formation of the bacterial peptidoglycan monomer unit. *Nat. Prod. Rep.*, 18:503–19, 2001.

- [24] Jean Van Heijenoort. Lipid Intermediates in the Biosynthesis of Bacterial Peptidoglycan. *Microbiology and Molecular Biology Reviews*, 71:620–35, 2007.
- [25] R. Merkel, P. Nassoy, A. Leung, K. Ritchie, and E. Evans. Energy landscapes of receptor-ligand bonds explored with dynamic force spectroscopy. *Nature*, 397:50–3, 1999.
- [26] Dorothy Becket, Elena Kovaleva, and Peter J. Schatz. A minimal peptide substrate in biotin holoenzyme synthetase-catalyzed biotinylation. *Protein Science*, 8:921–29, 1999.
- [27] Stanley Brown. Metal-recognition by repeating polypeptides. *Nature biotechnology*, 15:269–72, 1997.
- [28] Kenlynn E. Reed and John E. Cronan, Jr. *Escherichia coli* Exports Previously Folded and Biotinated Protein Domains. *The Journal of Biological Chemistry*, 266:11425–8, 1991.
- [29] B. Bouges-Bocquet, H. Villarroya, and M. Hofnung. Linker Mutagenesis in the Gene of an Outer Membrane Protein of *Escherichia coli*, LamB. *Journal of Cellular Biochemistry*, 24:217–228, 1984.
- [30] Dennis F. Kuck, Elliot L. Elson and Michael P. Sheetz. Forward transport of glycoproteins on leading lamellipodia in locomotile cells. *Nature*, 340:315–17, 1989.
- [31] Kenichi Suzuki, Ken Ritchie, Eriko Kajikawa, Takahiro Fujiwara, and Akihiro Kusumi. Rapid Hop Diffusion of G-Protein-Coupled Receptor in the Plasma Membrane as Revealed by Single Molecule Techniques. *Biophysical Journal*, 88:3659–80, 2005.
- [32] Nobuhiro Morone, Takahiro Fujiwara, Kotonon Murase, Rinshi S. Kasai, Hiroshi Ike, Shigeki Yuasa, Jiro Usukura and Akihiro Kusumi. Three-dimensional reconstruction of the membrane skeleton at the plasma membrane interface by electron tomography. *JCB*, 174:851–62, 2006.
- [33] Takahiro Fujiwara, Ken Ritchie, Hideji Murakoshi, Ken Jacobson, and Akihiro Kusumi. Phospholipids undergo hop diffusion in compartmentalized cell membrane. *The Journal of Cell Biology*, 157:1071–81, 2002.
- [34] Jennifer R. Robbins, Denise Monack, Sandra J. McCallum, Arturo Vegas, Estella Pham, Marcia B. Goldberg and Julie A. Theriot. The making of a gradient: IcsA (VirG) polarity in *Shigella flexneri*. *molecular Microbiology*, 41:861–72, 2001.
- [35] Sumita Jain, Peter van Ulsen, Inga Benz, M. Alexander Schmidt, Rachel Fernandez, Jan Tommassen, and Marcia B. Goldberg. Polar Localization of the Autotransporter Family of Large Bacterial Virulence Proteins. *Journal of Bacteriology*, 188:4841–50, 2006.

- [36] Anindya S. Ghosh and Kevin D. Young. Helical Disposition of Proteins and Lipopolysaccharides in the Outer Membrane of *Escherichia coli*. *Journal of Bacteriology*, 187:1913–22, 2005.
- [37] Miguel A. de Pedro, Christoph G. Grüfelder, and Heinz Schwarz. Restricted Mobility of Cell Surface Proteins in the Polar Regions of *Escherichia coli*. *Journal of Bacteriology*, 186:2594–2602, 2004.
- [38] J. Deich, E. M. Judd, H. H. McAdams, W. E. Moerner. Visualization of the movement of single histidine kinase molecules in live *Caulobacter cells*. *PNAS*, 101:15921–6, 2004.
- [39] So Yeon Kom, Zemer Gitai, Anika Kinkhabwala, Lucy Shapiro, W.E. Moerner. Single molecules of the bacterial actin MreB undergo directed treadmilling motion in *Caulobacter crescentus*. *PNAS*, 103:10929–34, 2006.
- [40] Julie S. Biteen, Michael A. Thompson, Nicole K. Tselentis, Grant R. Bowman, Lucy Shapiro, and W.E. Moerner. Super-resolution imaging in live *Caulobacter crescentus* cells using photoswitchable EYFP. *Nature methods*, 5:947–9, 2008.
- [41] Lili Nui and Ji Yu. Investigation Intracellular Dynamics of FtsZ Cytoskeleton with Photoactivation Single-Molecule Tracking. *Biophysical Journal*, 95:2009–16, 2008.
- [42] Lubert Stryer. *Biochemistry*. W. H. Freeman and Company, New York, 1995.
- [43] G. Udden, J. Bongaerts. Alternative respiratory pathways of *Escherichia coli*: energetics and transcriptional regulation in response to electrons acceptors. *Biochimica et Biophysica Acta*, 1320:217–234, 1997.
- [44] Nicholas J. Watmough, Myles R. Cheesman, Clive S. Butler, Richard H. Little, Colin Greenwood, and Andrew J. Thomsom. The Dinuclear Center of Cytochrome bo₃ from *Escherichia coli*. *Journal of Bioenergetics and Biomembranes*, 30:55–62, 1998.
- [45] Pierce Forget. The Bacterial Nitrate Reductases. *European Journal of Biochemistry*, 42:325–32, 1974.
- [46] Sean J. Elliott, Kenvin R. Hoke, Kerensa Heffron, Monica Palak, Richard A. Rothery, Joel H. Weiner, and Fraser A. Armstrong. Voltammetric Studies of the Catalytic Mechanism of the Respiratory Nitrate Reductase from *Escherichia coli*: How Nitrate Reduction and Inhibition Depend on the Oxidation State of the Active Site. *Biochemistry*, 43:799–807, 2004.
- [47] Hiroshi Kobayashi and Yasuhiro Anraku. Membrane-bound Adenosine Triphosphatase of *Escherichia coli*. *Journal of Biochemistry*, 71:387–99, 1972.

- [48] Donald B. Oliver, Rober J. Cabelli, Katherine M. Dolan, and Gregory P. Jarosik. Azide-resistant mutants of *Escherichia coli* alter the SecA protein, an azide-sensitive component of the protein export machinery. *PNAS*, 87:8227–8231, 1990.
- [49] Kirstine Berg-Sørensen, Lene Oddershede, and Henrik Flyvbjerg. Optical Tweezers as a Tool of Precision: Single-Molecule Mobility as Case Study. *SPIE proceedings, Photonics West*, January 2004.
- [50] J. H. Miller. *Experiments in Molecular Genetics*. Cold Spring Harbor Laboratory Press, New York, 1972.
- [51] Christopher K. Mathews, K. E. van Holde, Kevin G. Ahern. *Biochemistry*. Benjamin/Cummings, 1999.
- [52] Barbara A. Sampson, Rajeev Misra and Spencer A Benson. Identification and Characterization of a New Gene of *Escherichia coli* K-12 Involved in Outer Membrane Permeability. *Genetics*, 122:491–501, 1989.
- [53] Natividad Ruiz, Brian Falcone, Daniel Kahne, and Thomas J. Silhavy. Chemical Conditionality: A Genetic Strategy to Probe Organelle Assembly. *Cell*, 121:307–17, 2005.
- [54] Tao Wu, Juliana Malinverni, Natividad Ruiz, Seokhee Kim, Thomas J. Silhavy, and Daniel Kahne. Identification of a Multicomponent Complex Required for Outer Membrane Biogenesis in *Escherichia coli*. *Cell*, 121:235–45, 2005.
- [55] Lynn L Silver. Novel inhibitors of bacterial cell wall synthesis. *Current Opinon in Microbiology*, 6:431–438, 2003.
- [56] Dan Kahne, Catherine Leimkuhler, Wei Lu, and Christopher Walsh. Glycopeptide and Lipoglycopeptide Antibiotics. *Chem. Rev.*, 105:425–48, 2005.
- [57] Pedro M. Abreu, Paula S. Branco. Natural product-like combinatorial libraries. *Journal of the Brazilian Chemical Society*, 14:675–712, 2003.
- [58] Stanley Brown. Mutations in the gene for EF-G reduce the requirement for 4.5S RNA in the growth of *E. coli*. *Cell*, 49:825–33, 1987.
- [59] University of Wisconsin Madison. *E. coli* Genome Project.
- [60] Stanley Brown. Engineered Iron Oxide-Adhesion Mutants of the *Escherichia coli* Phage λ Receptor. *Proceedings of the National Academy of Sciences of the United States of America*, 89:8651–55, 1992.
- [61] Ulrike S.Eggert, Natividad Ruiz, Brian V. Falcone, Arthur A. Branstrom, Robert C. Goldman, Thomas J. Silhavy, Daniel Kahne. Genetic Basis for Activity Differences Between Vancomycin and Glycolipid Derivatives of Vancomycin. *Science*, 294:361–64, 2001.

- [62] Martti Vaara and Timo Vaara. Polycations as Outer Membrane-Disorganizing Agents. *antimicrobial agents and chemotherapy*, 24:114–22, 1983.
- [63] Martti Vaara and Timo Vaara. Polycations Sensitize Enteric Bacteria to Antibiotics. *antimicrobial agents and chemotherapy*, 24:107–13, 1983.
- [64] Andre Wiese, Thomas Gutschmann, Ulrich Seydel . Towards antibacterial strategies: studies on the mechanisms of interaction between antibacterial peptides and model membranes. *Journal of endotoxin Research*, 9:67–84, 2003.
- [65] Ahmad z. Sahalan, Ronald A. Dixon. Role of the cell envelope in the antibacterial activities of polymyxin B and polymyxin B nonapeptide against *Escherichia coli*. *Antimicrobial*, 31:224–7, 2008.
- [66] Thomas Gutschmann, Sven O. Hagge, Alexander David, Stefanie Roes, Arne Böhling, Malte U. Hammer, Ulrich Seydel. Lipid-Mediated resistance of Gram-negative bacteria against various pore-forming antimicrobial peptides. *Journal of Endotoxin Research*, 11:167–73, 2005.
- [67] Joris Messens, Jean-François Collet. Pathway of disulfide bond formation in *Escherichia coli*. *The International Journal of Biochemistry and Cell Biology*, 38:1050–62, 2006.
- [68] Stephanie Mangenot, Marion Hochrein, Joachim Rädler, and Lucienne Letellier. Real-Time Imaging of DNA Ejection from Single Phage Particles. *Current Biology*, 15:430–5, 2005.
- [69] University of California. Phage project.
- [70] rkm. Biology pictures.
- [71] Alex Evilevitch, Laurence Lavelle, Charles M. Knobler, Eric Raspaud, and William M. Gelbart. Osmotic pressure inhibition of DNA ejection from phage. *PNAS*, 100:9292–5, 2003.
- [72] Paul Grayson, Lin Han, Tabita Winther, and Rob Phillips. Maltose transport in *Escherichia coli* K12: Involvement of the bacteriophage lambda receptor. *PNAS*, 104:14652–7, 2007.
- [73] N. Gov. Membrane Undulations Driven by Force Fluctuations of Active Proteins. *PRL*, 93:268104–1–268104–4, 2004.
- [74] Patrick J. Loll and Paul H. Axelsen. The Structural Biology of Molecular Recognition by Vancomycin. *Annu. Rev. Biophys. Biomol. Struct.*, 29:265–89, 2000.

- [75] P. van Gelder, F. Dumas, I. Bartoldus, N. Saint, A. Prilipov, M. Winterhalter, Y. Want, A. Philippsen, J. Rosenbusch, and T. Schirmer. Sugar transport through maltoporin of *Escherichia coli*: Role of the greasy slide. *Journal of Bacteriology*, 184:2994–9, 2002.
- [76] Frederic C. Neihardt, Philip L. Bloch, and David F. Smith. Culture Medium for Enterobacteria. *Journal of Bacteriology*, 119:736–747, 1974.
- [77] L. Jauffred, T.H. Callisen, L.B. Oddershede. Visco-elastic Membrane Tethers extracted from *Escherichia coli* by Optical Tweezers. *Biophysical journal*, 93:1–8, 2007.
- [78] Sevec Szmelcman, Maurice Hofnung. Maltose transport in *Escherichia coli* K12: Involvement of the bacteriophage lambda receptor. *journal of bacteriology*, 124:112–8, 1975.
- [79] Winfried Boos and Howard Shuman. Maltose/Maltodextrin System of *Escherichia coli*: Transport, Metabolism, and Regulation. *Microbiology and Molecular Biology Reviews*, 64:204–29, 1998.
- [80] Valley Steward. Nitrate Respiration in Relation to Facultative Metabolism in Enterobacteria. *Microbiologica Reviws*, 52:190–232, 1988.
- [81] Ben C. Berks, Stuart J. Ferguson, James W. B. Moir, David J. Richardson. Enzymes and associated electron transport systems that catalyse the respiratory reduction of nitrogen oxides and oxyanions. *Biochimica et Biophysica Acta*, 1232:97–173, 1995.
- [82] Dirk-Jan Scheffers and Mariana G. Pinho. Bacterial Cell Wall Synthesis: New Insights from Localization Studies. *Microbiology and Molecular Biology Reviews*, 69:585–607, 2005.
- [83] Lynn L. Silver. Novel inhibitors of bacterial cell wall synthesis. *Current Opinion in Microbiology*, 6:431–38, 2003.
- [84] Min Ge, Zhong Chen, H. Russel Onishi, Joyce Kohler, Lynn L. Silver, Robert Kerns, Seketsu Fukuzawa, Christopher Thompson, Daniel Kahne. Vancomycin Derivates That Inhibit Peptidoglycn Biosynthesis Without Binding D-Ala-D-Ala. *Science*, 284:507–11, 1999.
- [85] Dorothy Beckett, Elena Kovaleva, and Peter J. Schatz. A minimal peptide substrate in biotin holoenzyme synthetase-catalyzed biotinylation. *Protein Science*, 8:921–929, 1999.
- [86] Akihiro Kusumi and Yasushi Sako. Cell surface organization by the membrane skeleton. *Current Opinion in Cell Biology*, 8:566–74, 1996.

- [87] Ken Ritchie, Ryota Lino, Takahiro Fujiwara, Kotono Murase and Akihiro Kusumi. The fence and picket structure of the plasma membrane of live cells as revealed by single molecule techniques (Review). *Molecular Membrane Biology*, 20:13–18, 2003.
- [88] Jörg Howe, Jörg Andrä , Raquel Conde, Maite Iriarte, Patrick Garidel, Michel H. J. Koch, Thomas Gutschmann, Ignacio Moriyón, and Klaus Brandenburg. Thermodynamic Analysis of the Lipopolysaccharide-Dependent Resistance of Gram-Negative Bacteria against Polymyxin B. *Biophysical Journal*, 92:2796–2805, 2007.
- [89] Haim Tsubery, Hertzog Yaakov, Sofia Cohen, Tal Giterman, Ariella Matityahou, Mati Fridkin, and Itzhak Ofek. Neopeptide Antibiotics That Function as Opsonins and Membrane-Permeabilizing Agents for Gram-Negative Bacteria. *Antimicrobial Agents and Chemotherapy*, 49:3122–28, 2005.
- [90] Vikrant M. Bhor, Celestine J. Thomas, Namita Surolia, and Avadhesh Surolia. Polymyxin B: An ode to an old antidote for endotoxic shock. *Molecular BioSystems*, 1:213–222, 2005.
- [91] Stefanie Roes, Ulrich Seydel, and Thomas Gutschmann . Probing the properties of Lipopolysaccharide Monolayers and Their Interaction with Antimicrobial Peptide Polymyxin B by Atomic Force Microscopy. *Langmuir*, 21:6970–8, 2005.
- [92] Klaus Brandenburg, Alexander David, Jörg Howe, Michel H. J. Koch, Jörg Andrä , and Patrick Garidel. Temperature Dependence of the Binding of Endotoxins to the Polycationic Peptides Polymyxin B and Its Nonapeptide. *Biophysical Journal*, 88:1845–1858, 2005.
- [93] Adrà Clausell, M. Antonia Busquets, Montserrat Pujol, Asunción Alsina, Yolanda Cajal . Polymyxin B-Lipid Interaction in Langmuir-Blodgett Monolayers of *Escherichia coli* lipids: A thermodynamic and Atomic Force Microscopy Study. *Biopolymers*, 75:480–490, 2004.
- [94] Hiroshi Nikaido. Molecular Basis of Bacterial Outer Membrane Permeability Revisited. *Microbiology and Molecular Biology Reviews*, 67:593–656, 2003.
- [95] Ning Yin, Ryan L. Marshall, Sannali Matheson and Paul B. Savage. Synthesis of Lipid A Derivatives and Their Interactions with Polymyxin B and Polymyxin B Nonapeptide. *J. Am. Chem. Soc.*, 125:2426–35, 2003.
- [96] Marina Katz, Haim Tsubery, Sofiya Kolusheva, Alex Shames, Mati Fridkin and Raz Jelinek. Lipid binding and membrane penetration of polymyxin B derivatives studied in biomimetic vesicle system. *Biochem J.*, 375:405–13, 2003.
- [97] Haim Tsubery, Itzhak Ofek, Sofia Cohen, Miriam Eisenstein, and Mati Fridkin,. Modulation of the Hydrophobic Domain of Polymyxin B Nonapeptide: Effect on Outer-Membrane Permeabilization and Lipopolysaccharide Neutralization. *Molecular Pharmacology*, 62:1036–1042, 2002.

- [98] Haim Tsubery, Itzhak Ofek, Sofia Cohen, Mati Fridkin. N-terminal modifications of PolyMyxin B nonapeptide and their effect on antibacterial activity. *Peptides*, 22:1675–81, 2001.
- [99] Haim Tsubery, Itzhak Ofek, Sofia Cohen, Mati Fridkin. The Functional Association of Polymyxin B with Bacterial Lipopolysaccharide Is Stereospecific: Studies on Polymyxin B Nonapeptide. *Biochemistry*, 39:11837–44, 2000.
- [100] Haim Tsubery, Itzhak Ofek, Sofia Cohen, Mati Fridkin. Structure-Function Studies of Polymyxin B Nonapeptide: Implications to Sensitization of Gram-Negative Bacteria. *J. Med. Chem.*, 43:3085–3092, 2000.
- [101] Primož Pritovšek, and Jurka Kidrič. Solution Structure of Polymyxins B and E and Effect of Binding to Lipopolysaccharide: An NMR and Molecular Modeling Study. *J. Med. Chem.*, 42:4604–13, 1999.
- [102] Peer-Joachim Koch, Joachim Frank, Jens Schüler, Clemens Kahle, and Hans Bradaczek. Thermodynamics and Structural Studies of the Interaction of Polymyxin B with Deep Rough Mutant Lipopolysaccharides. *Journal of Colloid and Interface Science*, 213:557–64, 1999.
- [103] Celestine J. Thomas, Beechanahalli P. Gangadhar, Namita Surolia, and Avadhesh Surolia. Kinetics and Mechanism of the Recognition of Endotoxin by Polymyxin B. *J. Am. Chem. Soc.*, 120:12428–34, 1998.
- [104] A. Wiese, M. Münstermann, T. Gutschmann, B. Lindner, K. Kawahara, U. Zähringer, U. Seydel. Molecular Mechanisms of Polymyxin B-Membrane Interactions: Direct Correlation Between Surface Charge Density and Self-Promoted Transport. *J. Membrane Biol.*, 162:127–138, 1998.
- [105] Martti Vaara. Agents That Increase the Permeability of the Outer Membrane. *Microbiological Reviews*, 56:395–411, 1992.
- [106] R. E. W. Hancock. Alterations in outer membrane permeability. *Ann. Rev. Microbiol.*, 38:237–64, 1984.

Real-time observations of single bacteriophage λ DNA ejections *in vitro*

Paul Grayson*, Lin Han[†], Tabita Winther[†], and Rob Phillips^{†‡}

Departments of *Physics and [†]Applied Physics, California Institute of Technology, Pasadena, CA 91125

Edited by Douglas C. Rees, California Institute of Technology, Pasadena, CA, and approved July 6, 2007 (received for review April 11, 2007)

The physical, chemical, and structural features of bacteriophage genome release have been the subject of much recent attention. Many theoretical and experimental studies have centered on the internal forces driving the ejection process. Recently, Mangenot *et al.* [Mangenot S, Hochrein M, Rädler J, Letellier L (2005) *Curr Biol* 15:430–435.] reported fluorescence microscopy of phage T5 ejections, which proceeded stepwise between DNA nicks, reaching a translocation speed of 75 kbp/s or higher. It is still unknown how high the speed actually is. This paper reports real-time measurements of ejection from phage λ , revealing how the speed depends on key physical parameters such as genome length and ionic state of the buffer. Except for a pause before DNA is finally released, the entire 48.5-kbp genome is translocated in ≈ 1.5 s without interruption, reaching a speed of 60 kbp/s. The process gives insights particularly into the effects of two parameters: a shorter genome length results in lower speed but a shorter total time, and the presence of divalent magnesium ions (replacing sodium) reduces the pressure, increasing ejection time to 8–11 s. Pressure caused by DNA–DNA interactions within the head affects the initiation of ejection, but the close packing is also the dominant source of friction: more tightly packed phages initiate ejection earlier, but with a lower initial speed. The details of ejection revealed in this study are probably generic features of DNA translocation in bacteriophages and have implications for the dynamics of DNA in other biological systems.

fluorescence | microscopy | virus | genome

The transfer of bacteriophage DNA from a capsid into the host cell is an event of great importance to biology and physics. In biology, DNA ejection was a key piece of evidence demonstrating that the genetic material was DNA and not protein (1), phages have long been used to insert foreign genes into bacteria (2), and phage-mediated DNA transfer between species is a challenge to theories of evolution (3). In physics, the translocation of DNA through a pore has been studied from the theoretical and experimental points of view (4–8). Because phage DNA ejection is such a well known example of this process, it is important to understand it from a quantitative point of view.

This paper addresses a longstanding, quantitative puzzle about phage DNA ejection: How fast is the ejection process? We use bacteriophage λ , a typical tailed phage, to answer this question. In a λ infection, first the phage tail binds to the *Escherichia coli* outer membrane protein LamB, triggering ejection. Then the genome, 48.5 kbp of double-stranded DNA, moves out of the phage head, through the tail, and into the cytoplasmic space, which requires force on the DNA directed into the cell. A force of tens of piconewtons (pN) is produced by the highly bent and compressed DNA within the capsid (9–11), but not much is known about how fast the DNA transfer occurs, except that ejection reaches completion *in vivo* in <2 min (12). One study used lipid vesicles incorporating LamB and filled with ethidium bromide: the DNA was ejected into the vesicles, causing an increase in fluorescence over ≈ 30 s (13). However, the $\approx 1,000$ molecules of ethidium bromide in each vesicle were enough for only the first 1 kbp of DNA (14). Also, because the ejections could have started at different times, that experiment says very

little about the DNA translocation process. This paper aims to resolve these challenges in describing the λ ejection process.

An important insight from theory is that frictional forces limit the speed of ejection, due to DNA rearrangement in the phage head or sliding forces in the tail (15, 16). Because the DNA is in a liquid state (17), we expect friction to behave at least somewhat like macroscopic hydrodynamic drag: stronger at higher speed or at smaller spacings between the moving parts. The DNA-tail interaction does not change during the ejection process, so we expect friction in the tail to remain constant. In contrast, friction in the head should be stronger when the spacing between the loops of DNA is small, i.e., at the beginning of ejection.

To quantify the rate of ejection, a single-phage technique is necessary. Single-phage ejections were first observed with fluorescence microscopy on phage T5, revealing an effect of the unique structure of the T5 genome: nicks in the DNA resulted in predefined stopping points and a stepwise translocation process, with speeds that were too high to be quantified, so that further analysis of the speed and source of friction was not possible (18). As we will show here, λ ejects its DNA differently from T5, following a continuous process that we can quantify with single-molecule measurements. This allows us to clarify the earlier vesicle-ejection results and study the speed of the ejection process. In fact, knowledge of the forces involved in ejection makes λ an ideal subject for study at the single-molecule level. By comparing the forces to the rate of ejection, we are able to quantify the friction and determine which source of friction actually dominates. Furthermore, we argue that only through systematic analysis of different phages is it possible to develop a complete picture of the DNA translocation process.

The key to checking quantitative ideas about bacteriophage ejection is to vary parameters that affect the process. Earlier, the genome length of λ was varied to investigate how it affects ejection force (11). In this paper we exploit the same strategy, using genome length as a control parameter, but this time to control the ejection dynamics. We expected that the dynamics only depends on the amount of DNA within the capsid, not on the length of the genome that was originally enclosed. A second parameter is the ionic composition of the solution, because monovalent cations lead to higher pressures than divalent cations (19). In fact, Mg^{2+} ions are commonly used to stabilize λ , but these ions are less important for the stability of mutants with shorter genomes (20). Here, we will compare a buffer containing Mg^{2+} to one containing Na^+ . The goal of the paper is to use these tunable parameters to dissect the DNA translocation process.

Author contributions: P.G. and R.P. designed research; P.G. and T.W. performed research; P.G. and L.H. contributed new reagents/analytic tools; P.G. analyzed data; and P.G. and R.P. wrote the paper.

The authors declare no conflict of interest.

This article is a PNAS Direct Submission.

[†]To whom correspondence should be addressed. E-mail: phillips@pboc.caltech.edu.

This article contains supporting information online at www.pnas.org/cgi/content/full/0703274104/DC1.

© 2007 by The National Academy of Sciences of the USA

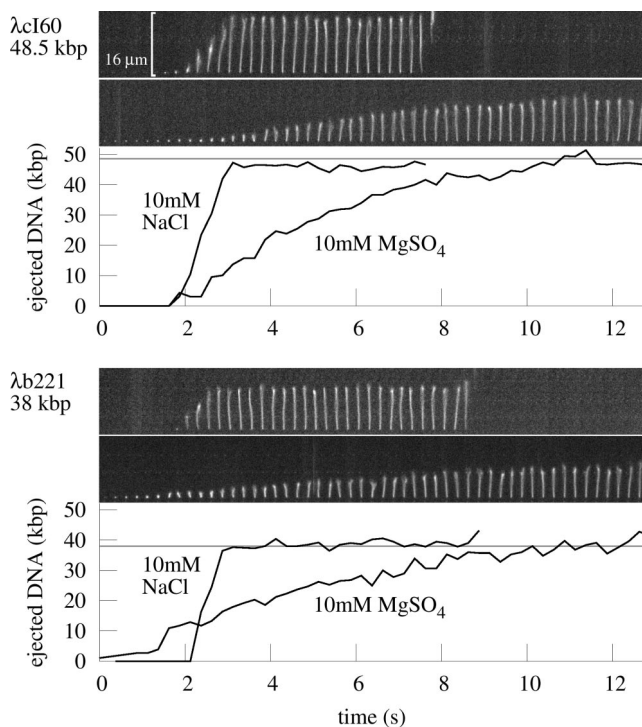


Fig. 1. Images: time series of single genome ejections from λ cI60 and λ b221, taken at a frame rate of 4 s^{-1} . For each of the phages, the ejection in buffer with 10 mM NaCl (Upper) is significantly faster than ejection in 10 mM MgSO_4 (Lower). The 16- μm scale bar is approximately the contour length of a 48.5-kbp piece of DNA. Graphs show length of the DNA that has emerged from the capsid at each time point, as computed by using a computer image-processing algorithm together with DNA length standards as described in the text.

The paper is organized as follows: in *Results*, we describe what we have observed about λ ejection using the single-molecule assay. In *Discussion*, we analyze these results, looking specifically at what they can tell us about the source of friction during ejection. We conclude by summarizing what we have learned about the ejection process, with recommendations for further work. Detailed procedures are given in *Methods*, and further details are available in [supporting information \(SI\) Text, SI Movies 1–4, SI Figs. 6–11, and SI Table 1](#).

Results

To reveal details of the λ ejection process, we measured the rate of ejection as a quantitative velocity with units of kbp/s, following recent work in which single phage T5 ejections could be seen by fluorescence microscopy (18): The λ capsids were bound to a microscope coverslip and washed with a dye/LamB solution to initiate ejection, with a high enough dye concentration to stain the DNA immediately after ejection. An oxygen-scavenging system reduced photodamage, allowing high frame-rate (4 s^{-1}) real-time measurement of the amount of DNA leaving the capsid (see *Methods* for details). As mentioned in Introduction, we can compare our results to models of the ejection process by varying the phage genome length and ion type. The genome length dependence was addressed by using two λ mutants, λ b221 (38 kbp) and λ cI60 (48.5 kbp), which together represent a range close to the maximum allowable range of DNA lengths for λ (21). To gain an understanding of the effects of various ions on the ejection process, we compared ejection in two buffers, with either Mg^{2+} or Na^+ ions at a concentration of 10 mM (see *Methods*). What we expected to see is that the force driving ejection is significantly reduced in the Mg buffer as compared with the Na buffer. These ions are significantly less concentrated

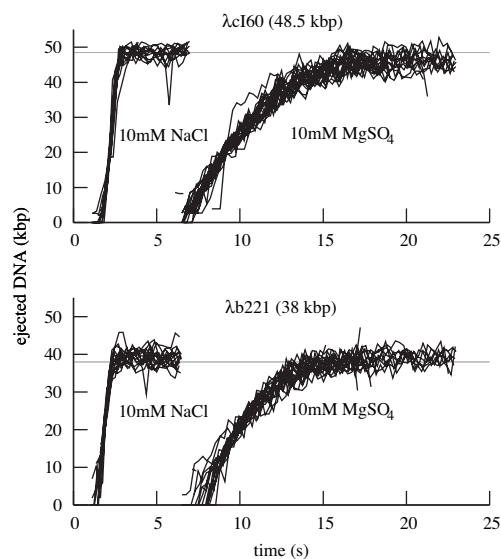


Fig. 2. Graphs of ejection trajectories, comparing NaCl and MgSO_4 buffers and two genome lengths. Single-ejection events were analyzed as described in the text, resulting in trajectories giving the length of DNA out of the capsid as a function of time. These trajectories are aligned and plotted for visual comparison; the offset of the starting time of the ejection is not used in further analysis. The graphs show that ejection proceeds on a time scale of $\approx 1 \text{ s}$ in NaCl buffer, or $\approx 10 \text{ s}$ in MgSO_4 buffer. The ejection speeds of phages with different genome lengths appear similar in this view.

than those within an *E. coli* cell, but the cytoplasmic concentrations are not relevant for the ejection process, which takes place when the capsid is bound to the outer surface of the cell.

Fig. 1 shows real-time views of genome ejection from λ . A total of 81 such single-molecule trajectories were selected from the video data and processed, representing different solution conditions, flow rates, and genome lengths. For each set of experimental conditions, the ejection followed a reproducible trajectory: except for experimental noise or photodamage, there were no apparent differences between events, as shown in Fig. 2. Fig. 3 shows the speed of the ejection process. As these graphs show, the translocation of DNA reaches a high rate of up to 60 kbp/s, slowing as it approaches a maximum extension near 100% ejection, after a total of 1–11 s. This is to be contrasted with the T5 genome, which exhibited multiple random pauses during the ejection process (18). At its maximum extension, however, the λ DNA remained attached for a random amount of time, seconds to minutes, often a long enough time that it was destroyed by photodamage before the release could be measured. Just as the pauses in the case of T5 were due to a feature of the T5 genome, this effect could be due to a unique feature of the λ genome: the 12-bp overhang at the end of the DNA might form nonspecific hydrogen bonds with the capsid protein. However, the present experimental technique does not have the resolution to address exactly how large the piece of DNA remaining within the capsid is.

Another important feature of the ejection process is the waiting time before translocation begins. Although all ejections proceed nearly identically once they have started, λ exhibits a random waiting time of seconds to minutes, during which time no visible DNA has emerged from the capsid. Fig. 4 shows the number of ejections that have been triggered as a function of time, with exponential fits to determine the approximate time constant t_0 of the waiting process.

Discussion

The previous section described the general features of the λ ejection process: a stochastic initiation process followed by a

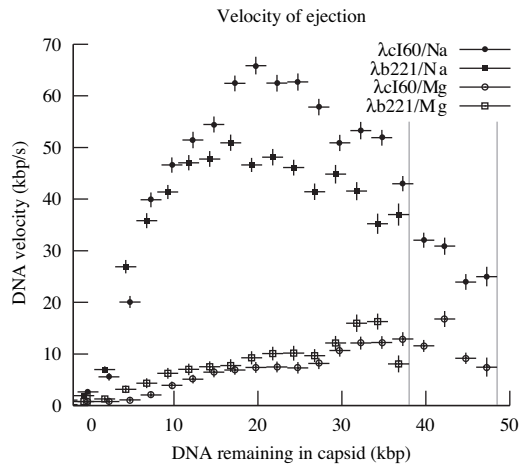


Fig. 3. Averaged speeds of DNA ejection for λ cI60 and λ b221. The plot shows the DNA ejection speed as a function of the amount of DNA within the capsid, averaged in bins of width 2.5 kbp (shown as the horizontal error bars.) Vertical error bars are computed from the standard deviation of the calibration data; there are additional systematic deviations in all curves due to inaccuracies in calibration at the different ionic conditions. The curves for phages of different genome lengths lie close to each other, whereas most of the variation is caused by the difference in buffer conditions. A maximum of ≈ 60 kbp/s is reached in NaCl buffer, whereas the maximum in MgSO_4 buffer is ≈ 17 kbp/s. Vertical gray lines represent the genome lengths of λ cI60 and λ b221.

continuous, reproducible translocation. Now we will discuss the quantitative details in light of recent theories that model the phage genome, predicting the forces that will be produced by compressed DNA during ejection, as shown in Fig. 5.

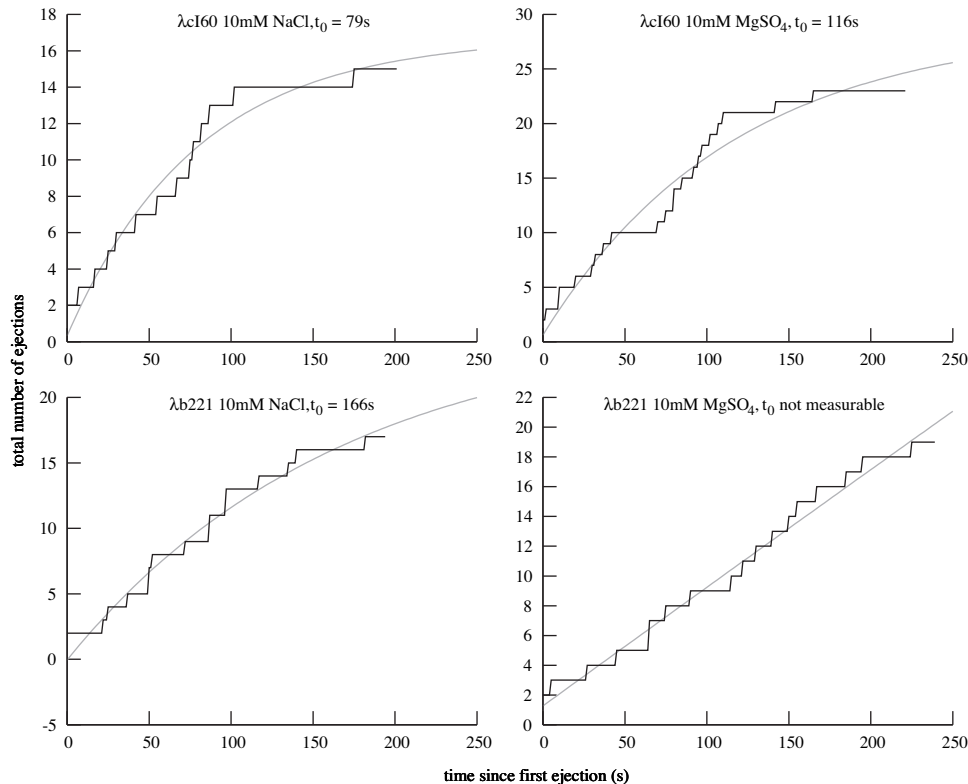


Fig. 4. The number of ejections that have been triggered as a function of time. For each experiment, the total number of ejections that had been observed was plotted as a function of time; these are the same ejections that were used for the analysis above. Also plotted are exponential least-squares fits of the form $a(1 - \exp(-t/t_0)) + b$, where t_0 is the time constant of triggering. To take into account the delay before LamB entered the flow chamber, we set $t = 0$ at the time of the first observed ejection.

For DNA translocation to initiate, some kind of molecular door that blocks the exit of the DNA must first open. Fig. 4 shows that the parameters known to affect pressure and velocity affect the waiting time before ejection, denoted by t_0 . For example, in Na buffer, λ cI60 has $t_0 = 79$ s and λ b221 has $t_0 = 166$ s. Here we have chosen to use an exponential function corresponding to a one-step kinetic process, because this is the simplest form that is supported by the data. In this case, the Arrhenius relation holds

$$\exp((E' - E)/k_B T) = t'_0/t_0 = 2.1, \quad [1]$$

where E and E' are the energies of the transition state for initiation of ejection in the two phages. This results in

$$E' - E = 3.1 \text{ pN nm}. \quad [2]$$

As shown in Fig. 5, the force F on the DNA with 48.5 kbp of DNA in the capsid is predicted to be 36 pN, whereas it is 23 pN with 38 kbp of DNA. How could the transition state energy be coupled to F ? In the transition state, the door may be partially open, having moved a distance Δx along the phage axis. In that case, we find

$$E' - E = \Delta x \cdot (F - F'); \quad \Delta x = 0.24 \text{ nm}. \quad [3]$$

Similarly, in Mg buffer, we find forces of 14 and 6.2 pN. For λ cI60, we find $t_0 = 116$ s, whereas the t_0 value for λ b221 is unmeasurable. Comparing λ cI60 in the two buffers, we get $\Delta x = 0.07$ nm, of the same order of magnitude as the value above. However, this method predicts a value of t_0 for λ b221 of ≈ 100 s, which should have been observable. It is possible that the

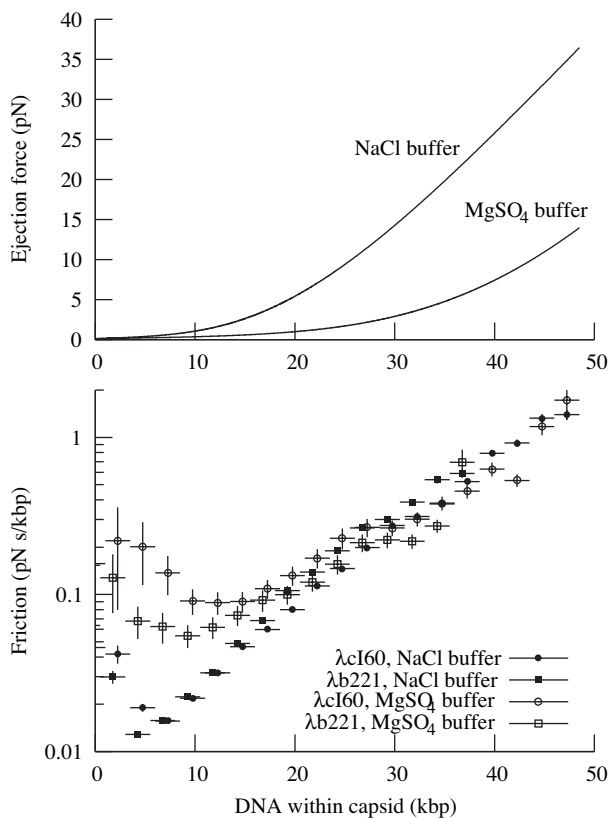


Fig. 5. The relationship between force and velocity. (*Upper*) Force on the DNA, as a function of the amount of DNA left within the capsid, according to theoretical calculations (M. Inamdar, personal communication). Calculations for both buffers were run according to the method of Purohit *et al.* (33), which requires two parameters, F_0 and c , that must be determined experimentally. We used $F_0 = 12,000$ pN/nm²; $c = 0.30$ nm for Mg buffer and $F_0 = 660$ pN/nm²; $c = 0.52$ nm for Na buffer, based on fitting to experimental data from Rau *et al.* (19). The calculations for Mg buffer were identical to those reported earlier (11). The force in Na buffer is significantly higher than that in Mg buffer. (*Lower*) Computed friction coefficient ϕ , showing the relationship between DNA packing within the capsid and its friction. The graph shows that ϕ generally increases with increasing DNA density. For low concentrations of DNA, ϕ is much lower for Na buffer than for Mg buffer. However, with more than ≈ 20 kbp in the capsid, ϕ becomes independent of the type of buffer. The value of ϕ appears to increase to a very high value when 100% of the DNA is packed. Error bars are computed as in Fig. 3.

change in buffer conditions has altered the details of the mechanism that initiates ejection.

The values of Δx given above have the right order of magnitude for a transition that involves, for example, the breaking of hydrogen bonds, suggesting that the waiting time distribution can tell us about the mechanics of the initiation process. However, we do not have enough data to make a claim about exactly what this process is.

After initiation, the DNA begins translocation through the phage tail, proceeding continuously with a varying speed until the entire genome has exited. We would like to understand the details of this process, with particular attention to the source of friction that limits the speed of translocation. Figs. 1 and 2 show that the presence of Mg²⁺ has a dramatic effect on the overall speed, with λcl60 taking ≈ 1.5 s to eject its DNA in Na buffer, which should be compared with 8–11 s in Mg buffer. The most obvious interpretation of this result, in agreement with the findings of bulk DNA pressure measurements (19), is that the higher pressure in Na buffer is responsible for the faster ejection.

However, this simplistic view is not entirely correct, as we discuss below.

Fig. 3 shows v for each set of parameters. As expected, v is a function only of the ionic conditions and the amount of DNA inside the capsid, independent of the original genome length. The graph shows that the maximum v is actually reached at an intermediate stage of ejection, whereas it is reduced by $\approx 50\%$ when the capsid is fully packed. The maximum of F is when the capsid is fully packed, so we know that v cannot simply be proportional to F . This suggests a modification to the simplistic idea of v being proportional to the force F with which the DNA is being ejected. The ratio of the two values represents the strength of the friction, which we denote by $\phi = F/v$.

Apparently, ϕ depends on the amount of DNA within the capsid. A reasonable interpretation is that when the capsid is fully packed, contact between strands of DNA or the capsid walls increases ϕ , slowing translocation below the maximum. It is also possible that ϕ will be different for Na and Mg buffers.

In Fig. 5 we plot ϕ as a function of the amount of DNA within the capsid, showing that the value of ϕ strongly depends on the amount of DNA in the capsid, increasing to ≈ 100 times its initial value as the phage becomes fully packed. In fact, over most of this range, ϕ is independent of all parameters except for the amount of DNA in the capsid. As discussed in Introduction, this dependence on DNA density strongly points to friction originating from hydrodynamic drag within the phage head rather than in the phage tail. The question now becomes whether we can understand the magnitude of ϕ theoretically. However, two challenges limit the development of models: First, the DNA remaining in the capsid will rearrange as it becomes progressively less dense; it is important to know how its structure changes to estimate how fast these changes can occur. The second is that the forces between DNA strands, water, ions, and the protein capsid are not well understood and are particularly difficult to calculate for the interaction of DNA with the narrowest part of tail. As a result, most theoretical modelers have “deliberately avoided” explicit calculations of the time scale of DNA translocation (15, 16, 22, 23). We believe that the data presented here will encourage the development of models that can quantitatively account for the actual ejection velocity.

In this paper, we have shown that the ejection of DNA from bacteriophage λ can reach speeds of up to 60 kbp/s, comparable to the lower bound of 75 kbp/s found for the translocation speed in T5 (18) and clarifying an earlier bulk experiment (13). The speed may also be compared with the slips of 10 kbp/s or greater observed during $\phi 29$ DNA packaging under force (24). This assay provides a quantitative way to look at parameters that might affect the ejection process: here, we have examined the effects of ions and the phage genome length, comparing them to expectations from theory. Other factors could be incorporated into the assay, such as external osmotic pressure, DNA-condensing agents, or DNA-binding proteins, in an effort to develop a better theoretical understanding of the ejection process. Additionally, because we have seen the ejection process from so many different points of view in λ , it would be interesting to know more about the forces and dynamics of DNA packaging in that phage. The ejection assay could also be replicated with other phages, to provide points of comparison to λ . In particular, $\phi 29$ has been shown to experience forces of up to 100 pN during packaging; its ejection could be significantly different from that of λ (24, 25).

We used SYBR Gold as a fluorescent marker for visualizing DNA, which may affect the translocation velocity, because the dye penetrated the capsid on a time scale of ≈ 10 min. The lowest possible dye concentration was used for this experiment, and dye was added immediately before ejection, which should minimize any dye-related effects. We did not notice any systematic difference between earlier or later ejections in each recording.

Despite the low dye concentration, staining of ejected DNA occurred on a time scale faster than the video frame rate: otherwise, the position of the DNA at the fixed end would have appeared to change during the ejection process.

Finally, it should be noted that the DNA ejection process *in vivo* may be quite different from what we observe here, due to osmotic pressure in the bacterial cytoplasm and the presence of proteins that can bind to and actively translocate DNA. No matter how high the internal force is when a phage is fully packed, it will drop to zero as the DNA exits the capsid, so it cannot be sufficient to complete ejection against the internal osmotic pressure of *E. coli*, which produces an outward force of several pN (11). A first attempt to mimic the cell interior could be made by including an osmotic stressing agent such as PEG in the ejection buffer. Several other forces potentially playing a role in ejection include proteins such as RNA polymerase that bind to DNA and produce an effective inward force by translocation or ratcheting (26), channels opened during the ejection process that allow water to rush in and produce drag on the DNA (27), and even molecular motors found in the phage capsid (28). For λ , it is not known what part of the process depends on the pressure in the capsid and what part relies on active transport. Further work to visualize the ejection process *in vivo* is probably the only way that this information could be revealed.

Methods

Buffers and Strains. Several buffers were used for *in vitro* ejection: Na buffer (10 mM Tris/10 mM NaCl, pH 7.8) was considered representative of buffers containing 100% monovalent cations, whereas Mg buffer (10 mM Tris/10 mM MgSO₄, pH 7.8) was considered representative of buffers containing \approx 100% divalent cations. TM buffer (50 mM Tris/10 mM MgSO₄, pH 7.4) was used in earlier ejection experiments (9, 11); we use it here for the preparation of the phages. Buffer A was used earlier for experiments on the DNA packaging process (24). Because of the 10-fold excess of NaCl, it is not clear which type of ion will dominate within the bacteriophage capsid. We found, in fact, that buffer A had an intermediate behavior: calibration DNA behaved identically to DNA in Mg buffer, but DNA translocation required \approx 4 s, between the values for the Na and Mg buffers (see [SI Table 1](#)).

Phages λ b221c126 (λ b221) and λ cI60 were extracted from single plaques and grown on *E. coli* C600 cells with the plate-lysis method on 50-ml supplemented tryptone-thiamine plates (20 g/liter agar, 10 g/liter tryptone, 5 g/liter NaCl, 2.5 g/liter MgSO₄, 13 mg/liter CaCl₂, 20 mg/liter FeSO₄, 2 mg/liter thiamine), which were covered with 20 ml of TM buffer after confluent lysis and incubated at room temperature for several hours or 4°C overnight. Phages were then purified by differential sedimentation and equilibrium CsCl gradients, resulting in 10¹² to 10¹³ infectious particles, as determined by titering on LB agar. After purification, the CsCl buffer was replaced with TM using 100,000 MWCO spin columns (Amicon).

The λ receptor LamB (maltoporin), required to trigger ejection, was extracted from the membranes of *E. coli* pop154 cells: these cells express a *lamB* gene from *S. sonnei* known to be compatible with a variety of λ strains, allowing ejection in the absence of chloroform (29, 30). An overnight culture was sonicated, then the membranes were pelleted, homogenized, and washed in 0.3% *n*-octyl-oligo-oxethylene (oPOE; Alexis Biochemicals catalog no. 500-002-L005) at 40°C for 50 min. A second wash was performed in 0.5% oPOE, followed by extraction in 3% oPOE at 37°C. LamB was affinity-purified in amylose resin and spin-filtered to replace the buffer with TM buffer containing 1% oPOE. Based on the sequence of LamB, it follows that a 1-cm absorbance of 1.0 at 280 nm corresponds to 0.34 mg/ml protein, which we use for computing LamB concentrations in the experiment. Accordingly, from 2 liters of cells we

were able to obtain at least 1 mg of protein, enough for many ejection experiments.

Single-Molecule Measurement. Our single molecule ejection assay essentially uses an earlier technique (18), with modifications for use with phage λ . A 5-mm-wide, 120- μ m-thick channel was constructed from double-sided adhesive sheets (Grace Biolabs). The channels were produced with laser cutting to assure reproducible dimensions (Pololu Corporation). Tygon tubing (inner diameter: 0.02 in) was epoxied to holes at each end of a glass slide. Before each observation, we cleaned a no. 1 coverslip by heating to 95°C in 0.5% Alconox detergent for 30–60 min, rinsing twice with water, and drying in a stream of air. Chambers were assembled, placed on a warm hot-plate for several seconds to seal, and used immediately after cooling. This cleaning process is critical for good imaging, and we noticed a significant degradation in image quality due to SYBR Gold/protein/glass interactions if the chambers were used just a few hours later.

Mg buffer containing 10¹⁰ pfu/ml λ cI60 or λ b221 was incubated with 4 μ g/ml DNase I at 37°C for 15 min to remove any prematurely released DNA. As a focusing aid, 0.1- μ m fluorescent beads were included at a dilution of \approx 10⁷. This phage-bead solution was added to the chamber and left at room temperature for 15 min or more, to allow the phages and beads to adhere to the surface of the coverslip. Then, at the microscope, the left end of the channel was coupled to a reservoir and the right end to a syringe pump, allowing a controlled left-to-right fluid flow along the channel that stretched out the DNA for visualization. To make the observations, the following three solutions were drawn through in succession: first, 800 μ l of Mg or Na buffer containing 1% oPOE to wash away unbound phage particles; second, 40 μ l of the same Mg or Na buffer plus 1% oPOE, 10⁻⁵ diluted SYBR Gold, and an oxygen-scavenging system containing 1% gloxy [gloxy: 17 mg of glucose oxidase (Sigma G2133–10KU) and 60 μ l of catalase (Roche 10681325) in 140 μ l Mg buffer], 0.4% glucose, and 1% 2-mercaptoethanol (31); and third (after sufficient dye was present for observation of the earliest ejections), the same buffer with 2.5 μ g/ml LamB added. This concentration of LamB was required to make binding occur faster than \approx 10 s (data not shown). Single ejections were observed on a Nikon inverted microscope using a 100 \times , 1.4 NA oil immersion objective at ambient temperature (\approx 28°C). The illumination source was a 100-W mercury lamp, used at full intensity. Images were acquired at 4 s⁻¹ with a Photometrics Coolsnap FX camera. Example movies are available in [SI Movies 1–4](#).

Many individual DNA ejections were visible in each acquired image sequence. Before analysis, each ejection was checked for various artifacts that would interfere with processing: overlap with other strands or the edge of the field of view, sticking of DNA ends to the glass, or breaking of the DNA strand. Overlap is unavoidable, whereas the sticking and breaking were caused by the intense illumination and greatly ameliorated by the oxygen-scavenging system. The ejections were analyzed by using a custom difference-of-gaussians filter running within the GNU Octave programming language; for each frame, the program identified the shape of the DNA and recorded its extension in the direction of the flow. See [SI Text](#) for details of the image processing routine, including source code.

Lengths were calibrated by using λ DNAs tethered to specially prepared chambers. The goal was to examine the function that relates the size of a DNA image in pixels to three variables: its length in base pairs, the flow rate, and the ionic composition of the solution. We obtained λ DNA (New England Biolabs) and modified it by using Klenow exo⁻ (New England Biolabs) to add biotin-11-dUTP (Roche) to one end, as a length standard equivalent to an entire piece of ejected DNA from λ cI60. Other length standards were then prepared by digesting aliquots of the DNA with restriction enzymes. The DNAs were attached to

streptavidin (Sigma) on the surface of a coverslip, and flows of various magnitudes were applied. Images were collected and analyzed identically to the images from the ejection videos. It was found that the DNA fit well to the form

$$\text{extension} = 460 \text{ nm} + 0.34 \text{ nm/bp} \cdot (L - L_0 \cdot (1 - e^{-L/L_0})),$$

[4]

where 460 nm was the minimum feature size observable by our technique and L is the length of the DNA fragment in base pairs (data shown in *SI Text*) The parameter L_0 is a function of flow rate; at $L = L_0$, the DNA is stretched out to 37% of its contour length by the flow. When $L \ll L_0$, there is no observable stretching, and when $L \gg L_0$, the DNA will appear shorter than its actual length by L_0 . The equation we used for fitting is not derived from any physical principles, it is just intended to be a smooth curve having the above properties without introducing any parameters other than L_0 . We found $L_0 = 18$ kbp for Mg buffer and 8 kbp for Na buffer at a flow rate of 40 $\mu\text{l}/\text{min}$. This flow was determined to have no significant effect on the ejection

process (see *SI Text*) so it was used throughout the experiment. We note that the physics of tethered DNA in a shear flow is an interesting physical problem in its own right that may have interesting dynamics that would not be completely captured by a time-independent expression like Eq. 4 (32).

We thank A. Graff (University of Basel, Basel, Switzerland) and E. Berkane (University of Würzburg, Würzburg, Germany) for providing protocols for the purification of λ MB and the pop154 *E. coli* strain. Michael Feiss (University of Iowa, Ames, IA) kindly sent us samples of the λ b221c126 and λ cI60 phages used here. M. Inamdar (ITT, Bombay, India) kindly provided data from his calculations on the pressure within λ . We thank Douglas Rees, S. Fraser, and G. Jensen for laboratory space, and I. Molineux, J. Widom, J. Kondev, W. Gelbart, C. Knobler, A. Grosberg, M. Rubinstein, and others for very helpful conversations; and S. Quake as well as the anonymous reviewers for critical reading of the manuscript. This work was supported by a grant from the Keck Foundation (to R.P.), a National Institutes of Health Director's Pioneer Award (to R.P.), and National Science Foundation Grant CMS-0301657 (to R.P.). P.G. was partially supported by a National Science Foundation graduate research fellowship.

- Hershey AD, Chase M (1952) *J Gen Physiol* 36:39–56.
- Morse ML, Lederberg EM, Lederberg J (1956) *Genetics* 41:142–156.
- Homma K, Fukuchi S, Nakamura Y, Gojobori T, Nishikawa K (2007) *Mol Biol Evol* 24:805–813.
- Heng JB, Aksimentiev A, Ho C, Marks P, Grinkova YV, Sligar S, Schulten K, Timp G (2006) *Biophys J* 90:1098–1106.
- Smeets RM, Keyser UF, Krapf D, Wu MY, Dekker NH, Dekker C (2006) *Nano Lett* 6:89–95.
- Chang H, Venkatesan BM, Iqbal SM, Andreadakis G, Kosari F, Vasmatzis G, Peroulis D, Bashir R (2006) *Biomed Microdevices* 8:263–269.
- Harrell CC, Choi Y, Horne LP, Baker LA, Siwy ZS, Martin CR (2006) *Langmuir* 22:10837–43.
- Liu H, Qian S, Bau HH (2007) *Biophys J* 92:1164.
- Evilevitch A, Lavelle L, Knobler CM, Raspaud E, Gelbart WM (2003) *Proc Natl Acad Sci USA* 100:9292–9295.
- Evilevitch A, Gober JW, Phillips M, Knobler CM, Gelbart WM (2005) *Biophys J* 88:751–756.
- Grayson P, Evilevitch A, Inamdar MM, Purohit PK, Gelbart WM, Knobler CM, Phillips R (2006) *Virology* 348:430–436.
- Garcia LR, Molineux IJ (1995) *J Bacteriol* 177:4066–4076.
- Novick SL, Baldeschwieler JD (1988) *Biochemistry* 27:7919–7924.
- Garcia HG, Grayson P, Han L, Inamdar M, Kondev J, Nelson PC, Phillips R, Widom J, Wiggins PA (2007) *Biopolymers* 85:115–130.
- Gabashvili IS, Grosberg A Yu. (1991) *Biofizika* 36:788–793.
- Gabashvili IS & A. Grosberg., (1992) *J Biomol Struct Dyn* 9:911–920.
- Strey HH, Parsegian VA, Podgornik R (1997) *Phys Rev Lett* 78:895.
- Mangenot S, Hochrein M, Rädler J, Letellier L (2005) *Curr Biol* 15:430–435.
- Rau DC, Lee B, Parsegian VA (1984) *Proc Natl Acad Sci USA* 81:2621–2625.
- Parkinson JS, Huskey RJ (1971) *J Mol Biol* 56:369–384.
- Feiss M, Fisher RA, Crayton MA, Egner C (1977) *Virology* 77:281–293.
- Spakowitz AJ, Wang ZG (2005) *Biophys J* 88:3912–3923.
- Inamdar MM, Gelbart WM, Phillips R (2006) *Biophys J* 91:411–420.
- Smith D, Tans S, Smith S, Grimes S, Anderson D, Bustamante C (2001) *Nature* 413:748–752.
- Fuller, Derek N, Rickgauer, John Peter, Jardine, Paul J, Grimes, Shelley, Anderson, Dwight L, Smith, Douglas E (2007) *Proc Natl Acad Sci USA* 104:11245–50.
- Kemp P, Gupta M, Molineux IJ (2004) *Mol Microbiol* 53:1251–1265.
- Molineux, Ian J (2006) *Virology* 344:221–229.
- González-Huici V, Salas M, Hermoso JM (2006) *Gene* 374:19–25.
- Roa M, Scandella D (1976) *Virology* 72:182–194.
- Graff A, Sauer M, Gelder P Van & Meier W (2002) *Proc Natl Acad Sci USA* 99:5064–5068.
- Yildiz A, Forkey JN, McKinney SA, Ha T, Goldman YE, Selvin PR (2003) *Science* 300:2061–2065.
- Doyle PS, Ladoux B, Viovy JL (2000) *Phys Rev Lett* 84:4769–4772.
- Purohit PK, Kondev J, Phillips R (2003) *Proc Natl Acad Sci USA* 100:3173–3178.

Effect of energy metabolism on protein motility in the bacterial outer membrane

Tabita Winther
The Niels Bohr Institute,
University of Copenhagen, 2100 Copenhagen Ø, Denmark

Lei Xu
The Niels Bohr Institute,
University of Copenhagen, 2100 Copenhagen Ø, Denmark

Kirstine Berg-Sørensen
Department of Physics, Technical University of Denmark
2800 Lyngby, Denmark

Stanley Brown
Department of Biology
2200 Copenhagen NV, University of Copenhagen
Denmark

Lene B. Oddershede¹
The Niels Bohr Institute,
University of Copenhagen, 2100 Copenhagen Ø, Denmark

¹Corresponding author: L.B.O., The Niels Bohr Institute, Blegdamsvej 17, DK-2100 Copenhagen Ø, E-mail: oddershede@nbi.dk

Abstract

We demonstrate the energy dependence of the motion of a porin, the λ -receptor, in the outer membrane of living *Escherichia coli* by single molecule investigations. By poisoning the bacteria with arsenate and azide, the bacterial energy metabolism was stopped. The motility of individual λ -receptors significantly and rapidly decreased upon energy depletion. We suggest two different causes for the ceased motility upon comprised energy metabolism: One possible cause is that the cell uses energy to actively wiggle its proteins, this energy being one order of magnitude larger than thermal energy. Another possible cause is an induced change in the connection between the λ -receptor and the membrane structure, for instance by a stiffening of part of the membrane structure. Treatment of the cells with ampicillin, which directly targets the bacterial cell wall by inhibiting cross-linking of the peptidoglycan layer had an effect similar to energy depletion and the motility of the λ -receptor significantly decreased. Since the λ -receptor is closely linked to the peptidoglycan layer we propose that λ -receptor motility is directly coupled to the constant and dynamic energy consuming reconstruction of the peptidoglycan layer. The result of this motion could be to facilitate transport of maltose-dextrins through the porin.

Key words: *Escherichia coli*; lambda receptor; diffusion; ampicillin; peptidoglycan; optical tweezers

Introduction

Insight into membrane protein motility is important in order to understand nutrient uptake and regulatory mechanisms, and for procaryotes also to understand the action of antibiotics. There have been numerous investigations of mobility of proteins in the membranes of eucaryotic cells (1–3), but few on the mobility of proteins in the outer membranes of living procaryotic cells (4–7). Membrane proteins cannot be viewed as isolated structures, their function is deeply dependent on their environment, the membrane, as well as energy availability and regulatory mechanisms. For lipid bilayers it has been theoretically predicted that there should be a connection between the energetic activation of proteins and the membrane compartmentalization (8). Also, the spatial organization and oligomerization of bacteriorhodopsin embedded in artificial membranes has been shown to depend on photoactivation; at particular protein concentrations, a decrease in protein motility was observed upon photoactivation (9). In this paper we further investigate the possible influence on energy availability on protein motility in the membrane of a living *E. coli*.

The outer membrane of gram-negative bacteria is an asymmetric structure that functions as a permeability barrier allowing for transport predominantly through specific pores and channels (10). The main components of the outer part of the cell wall are the outer leaflet consisting of lipopolysaccharides, the inner leaflet consisting of phospholipids, and the peptidoglycan layer, a strong structure which enables the bacterium to maintain a large osmotic pressure gradient across the cell wall. The λ -receptor is an integral outer membrane protein, which is responsible for the transport of maltodextrins across the outer membrane (11), and it is proposed to be attached to the peptidoglycan layer (12). As it is the receptor for bacteriophage lambda it has been studied for more than 40 years and the regulation as well as the genetics of the receptor is well understood. There can easily be thousands of λ -receptors present in the outer membrane, and they appear to be fairly randomly distributed across the entire membrane (6, 13, 14). *In vivo* studies of the mobility of a single λ -receptor consistently found that the λ -receptor performs 'wiggling motion' which can be characterized as a confined diffusional motion within the outer membrane (4–6).

In the present work, we examined the role of energy metabolism on the motility of a single λ -receptor in the outer membrane of *E. coli*. In metabolically competent cells we monitored the motion of a single λ -receptor using

both beads and quantum dots, thus clarifying the magnitude of the confined diffusion (4, 6). To study the effect of a comprised energy metabolism we monitored the motility of the same receptor both before and after energy depletion of the cells by arsenate which stops ATP synthesis and azide which stops electron transport. This treatment gave rise to a significant and rapid decrease of motility. We invoke a model with two possible causes for the observed decrease in motility, one cause could be that a metabolically competent cell spends energy which results in a wiggling of its λ -receptors. Another possible cause could be a change in the membrane structure caused by energy depletion. To pinpoint the biological cause of the observed effects, we treated the cells with ampicillin, an inhibitor of peptidoglycan crosslinking. The effect of ampicillin was to efficiently stop the motion of the receptor. Based on these observations we propose that the λ -receptor through its firm connection to the peptidoglycan layer uses the energy dependent dynamic re-construction of this layer to perform a wiggling motion.

Materials and methods

Bacterial strains The strains used were derived from S2188 (15), an *E. coli* K12 strain which has a deletion in the *lamB* gene. A plasmid harboring the biotinylated λ -receptor was then inserted into strain pLO16 which was used throughout the present study, for a more detailed description see Ref.(4), where it is also proven that the efficiency of the biotinylation is very low, on average less than one receptor per bacterium is biotinylated. This greatly reduces the risk of having a bead attached to more than one receptor simultaneously.

Growth and preparation of bacteria Single colonies of bacteria were grown at 37 C on YT agar plates (16) supplemented with 25 g/ml chloramphenicol. A single colony was suspended in M63 salts (17) containing 1 μ g/ml B1, 25 μ g/ml chloramphenicol, 0.1% casein hydrolysate, and 0.2% glycerol. The bacteria were grown over night in shaking water bath at 37 °C. Thereafter 0.1ml of suspended bacteria was diluted into 3ml fresh MOPS media (18) where they were grown until log-phase, still at 37 °C. MOPS was chosen as growth medium as it can be phosphate-free and therefore is well suited as medium also during poisoning with arsenate: The poisoning has to be carried out in a phosphate free solution, because the metabolic inhibition by arsenate

is caused by its resembling of the phosphate group that participates in the energy transfer. After reaching log-phase, isopropyltriagalactoside (IPTG) was added to a final concentration of 0.5 mM, and the bacteria were grown for an additional half hour. IPTG is used to induce the expression of the λ -receptor. One milliliter of this culture was then centrifuged for 5 min at $1673 \times g$ and the pellet was resuspended in buffer. The buffer used throughout the experiments was a KCl-potassium phosphate (10 mM potassium phosphate, 0.1 M KCl, pH 7) buffer. The beads used were streptavidin-coated polystyrene spheres from Bangs Laboratories, Inc. (Fishers, IN) most often with a diameter of $0.44 \mu\text{m}$. The remaining parts of the preparation procedure was performed at room temperature (22°C): The beads were washed by suspension in millipore water and thereafter centrifuging them at $1673 \times g$ for 5 min. The supernatant was discarded and the beads resuspended in buffer and sonicated for at least 15 min to disrupt aggregates. To study the bacteria in the microscope, perfusion chambers were made. On a poly-L-lysine coated coverslip two pieces of double sticky tape were put together to form a chamber and another coverslip was then attached as the lid of the chamber. To allow the bacteria to attach to the poly-L-lysine coated surface, the bacteria were incubated at room temperature for 20 min. Heparin (12.5 mg/ml) was perfused into the chambers and incubated at room temperature for 15 min. The heparin layer passivates the charges of the poly-L-lysine, which thereby minimizes the attraction between the poly-L-lysine coated coverslip and the streptavidin-coated beads (4). The chambers were then washed four times with buffer, after which the washed streptavidin-coated beads were flushed in and left to adhere to biotinylated receptors for 15 min, still at room temperature. To remove excess beads, the chambers were then washed until they appeared clear. They were washed with MOPS media with the difference from the MOPS mentioned above that the glycerol was replaced with glucose. Glucose was used to support anaerobic growth in the closed chambers. The chambers were inverted and stored over a water bath at 5°C until use.

Optical tweezers setup The optical tweezers is based on a Spectra-Physics Millennia Nd:YVO₄ laser implemented in an inverted Leica DM IRBE microscope. The laser light is tightly focused by a Leica objective (100x oil NA 1.4 PL APO), after passage of the sample the light is collected by an oil immersion condenser and imaged onto a photo-diode. Two types of photo-diodes were used, one was a quadrant photodiode (Hamamatsu S5981 Si-PIN) the other a position sensitive diode (Pacific Silicon Detectors DL100-

7PCBA3). With this setup we can measure forces and distances in the piconewton and nanometer regimes with a time resolution of MHz. A detailed description of the setup can be found in (19). The duration of an optical tweezers measurement is on the order of seconds, and the sampling rate was 22000 Hz, giving a temporal resolution of 46 μ s. To ensure that the mobility of exactly the same receptor was recorded before and after poisoning the entire experiment was video recorded using a Sony XC-ES50 CCD camera. The experiments which included visualization of individual quantum dots were performed in a Leica SP5 confocal microscope equipped with an Andor sXon+ cooled EMCCD camera and a normal fiber coupled Leica Hg excitation source. The laser power delivered at the sample was around 10 mW and the total exposure time on the order of seconds. At such low laser power and low exposure time no physiological damage has been detected on optically trapped bacterial species (20).

Experiments with beads as markers The first step in the experimental procedure was to trap a free bead and perform a force calibration of a bead at the same height as a bead attached to a λ -receptor (4). Next, we found a bead attached to a lambda receptor, this attachment being characterized by a 'wiggling' motion of the bead (4). If a bead is not specifically attached, it does not perform this wiggling motion(4) and it can be pulled away by an optical trap thus creating a tether consisting of outer membrane material (21). In the present investigation, we centered the optical trap on a bead which was specifically attached to a λ -receptor and recorded a time series of its motion using the photodiode and custom made Labview programs.

Energy depletion After the steps described in the above paragraph, the liquid in the perfusion chambers was exchanged by flushing 20 μ l of an arsenate and azide poison mixture through the chamber five times. The poison mixture consisted of phosphate free MOPS supplemented with 20 mM NaN_3 and 1 mM KH_2AsO_4 . This procedure was repeated after a waiting period of roughly 10 min. This tedious procedure of poisoning ensures that all the liquid in the perfusion chamber is replaced with the poisonous one and that the poison has time to affect the cells. Another time series of the positions visited by the same λ -receptor was recorded after poisoning.

Ampicillin In the experiments with ampicillin the cells were grown in M63 as described above. After reaching log-phase the M63-IPTG solution was supplemented by 100 μ g/ml ampicillin and the cells were grown for at least 1 hour with ampicillin present. Then the remaining part of the procedure outlined in 'Growth and preparation of bacteria' was conducted, though

with the modification that all solutions contained 12 % sucrose. The sucrose was included to osmotically stabilize cells with compromised cell walls. Three types of experiments were made: i) Ampicillin was present both during growth and during measuring. ii) Ampicillin was present during growth but the measurement procedure was performed in M63 without ampicillin. iii) A control where ampicillin was not present neither during growth nor during the measurement but everything else was as in cases i) and ii).

Experiments with quantum dots as markers The preparation of these samples were as described above in the 'Growth and preparation of bacteria' section (but in M63) until the point where the beads were added apart from the fact that the IPTG concentration was raised to 1mM. The streptavidin coated CdSe quantum dots (Invitrogen, emission wavelength 655 nm, outer diameter \sim 15 nm) were diluted 1/10000 into the growth media (M63), and after addition of 10 μ L of the quantum dot solution to the samples, they were sealed. The sample was incubated for 30 minutes to allow the quantum dots to attach to the receptor before the experiment was initiated. The motion of the quantum dot was observed using an EMCCD camera, taking 50 seconds time series with a repetition rate of 10 Hz. All frames were overlaid in a stack and for each pixel the brightest pixel value was chosen for a final, summarized picture. This final picture provided an overview of the total excursions of the quantum dot during the 50 seconds. The pixels which were not visited appeared dark, those visited appeared brighter. Each pixel corresponded to 25 nm. We only used quantum dots to visualize lambda receptors on metabolically competent bacteria.

Data Analysis

The optical tweezers exert a harmonic force on the trapped bead, $F = -\kappa(x_{\text{bead}} - x_{\text{trap}})$, where κ is denoted the spring constant of the optical trap, x_{bead} is the position of the bead and x_{trap} is the equilibrium position of the optical trap. Similar equations exist for the two orthogonal directions, but as we have chosen only to analyze receptors which sit on top of the bacteria seen from the microscope's point of view, and since the motion of a λ -receptor is isotropic in the lateral directions (4), it suffices to only consider the x direction in the following analysis. The timeseries of the bead's motion is measured in Volts by the photodiodes, and is easily converted to meters,

e.g., using the procedures written in (19). When performing this calibration procedure it is important to account for aliasing and possible filtering by the photodiode and other filters present and we did so using the MatLab programs described in (22).

The bead and the protein are joined through a biotin-streptavidin linkage, which is described as a harmonic spring with spring constant κ_{bs} . The potential felt by the protein in the membrane is also well described by a harmonic potential (4), with spring constant κ_{cw} . This spring constant describes the connection to the membrane structure, and an alternation of the cell wall properties would appear in our model as a change in κ_{cw} . The protein also feels some frictional force from the membrane, the friction coefficient being denoted γ_{prot} . Finally, both the bead and the protein are subject to stochastic forces due to the random bombardment by solvent molecules. These stochastic forces are denoted F_{bead} and F_{prot} and are assumed to have the properties of white noise, i.e. vanishing expectation value and delta-function auto-correlations. F_{bead} and F_{prot} vary with time and temperature, T . The above definitions as well as the following two coupled equations of motion for respectively the bead and the protein, are identical to those outlined in Ref.(4):

$$\begin{aligned} M_{bead}\ddot{x}_{bead} &= -\kappa(x_{bead} - x_{trap}) + \kappa_{bs}(x_{prot} - x_{bead}) - \gamma_{bead}\dot{x}_{bead} + F_{bead}(1) \\ M_{prot}\ddot{x}_{prot} &= -\kappa_{cw}(x_{prot} - x_{cw}) - \kappa_{bs}(x_{prot} - x_{bead}) - \gamma_{prot}\dot{x}_{prot} + F_{prot}(2) \end{aligned}$$

Here, M_{bead} and M_{prot} are the masses of bead and protein.

Using this model and typical data sets, it turns out that the total spring constant felt by the bead is given by $\kappa_{tot} = \kappa + \kappa_{cw}$ (4). When a measurement is done with the optical tweezers system, one obtains a timeseries of the positions visited by the bead. The corresponding histogram is well described by a Gaussian distribution with standard deviation σ :

$$\sigma^2 = \frac{k_B T}{\kappa + \kappa_{cw}} \quad (3)$$

From this expression and the determination of κ from calibration, κ_{cw} can be found. Subsequently, the standard deviation of the positions visited by the protein, σ_λ , can be found:

$$\sigma_\lambda^2 = \frac{k_B T}{\kappa_{cw}} \quad (4)$$

Experimentally, a narrowing of the position histogram, the width of which is described by σ_λ , is observed upon energy depletion. Thus, Equation 4 suggests two interpretations of this narrowing, either T decreases or κ_{cw} increases, these two interpretations are modeled as A or B in the following.

Effect of energy depletion

We propose two ways of modeling the effect of energy depletion:

Model A We assume that the λ -receptor is actively moved, made to 'wiggle' in a metabolically competent cell. In other words, its total energy is a sum of two terms, one originating from the thermal motion, the other from an active motion (where the cell spends energy to perform this motion):

$$E_{tot} = E_{thermal} + E_{active}. \quad (5)$$

Model A is implemented in Equations 1 and 2 by using an artificial temperature, T_{bac} , to describe the total energy: $E_{tot} = \frac{1}{2}k_B T_{bac}$. T_{bac} is then put into Equation 2 in the stochastic force term. Hence, in the fitting routines, T_{bac} is allowed to vary and all other parameters are kept fixed while comparing datasets from metabolically competent cells to energy depleted cells. Model A is illustrated in Figure 1, where a 'pick-up truck' is drawn as the active mover of the λ -receptor before energy depletion.

Model B We assume that the effect of energy depletion predominantly alters the membrane structure and that this gives rise to a change of κ_{cw} . Hence, in the fitting routines, κ_{cw} is allowed to vary and all other parameters, including temperature, are kept fixed while comparing datasets from metabolically competent cells to energy depleted cells. Model B is also illustrated in Figure 1 where the change in the cell wall is drawn as an aggregation of membrane proteins around the λ -receptor and as a stiffening of the attachment of the λ -receptor to the peptidoglycan layer.

In Equations 1 and 2 the inertial terms are significantly smaller than the other terms and may be neglected. Thus simplified, Equations 1 and 2 are Fourier transformed and the power spectrum of the position of the bead,

$P_{\text{bead}}(f)$, is derived: $P_{\text{bead}}(f) \propto |\langle \tilde{x}_{\text{bead}}(f) \rangle|^2$ where $\tilde{x}_{\text{bead}}(f)$ is the Fourier transformed of positions, $x(t)$. The general result is

$$P_{\text{bead}}(f) = \frac{\mathcal{D}_{\text{bead}}}{2\pi^2} \cdot \frac{(b+c)^2 + r^2(f/f_c)^2 + trb^2}{\mathcal{D}} \quad (6)$$

with

$$\begin{aligned} \mathcal{D} = & f_c^2 (r^2(f/f_c)^4 + ((b+c)^2 + 2br^2 + r^2b(2+b^2))(f/f_c)^2 \\ & + (2bc(b+c) + (b+c)^2 + b^2c^2)) \end{aligned} \quad (7)$$

and where we have introduced the ratios

$$r = \frac{\mathcal{D}_{\text{bead}}}{\mathcal{D}_{\text{prot}}}; \quad b = \frac{\kappa_{\text{bs}}}{\kappa}; \quad c = \frac{\kappa_{\text{cw}}}{\kappa}; \quad f_c = \frac{\kappa}{2\pi\gamma_{\text{bead}}} \quad t = \frac{T_{\text{bac}}}{T}. \quad (8)$$

The way in which the general expression in Eq. (6) is fitted to experimental data depends on which model is invoked but in all cases the data sets originating from metabolically competent and comprised cells are fitted simultaneously. In model A, $t=1$ for the metabolically competent cells, but t is allowed to vary for the energy depleted cells. In model B, κ_{cw} is allowed to have one value for the metabolically competent cells and another, $\kappa_{\text{cw,p}}$, for the energy depleted (poisoned) cells. All other parameters are assumed identical for metabolically competent and comprised cells in the simultaneous fitting procedure.

Results

Normal motion as revealed through quantum dot attachment

In order to determine the motility of a λ -receptor in a metabolically competent cell, we specifically attached a quantum dot to individual receptors. For each attached quantum dot, blinking was observed, which ensured that the signal originated from a single quantum dot. Analysis of timeseries of positions of individual quantum dots showed that a quantum dot attached to a λ -receptor always stays within a region of $\simeq 50$ nm. This is completely consistent with earlier results (4, 5) as well as present results using micron-sized beads as handles. The remaining experiments of this work were done

with 0.44 μm beads as handles because these beads have the advantage over quantum dots that their motion can easily be monitored by the optical tweezers with superior temporal and spatial resolution as compared to the image based techniques.

Energy depletion

In all samples the motion of the exact same λ -receptor was recorded before and after energy depletion. A timeseries showing the positions visited by the bead attached to the receptor before (blue) and after (red) energy depletion is shown in Figure 2. The distributions of positions visited by an individual receptor, both before and after energy depletion are well fitted by Gaussian functions (shown as full lines in the left inset of Figure 2). The right inset of Figure 2 shows a scatter plot of the positions visited before and after energy depletion. It is clear that the λ -receptor moves less after energy depletion. In total 29 experiments were done and they all showed a decrease in motility. This effect was also clearly visible by eye in the microscope, and it was observable immediately after the poisoning flushing procedure, which took a couple of minutes. I.e., the effect sets in rapidly, faster than two minutes.

This decrease of λ -receptor motility can be quantified by comparing the standard deviation of the position histograms (as shown in the left inset of Figure 2 before and after energy depletion. For $n=29$ data sets we got $\sigma_{before} = (7.17 \pm 0.56)$ nm (mean \pm SEM) and $\sigma_{after} = (2.98 \pm 0.36)$ nm. To test whether these numbers are significantly different a students T-test was performed. The p-value gives the probability that the observed difference between the two populations is accidental. In other words, a low p-value supports the hypothesis of a significant change in motility upon energy depletion. The outcome of this analysis was that the p-value = 3.6×10^{-7} . Hence, there is a significant change in motility of the λ -receptor upon energy depletion of the cell.

As a control, we investigated whether the exchange of media could be the cause of change of λ -receptor motility. The experiment mentioned above was repeated, but without azide and arsenate in the flushed in media. The result was that σ_{before} was not significantly different from σ_{after} . Hence, the observed change in motility was not simply an artifact of the flushing procedure.

The standard deviation of the bead, σ , gives clues about the motion of the bead linked to the receptor and hence, it indirectly provides information

on the motion of the receptor itself. With the knowledge of κ and κ_{cw} we used Equation 4 to find σ_λ , the standard deviation of the motion of the λ -receptor without the effect of the optical trap. Using all the above mentioned datasets we found that for a normal metabolically competent cell $\sigma_{\lambda,before} = (10.3 \pm 1.6)$ nm. For an energy depleted cell $\sigma_{\lambda,after} = (4.4 \pm 0.4)$ nm. A Students T-test gives $p = 3.5 \times 10^{-4}$, in other words, the probability that the observed difference between the two populations is accidental is very low. Energy depletion of the cell causes a significant motility change for the λ -receptor.

For data acquisition we used two different types of photodiodes, a quadrant photodiode (QPD) and a position sensitive diode (PSD). Each photodiode has advantages and disadvantages, e.g., the quadrant photodiode has a pronounced filtering effect on frequencies above 10 kHz (23) but has a very low noise on the low-frequency part. The position sensitive diode has a 3dB frequency that is somewhat larger than for the QPD, maybe around 100 kHz, but it is a bit more noisy in the low frequency regime. Hence, for the above mentioned analysis of σ both types of photodiodes could be employed, but for analysis of the power spectra, where the high-frequency regime is important, only the data acquired by the PSD could be used. Figure 3 shows a power-spectral analysis of one dataset acquired by the PSD. The upper set of data points originate from metabolically competent cells, the lower set originate from the same λ -receptor but after energy depletion. Equation 6 stated in terms of Model A (full lines in Figure 3) was simultaneously fit to both data sets. The inset shows the quality of the fit by dividing the data by the fit, ideally the distribution should be frequency independent and 1/3 of the data points should be outside the two lines, each of which is located one standard deviation from 1.

Power-spectral analysis of all datasets acquired by the PSD allowed us to fit the data both by model A and model B. The outcome was that the χ^2 value from model A was smaller than that of model B in 10 out of 12 cases, in one case the two values were indistinguishable. Fits of model A gave values for $\frac{T_{bac}}{T}$ and there seemed to be no dependence of this ratio on the stiffness of the optical trap (see supplementary information). The average value found for $\frac{T_{bac}}{T} = 10.5 \pm 3.8$. Fits of model B to the power spectral data sets gave values for $\frac{\kappa_{cw,p}}{\kappa_{cw}} = 27.6 \pm 12.4$ and again, there was no dependence of this ratio on the stiffness of the optical trap.

The ratios $\frac{T_{bac}}{T}$ and $\frac{\kappa_{cw,p}}{\kappa_{cw}}$ obtained from power-spectral analysis are equivalent to numbers which can be extracted from analysis of histograms as shown

in the inset of Figure 2. As evident from Equation 3, the ratio $\frac{T_{\text{bac}}}{T}$ (model A) is equivalent to $\frac{\sigma_{\text{before}}^2}{\sigma_{\text{after}}^2}$. The values of $\frac{T_{\text{bac}}}{T}$ obtained from histogram analysis is also shown in supplementary information. From Equation 4 it is evident that the ratio $\frac{\kappa_{\text{cw,p}}}{\kappa_{\text{cw}}}$ (model B) is equivalent to $\frac{\sigma_{\lambda,\text{before}}^2}{\sigma_{\lambda,\text{after}}^2}$. The values of $\frac{T_{\text{bac}}}{T}$ and $\frac{\kappa_{\text{cw,p}}}{\kappa_{\text{cw}}}$ obtained by analyzing the histograms are in accordance with those obtained by power-spectral analysis (on a 5 % significance level in a Students T-test).

Following treatment with ampicillin we observed no change in cell shape. Therefore, damage to the cell wall was minor. Due to the length of time necessary to regenerate the cell wall after removal of ampicillin we did not examine the same λ -receptor before and after regeneration. Instead, different populations were investigated. We had a population (i) (described in the Materials and Methods section), 38 datasets, which had been growing in ampicillin and where ampicillin was present during the preparation and measurement procedure, a population (ii) 28 datasets which had been growing in ampicillin but where ampicillin was not present during the preparation and measurement procedure, and finally a control (iii) 24 datasets without ampicillin but with all other parameters the same. Figure 4 shows a time trace from a typical control cell (blue) and from a typical ampicillin treated cell population (i) (red). There is a clear change in motility. This is also true if one considers all investigated cells: $\sigma_{\text{control}} = (11.32 \pm 0.89)$ nm and $\sigma_{\text{ampicillin,i}} = (3.43 \pm 0.32)$ nm. A Students T-test gives a p-value of 2.1×10^{-14} . Hence, there is a very significant decrease in λ -receptor motility in cells treated and measured with ampicillin in comparison to the control. If, on the other hand, the cells were allowed to regenerate during the preparation and measurement procedure (which took around 1 hour) it seemed that the λ -receptor could resume motion, the values quantifying the motility were $\sigma_{\text{control}} = (11.32 \pm 0.89)$ nm and $\sigma_{\text{ampicillin,ii}} = (10.25 \pm 0.70)$ nm. A Students T-test gives a p-value of 0.11. Hence, the populations ii and iii are not significantly different.

Discussion

In performing our analysis of the motility of λ -receptors in the outer membrane of *E. coli* we utilize the inefficient conjugation of biotin to proteins exported from the cytoplasm (24, 25). This allows us to limit the number of

λ -receptors able to bind streptavidin to fewer than one per cell on average (4). In this and our previous studies (4, 5), we found the λ -receptor diffused within a confined range of approximately 50 nm. Our previous analysis used only down to 0.44 micron streptavidin-coated spheres to visualize the movement of the biotinylated λ -receptors. It was hypothesized (6) that the large size of the spheres could hide a subpopulation with larger motility, as observed for a subset of lambda-receptors monitored with 20 nm gold nanoparticles (6). To address this concern, we conducted single-particle tracking analysis using streptavidin-coated quantum dots. Using quantum dots 15 nm in diameter we again observed diffusion limited to 50 nm domains, hence, the size of the handle cannot be the cause. The strains used in the present investigation and in Refs.(4, 5) had on average less than one binding site per bacterium. The strains used in Ref.(6), had all λ -receptors expressing gold-binding sites, hence, potentially the 20 nm gold nanobeads could bind to hundreds or thousands λ -receptors available on a single bacterium. As the point spread function of a 20 nm gold nanoparticle is approximately 300 nm, two or more particles closer than 300 nm would appear as one point when imaged by light microscopy. A centroid tracking routine utilizes the picture from the microscope, although it can reliably track one particle with a resolution down to 10 nm, it is not able to track the centroid of a particle if its point spread function overlaps with those of other particles. Therefore, the sub-population of λ -receptors observed in Ref.(6) postulated to move distances of 300 nm could be caused by two or more gold nanoparticles located within each others point spread function.

Upon energy depletion of the cells by azide and arsenate there was a significant decrease of motility of the λ -receptor. The change in motility occurred rapidly, on a timescale faster than minutes. One of the actions of azide is to block electron transport. In the absence of phosphate arsenate blocks ATP synthesis. Hence, with these two poisons the cells had their energy metabolism effectively stopped. There have been several theoretical reports predicting a correlation between protein motility and the energetic state of the membrane, e.g., in Refs.(8, 26). However, to our knowledge, the effect of energy on the motility of membrane proteins has not been observed before. The fact that we clearly see a connection between the energetic state of the bacterium and the motility of the λ -receptor signifies first of all that the bacterium uses energy moving the λ -receptor. A highly energetically optimized system as a bacterium would never waste its energy, therefore there must be a benefit to this motion. Secondly, the fact that the λ -receptor moves

more in a metabolically competent cell than in an energy depleted cell at the same temperature means that its motion cannot be attributed to thermal fluctuations alone. Our observations of energy dependence in the movement of the λ -receptor should be considered when comparing diffusion in artificial membranes to diffusion in the membranes of living bacterial cells.

To elucidate the cause of the observed decrease of λ -receptor motility we invoked two models; model A assumed that the change in motility was caused by some ATP based activation energy which the bacterium uses to wiggle its λ -receptor when it is in a metabolically competent state. A fit of model A to the data showed that this activation energy, E_{active} from Equation 5, should be approximately 9 times larger than the thermal energy of the λ -receptor. Model B assumed that the observed decrease of λ -receptor motility was caused by a change in the stiffness of the attachment between the λ -receptor and the cell wall, κ_{cw} . A fit of model B to the data revealed that κ_{cw} should increase by a factor of approximately 28 upon energy depletion. The biological causes of such a stiffening could, for instance, be an aggregation of proteins around the λ -receptor, a stiffening of the lipids in the membrane, or a stiffening of the peptidoglycan layer, to which the λ -receptor is assumed attached (12). A χ^2 test of the two models is in favor of model A. However, in reality, the reduced motility is probably influenced by a mixture of both mechanisms. For convergence reasons, it was not possible to let too many parameters flow in the data analysis and we had to make separate fits of models A and B to the data.

To shed more light on the biological cause of the wiggling motion of the λ -receptor we also performed experiments where the peptidoglycan was damaged by ampicillin, a common antibiotic. Ampicillin hinders crosslinking of peptide bonds in the peptidoglycan layer and hence, inhibits the constant dynamic remodeling of the peptidoglycan layer. The result of ampicillin treatment was to efficiently stop the motion of the λ -receptor. However, if the cells were allowed to revive without ampicillin present, the receptors resumed the same motility as in the untreated cells. The decrease in motility upon ampicillin treatment is consistent with the results from Ref.(12) where the λ -receptor is postulated to be attached to the peptidoglycan, firmly enough to withstand SDS treatment. The fact that the λ -receptor resumes its motion upon removal of ampicillin suggests that the motility of the λ -receptor is very closely linked to the dynamic re-construction of the peptidoglycan layer.

Why would a bacterium spend energy moving its λ -receptor in the membrane? As the role of the λ -receptor is to facilitate the diffusion of maltodex-

trins across the outer membrane of Gram-negative bacteria, it is likely that the observed motility assists this task. It has been shown by crystallography that the λ -receptor has a so-called 'Greasy slide' consisting of six contingent aromatic residues, to which maltooligosaccharide binds during its guided diffusion into the cell (27, 28). We suggest that the motility of the receptor, the 'wiggling motion' (4, 6), assists in the guided diffusion, maybe by shaking the polymer loose from the greasy slide. An effect somehow parallel to the shaking of a salt container in order to overcome compactification of the salt crystals such that gravity can force salt onto your plate. The parallel of gravity would be the electrochemical potential favoring a cytoplasmic position of the polymer. We suggest that the binding of the λ -receptor to the peptidoglycan layer is a convenient way to make the receptor actively move, the natural and constant re-construction of the peptidoglycan will simply make anything connected to it move as well. When the cell is depleted of energy (e.g. by azide and arsenate poisoning), this energy consuming re-construction of the peptidoglycan cannot take place anymore and the λ -receptor stops moving. Another way to stop the motion is to directly target the peptidoglycan by ampicillin, which has a similar effect.

Future investigations will include observations of motility of other bacterial outer membrane proteins, among those which are not known to link to the peptidoglycan layer. Also, it is a very interesting question whether a similar effect is present in eucaryotic cells with a very different membrane structure.

Conclusion

We investigated the motility of a single λ -receptor in the outer membrane of *E. coli* and the dependence on energy metabolism. In an energetically competent cell, experiments using quantum dots as markers showed, in accordance with part of earlier literature (4, 5), that all λ -receptors performed a confined diffusion with a typical range of 50 nm. Poisoning the cell by azide and arsenate which stops energy metabolism, causes a rapid and significant decrease of motion of the λ -receptor. We propose a model with two possible causes of this decreased motility in energy depleted cells, one possible cause could be that an energetically competent cell actively uses energy to move the λ -receptor, this energy would be approximately one order of magnitude larger than thermal energy. Another cause could be that the attachment

between the λ -receptor and the membrane structure changes, e.g. by an aggregation of proteins or a stiffening of some part of the membrane structure. To further pinpoint the biological cause of the observed decreased motility, the effect of ampicillin treatment was investigated. Ampicillin directly targets the peptidoglycan layer, hindering transpeptidase action. Ampicillin effectively stopped the motility of the λ -receptor but we also observed that this effect was reversible. In summary, we propose that the λ -receptor is linked to the peptidoglycan layer and that the observed motility of the λ -receptor is directly linked to the energy dependent dynamic reconstruction of the peptidoglycan layer.

Acknowledgments

We are very grateful for discussions with T. Silhavy, K. Sneppen, R. Lipowsky and T. Heimburg. We deeply appreciate help from L. Jauffred with the quantum dot experiments.

References

1. Nakada, C., K. Ritchie, Y. Oba, M. Nakamura, Y. Hotta, R. Iino, R. Kasai, K. Yamaguchi, T. Fujiwara, and A. Kusumi. 2003. Accumulation of anchored proteins forms membrane diffusion barriers during neuronal polarization. *Nature Cell Biology* 5:626–632.
2. Suzuki, K., K. Ritchie, E. Kajikawa, T. Fujiwara, and A. Kusumi. 2005. Rapid Hop Diffusion of a G-Protein-Coupled Receptor in the Plasma Membrane as Revealed by Single-Molecule Techniques. *Biophysical Journal* 88:3659–3680.
3. Ritchie, K., and J. Spector. 2007. Single molecule studies of molecular diffusion in cellular membranes: Determining membrane structure. *Biopolymers* 87:95–101.
4. Oddershede, L., J. Dreyer, S. Grego, S. Brown, and K. Berg-Sørensen. 2002. The Motion of a Single Molecule, the λ -receptor, in the Bacterial Outer Membrane. *Biophysical Journal* 83:3152–3161.

5. Oddershede, L., H. Flyvbjerg, and K. Berg-Sørensen. 2003. Single-molecule experiment with optical tweezer improved analysis of the diffusion of the λ -receptor in *E. coli*'s outer membrane. *J. Phys.: Condens Matter* 15:S1737–S1746.
6. Gibbs, K., D. D. Isaac, J. Xu, R. W. Hendrix, T. J. Silhavy, and J. A. Theriot. 2004. Complex spatial distribution and dynamics of an abundant *Escherichia coli* outer membrane protein, LamB. *Molecular Microbiology* 53:1771–1783.
7. de Pedro, M., C. Grunfelder, and H. Schwarz. 2004. Restricted mobility of cell surface proteins in the polar regions of *Escherichia coli*. *J. Bacteriol.* 1:2594–2602.
8. Sabra, M., and O. Mouritsen. 1998. Steady-State Compartmentalization of Lipid Membranes by Active Proteins. *Biophysical Journal* 74:745–752.
9. Kaya, N., D. Wiersma, B. Poolman, and D. Hoekstra. 2002. Spatial Organization of Bacteriorhodopsin in Model Membranes. *The Journal of Biological Chemistry* 277:39304–39311.
10. Nikaido, H. 2003. Molecular Basis of Bacterial Outer Membrane Permeability Revisited. *Microbiology and Molecular Biology Reviews* 67:593–656.
11. Szmelcman, S., and M. Hofnung. 1975. Maltose transport in *Escherichia coli* K-12: Involvement of the bacteriophage lambda receptor. *Journal of Bacteriology* 124:112–118.
12. Gabay, J., and K. Yasunaka. 1980. Interaction of the *lamB* protein with the peptidoglycan layer in *Escherichia coli* k12. *Eur. J. Biochem.* 104:13–18.
13. Ryter, A., H. Shuman, and M. Scharwartz. 1975. Integration of the Receptor for Bacteriophage Lambda in the Outer Membrane of *Escherichia coli*: Coupling with Cell Division. *Journal of Bacteriology* 122:295–301.
14. Vos-Scheperkeuter, G., E. Pas, G. Brakenhoff, N. Nanninga, and B. Witholt. 1984. Topography of the Insertion of LamB Protein into the Outer Membrane of *Escherichia coli* Wild-Type and lac-lamB Cells. *Journal of Bacteriology* 159:440–447.

15. Brown, S. 1997. Metal-recognition by repeating polypeptides. *Nature Biotechnology* 15:269–272.
16. Miller, J. 1972. Experiments in Molecular Genetics. Cold Spring Harbor Laboratory Press, New York.
17. Pardee, A., F. Jacob, and J. Monod. 1959. The genetic control and cytoplasmic expression of "inducibility" in the synthesis of beta-galactosidase by *E. coli*. *J. Mol. Biol.* 1:165–178.
18. Neidhardt, F., P. Bloch, and D. Smith. 1974. Culture Medium for Enterobacteria. *Journal of Bacteriology* 119:736–747.
19. Oddershede, L., S. Grego, S. Nørrelykke, and K. Berg-Sørensen. 2001. Optical Tweezers: Probing Biological Surfaces. *Probe Microscopy* 2:129–137.
20. Rasmussen, M., L. Oddershede, and H. Siegumfeldt. 2008. Optical tweezers cause physiological damage to *E. coli* and *Listeria* bacteria. *Applied and Environmental Microbiology* 74:2441–2446.
21. L.Jauffred, T. Callisen, and L. Oddershede. 2007. Viscoelasticity of bacterial tethers. *Biophysical Journal* 93:1–8.
22. Hansen, P., I. Tolic-Nørrelykke, H. Flyvbjerg, and K. Berg-Sørensen. 2006. Tweezercalib 2.0: Faster version of a MatLab package for precision calibration of optical tweezers. *Computer Phys. Comm.* 174:518–520.
23. Berg-Sørensen, K., L. Oddershede, E.-L. Florin, and H. Flyvbjerg. 2003. Unintended Filtering in Typical Photodiode Detection System for Optical Tweezers. *Journal of Applied Physics* 93:3167–3176.
24. Reed, K., and J. J.E. Cronan. 1991. Escherichia coli exports previously folded and biotinylated protein domains. *J. Biol. Chem.* 266:11425–11428.
25. Jander, G., J. J. E. Cronan, and J. Beckwith. 1996. Biotinylation in vivo as a sensitive indicator of protein secretion and membrane protein insertion. *J. Bacteriol.* 178:3049–3058.
26. Gov, N. 2004. Membrane Undulations Driven by Force Fluctuations of Active Proteins. *Physical Review Letters* 93:1–4.

27. Schirmer, T., T. Keller, Y.-F. Wang, and J. Rosenbusch. 1995. Structural basis for sugar translocation through maltoposin channels at 3.1 Å resolution. *Science* 267:512–514.
28. van Gelder, P., F. Dumas, I. Bartoldus, N. Saint, A. Prilipov, M. Winterhalter, Y. Want, A. Philippsen, J. Rosenbusch, and T. Schirmer. 2002. Sugar transport through maltoporin of *Escherichia coli*: Role of the greasy slide. *Journal of Bacteriology* 184:2994–2999.

Figure Legends

Figure 1.

An illustration of Models A and B for the effect of energy depletion. The λ -receptor is a trimer located in the outer membrane of *E. coli* bacteria, it is assumed to connect to the peptidoglycan layer (12). In **model A** the λ -receptor in a metabolically competent cell is assumed to be actively moved, the cell spends energy to wiggle the λ -receptor. This is illustrated by the pick-up truck moving the protein around before energy depletion. In **model B** the energy depletion somehow modifies the membrane structure. We have illustrated this change of membrane structure by moving other membrane proteins closer to the λ -receptor and by making the attachment to the peptidoglycan layer stronger.

Figure 2.

Effect of energy depletion. The graph shows the position as a function of time of a bead attached to a λ -receptor. The motility of the same receptor is shown both before (blue) and after (red) the energy poisoning by azide and arsenate. The left inset shows a histogram of the positions visited both before (blue broad histogram) and after (red narrow histogram) poisoning. The right inset shows a scatter plot of the positions visited by the bead-receptor complex both before (blue) and after (red) energy depletion.

Figure 3.

Power spectra calculated from the position time series of the λ -receptor before (upper set of data points) and after (lower set of data points) energy depletion. The full lines overlaying the data show a fit of the model, Eq. (6) to the data and inserts display scatter plots, demonstrating the quality of the fits. The data are fitted by Model A.

Figure 4.

The effect of treating the cells with ampicillin. The graph shows the position as a function of time of a bead attached to a λ -receptor. The motility of a receptor is shown both without (blue) and with (red) treatment by ampicillin. The left inset shows a histogram of the positions visited both without (blue

broad histogram) and with (red narrow histogram) ampicillin. The right inset shows a scatter plot of the positions visited both without (blue) and with (red) ampicillin.

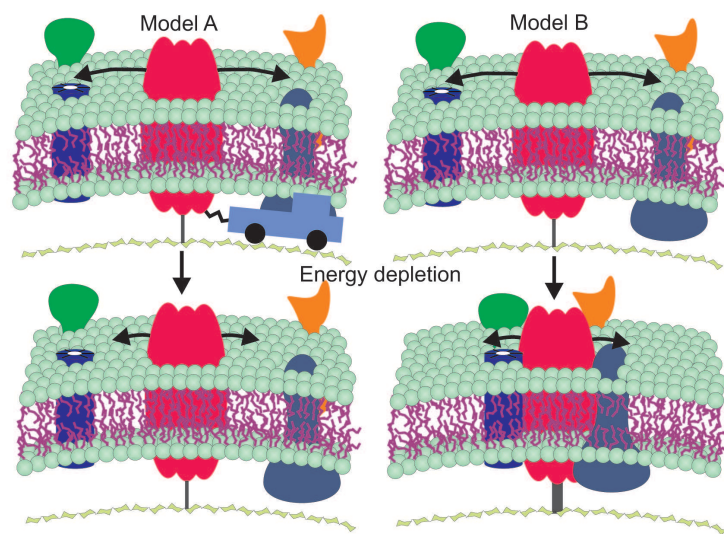


Figure 1:

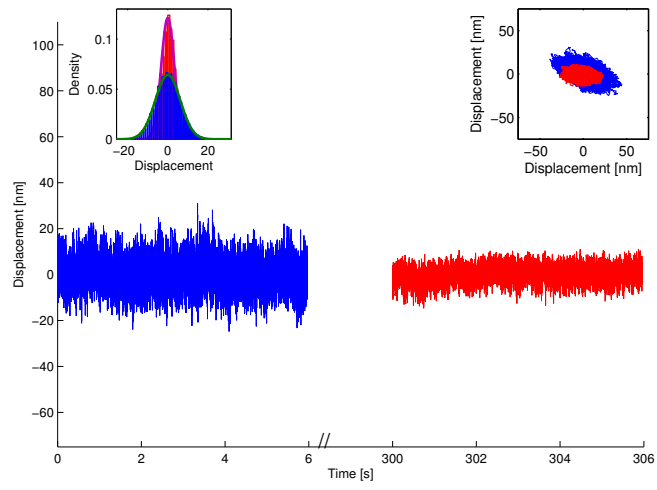


Figure 2:

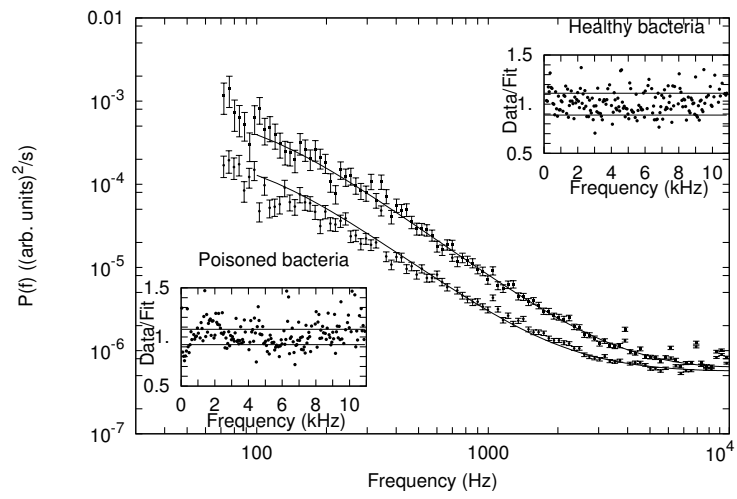


Figure 3:

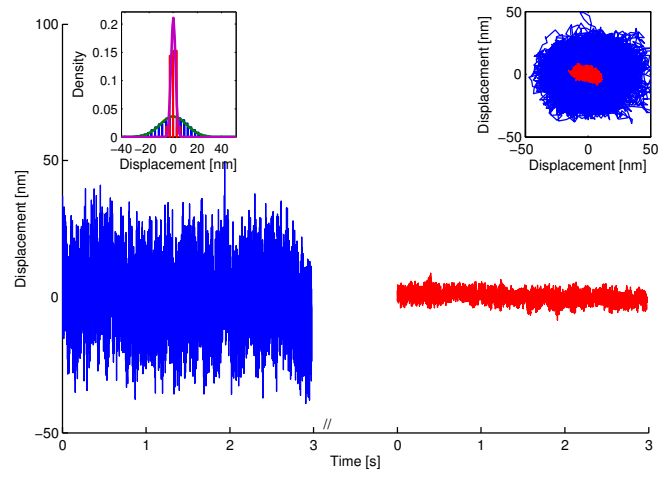


Figure 4:

Effect of antibiotics and antimicrobial peptides on single protein motility

Tabita Winther and Lene Oddershede*

The Niels Bohr Institute, University of Copenhagen, Blegdamsvej 17, DK-2100 Copenhagen, Denmark

Abstract:

Following the movement of individual molecules of a bacterial surface protein *in vivo* we investigated the effects of antibiotics and antimicrobial peptides on protein motility and membrane structure. In previous work we engineered the λ -receptor of *Escherichia coli* such that less than one receptor per cell is *in vivo* biotinylated and can bind to a streptavidin coated bead. Such a bead served as a handle for the optical tweezers to follow the motion of an individual receptor. In an un-perturbed living cell the λ -receptor performs a confined diffusive motion. The λ -receptor links to the peptidoglycan layer, and indeed, a perturbation of the peptidoglycan layer had a pronounced effect on the motility of the receptor: The motility significantly decreases upon treatment with vancomycin or ampicillin, to study the effect of vancomycin we used strains with increased membrane permeability. As the motility of an individual receptor was monitored over an extended amount of time we were able to observe a temporal evolution of the action of vancomycin. Antimicrobial peptides (AMPs) are alternatives to conventional antibiotics in the treatment of bacterial infections. Therefore, we also investigated the effect of the toxic AMP polymyxin B (PMB) which targets both the outer and inner membranes and kills the organism. PMB significantly decreased the motility of the lambda-receptor. On the basis of these findings we confirm that the λ -receptor is firmly attached to the peptidoglycan layer, and that an antibiotic or AMP mediated destruction of the dynamic peptidoglycan synthesis decreases the receptor motion.

Keywords:

Antibiotics; ampicillin; vancomycin; antimicrobial peptides; single molecule biophysics; lambda-receptor; *E. coli*; peptidoglycan

* Corresponding author. Email: oddershede@nbi.dk

Introduction:

The vast majority of previous investigations regarding the action of antibiotics and antimicrobial peptides have been performed by ensemble experiments, such yielding average information regarding the influence of a particular potential drug. Ensemble studies have been and are by far the most common way to investigate biological phenomenon, and they are the standard against which single molecule experiments are compared. The rapid evolution of single molecule biophysics have proven, however, that studies on the single molecule level can reveal spatial and temporal inhomogeneities, which are hidden in ensemble studies. Such inhomogeneities can be important and carry fundamental information regarding the basic function of a given bio-molecule. One beautiful example is that of polymerase, where single molecule studies have revealed information regarding the working mechanism, energy turn-over, typical speeds and forces, this type of information being hidden in ensemble studies [1, 2].

The bacterial outer membrane structure is a typical target both for antibiotics and antimicrobial peptides and the motility of outer membrane proteins can therefore be used as an indirect measure of their action. The diffusion of individual proteins has been studied mainly in eucaryotic cells, for a review see [3]. Only very few experimental investigations have reported on the diffusion of single proteins in the outer membrane of metabolically competent procaryotic cells [4, 5, 6]. These investigations focused on the motility of the λ -receptor in the outer membrane of *E. coli*. The λ -receptor is an 18 stranded β -barrel with the purpose of transporting maltodextrins across the outer membrane and is also the receptor of bacteriophage lambda. The λ -receptor is an integral outer membrane protein attaching firmly to the peptidoglycan layer [7]. Here we used an engineered λ -receptor [4], where we inserted a biotin acceptor site into an external loop of the protein. In energetically competent cells, the λ -receptor performs a confined diffusional motion, a 'wiggling' motion, within a range of approximately 50 nm [4, 5, 8]. This motility of the λ -receptor has recently been shown to be energy dependent and to decrease significantly upon energy depletion of the cell [8]. It was also proposed that the observed motility of the λ -receptor was an result of its close linking to the peptidoglycan layer, which performs a constant, dynamic, and energy consuming re-construction, and that the purpose of linking the λ -receptor to the peptidoglycan layer was to 'wiggle' the protein, which then, in turn, could facilitate transport of maltodextrins through the porin.

In the present investigation we used the λ -receptor as a tracer to monitor the action of vancomycin and ampicillin, two common antibiotics hindering peptidoglycan synthesis, on the outer membrane of *E. coli*. Also, we investigated the effect of the antimicrobial peptides, polymyxin B (PMB) and polymyxin B-nonapeptide (PMBN), on λ -receptor motility. PMB is a common antimicrobial peptide, which is known to increase inner and outer membrane permeability and kill the microorganism. PMBN is a truncated derivate of PMB and only increases outer membrane permeability. Both these drugs are known to act rapidly and in very small doses [9]. The paper is organized such that the methods and results of applying each drug is presented individually. The discussion unifies all results into a model of how antibiotics and antimicrobial peptides act on a single protein in the outer bacterial and which implications this has for our understanding of the attachment of the λ -receptor in the outer bacterial membrane.

Position measurements:

In order to find the positions visited by the λ -receptor a streptavidin coated polystyrene bead was attached to the receptor and used as a handle for position-measuring optical tweezers. The λ -receptor was *in vivo* biotinylated, the efficiency of the biotinylation being very low; on average less than one λ -receptor per bacterium had biotin attached to an extra cellular site. This ensures that each streptavidin coated bead was only attached to a single biotinylated λ -receptor. The strains were derived from S2188 [10] and the biotinylation procedure and controls are described in Ref. [4]. The motion of the protein can be deduced from the motion of the bead [4], and the motion of the bead was monitored by optical tweezers based on a Nd:YVO₄, wavelength 1064 nm. The trap was implemented in a Leica inverted microscope DM IRBE and the forward scattered light collected by a quadrant photodiode (Hamamatsu S5981). For a detailed description of the settings and how the laser signal is converted to position measurements please see Refs. [4, 8]. The laser power delivered at the sample was around 10 mW and the total exposure time a couple of seconds. At such low exposure doses there is no detectable physiological damage on bacterial species, even if they are in the most intense region of the trap [11]. The first step in the position measurement procedure was to trap a bead free in solution and perform a force calibration at the same height as a bead attached to a λ -receptor [4]. Secondly, we measured a time-series of the positions of a bead attached to a λ -receptor, this attachment being characterized by a ‘wiggling’ motion of the bead [4]. Unspecifically attached beads did not ‘wiggle’ and if an unspecifically attached bead is pulled away from the bacterium using the optical tweezers, a viscoelastic tether composed of membrane material will be extracted [12].

Vancomycin:

Vancomycin blocks peptidoglycan synthesis and is normally used against gram positive bacteria lacking the outer membrane part. Vancomycin is too large to pass the outer membrane of normal gram negative bacteria. However, gram negative bacteria with the mutation of increased outer membrane permeability (*imp*) are susceptible to larger molecules as vancomycin or bile salts. Increased membrane permeability in *E. coli* was found in 1989 [13], and it was recently established that this was due to the absence of one of two outer membrane proteins [14, 15]. To test the action of vancomycin we made *imp* strains as described below.

Strains: To conduct these experiments we needed a strain with increased outer membrane permeability, without pili, and without un-modified λ -receptors. Thomas Silhavy and Natividad Ruiz kindly provided strain NR701, which is MC4100 *imp4213 yfhS::Tn10*. We used a P1 transduction to transfer *imp4213* in the strain S1964 [16]. To follow the transfer of *imp4213*, the gene of arabinose was chosen as a marker. NR701 is *ara-*, so first we made it *ara+*. To complete the P1 transduction a single phage colony was obtained by growing P1vir on the bacteria S971 [17]. The single phage colony was used on MG1655 to transfer *ara+* into NR701. Then *ara+ imp4213* was co-transduced into S1964 [16] which is without pili, is *ara::Tn10* and has no λ -receptors. This strain was termed TM14. Then the plasmid pLO16 [4] coding for the modified λ -receptors was

inserted. A successful insertion of *imp4213* was controlled by sensitivity to bile salts and no growth in the presence of a SDS disk.

Methods: Bacterial colonies were grown over night at 37 °C on YT agar [18] supplemented with 25 µg/ml chloramphenicol. A single colony was picked and suspended into M63 media [19] containing 1 µg/ml B1, 25 µg/ml Chloramphenicol, 0.1 % casein hydrolysate, and 0.2 % glycerol. The bacteria were grown in shaking water bath over night at 37 °C. 0.1 ml of the overnight culture was then diluted into 3 ml of fresh M63 media and grown at 37 °C until log-phase. To induce the expression of the λ -receptor 3 ml of fresh M63 media supplemented with IPTG was added to a final IPTG concentration of 0.5mM. The bacteria were grown for an additional ½ hour with IPTG. 1 ml cell culture was spun down at 5000 rpm for 5 minutes and the cells resuspended in 100 µl buffer. The buffer used throughout the experiments was 10 mM potassium phosphate, 0.1 M KCl, pH 7. The procedure until this point was carried out at 37 °C, after this point at room temperature unless otherwise stated.

The beads used were streptavidin-coated polystyrene beads with a diameter of ~ 0.5 µm (Bangs Laboratories, Inc). The beads were suspended in millipore water and centrifuged at 1673 x g for 10 min. The supernatant was discarded and the beads resuspended in buffer and sonicated for at least 15 min to remove aggregates. To immobilize the bacteria a droplet of 10 mM poly-l-lysine was spread on a 0.17 mm coverslip and left to dry. This coverslip formed the bottom of a perfusion chamber. 10 µl of the bacterial solution was perfused into the chamber, this step was repeated. The bacteria were left for 15-25 minutes to adhere to the surface. Ten microliters of 12.5 mg/ml heparin supplemented was flushed into the samples and left for 15 minutes. Heparin decreases the attraction between the surface and the streptavidin-coated beads. The samples were rinsed four times with buffer. 10 µl washed streptavidin coated polystyrene beads was then perfused into the chamber and left for 15 minutes to attach to the λ -receptors. Finally, the chamber was flushed 3-5 times with M63 glucose media. Glucose was used as a carbon source inside the perfusion chambers to support anaerobic growth. The chambers were stored at 4°C until use.

The positions of beads attached to λ -receptors in untreated cells were measured as described above. Thereafter the the cells were treated with vancomycin by flushing 20 µl of 0.08 mg/ml vancomycin in M63 glucose through the chamber 5 times. This concentration is 100 × MIC [20]. After a delay of roughly 3 min the chamber was flushed 5 times again with vancomycin solution and finally, the mobility of the exact same λ -receptor was measured again.

Results: Figure 1 shows a timeseries of positions visited by a single λ -receptor before and after treatment with vancomycin, note that it is exactly the same receptor which is monitored both before and after treatment. The gap in the timescale denotes the time where the vancomycin treatment takes place. The right inset shows the distribution of the visited positions before (broad histogram) and after (narrow histogram) vancomycin treatment, full lines are Gaussian fits. The left inset shows a scatterplot of the positions visited before (black) and after (grey) vancomycin treatment.

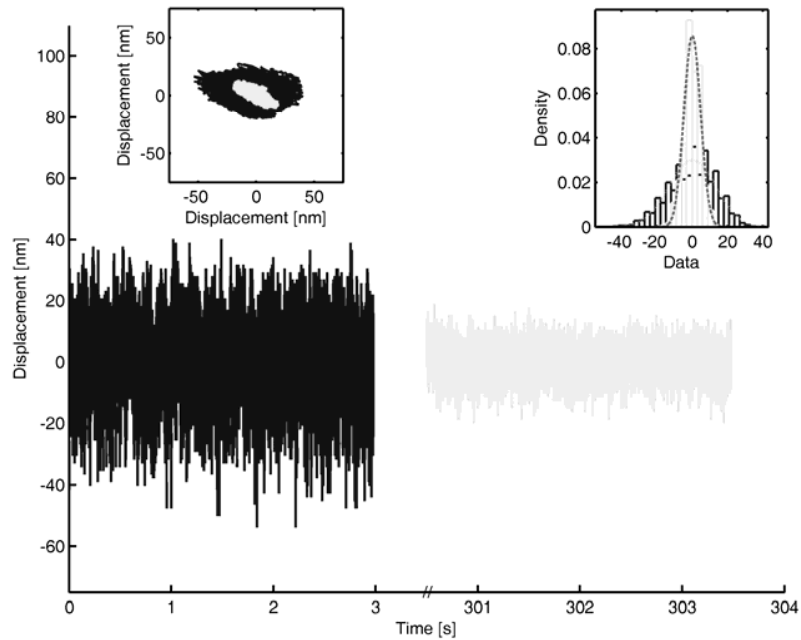


Figure 1: Effect of vancomycin treatment. Time series of positions visited by an individual λ -receptor before (black) and after (grey) vancomycin treatment. The right inset shows a histogram of positions visited before (broad histogram) and after (narrow) vancomycin treatment. The left inset shows a scatterplot of positions visited before (black) and after (grey) vancomycin treatment.

From Figure 1 it is clear that the motility of the λ -receptor decreases upon treatment with vancomycin. We have chosen to quantify the motility of the λ -receptor by the width of the position histograms (inset of Figure 1), the larger the standard deviation of the histogram, σ , the more motile the λ -receptor. Before vancomycin treatment the standard deviation of the receptor bead complex was $\sigma_{\text{before}} = (9.6 \pm 0.97)$ nm (mean \pm SEM), and after treatment $\sigma_{\text{after}} = (3.4 \pm 0.44)$ nm, $n = 10$. To test whether these two numbers are significantly different a Student's T-test was made. The resulting p-value gives the probability that the observed difference is accidental. In other words, a low p-value supports the hypothesis that the numbers are significantly different. A T-test on the σ values with and without vancomycin gave $p = 0.0002$. Hence, we conclude that the motility of a λ -receptor in an untreated cell is significantly larger than in a cell treated with vancomycin.

The cells were grown at 37°C and the measurements shown in Figure 1 and the numbers given above were from experiments performed at room temperature (22°C). Using a heated sample and objective holder we also performed similar measurements at 37°C . The results obtained at 37°C ($n=10$) were indistinguishable from those performed at 22°C ($n=10$), however, they were more noisy which is probably because the experiments were technically more difficult and the temperature was higher.

We also monitored the possible time evolution of the λ -receptor motility pattern upon vancomycin treatment. Immediately after vancomycin treatment the motility had decreased, hence, vancomycin seemed to have a rapid effect. Both at 22 °C and 37 °C the motility of the receptor was a bit higher after 15 minutes than immediately after treatment. After 30 minutes the motility was smaller than after 0 minutes, and also significantly smaller than after 15 minutes (on a 5 pct. significance level). Hence, there seems to be an evolution of λ -receptor motility as a function of time after beginning of vancomycin treatment: The treatment seems to have a rapid effect (after 0-3 minutes), then the receptor regains some motility, and finally (after 30 minutes), motility is down to a minimum, possibly corresponding only to thermal fluctuations.

Ampicillin:

Ampicillin is a common antibiotic, efficient towards gram negative bacteria and hindering peptidoglycan synthesis. The effect on λ -receptor motility of ampicillin treatment with was first reported in [8] but for sake of completeness the results are briefly reviewed here.

Strains: The strains used are *E. coli* K12 S2188 [10] harboring the pLO16 plasmid [4].

Methods: In the experiments with ampicillin the procedure was largely as described under ‘Vancomycin methods’. However, one important difference is that all solutions (starting from the 3 ml fresh M63 into which the overnight culture was diluted) were supplemented with 12 % sucrose. Sucrose was supplemented in order to osmotically stabilize cells with comprised cell walls. After reaching log-phase the M63-IPTG solution was supplemented with 100 $\mu\text{g/ml}$ ampicillin. Due to the length of time needed for the action of ampicillin and to regenerate the cell wall after ampicillin treatment we did not examine the same λ -receptor before and after treatment, different populations were observed. Three types of experiments were conducted: 1) With ampicillin present both during growth and during the measurement procedure. 2) With ampicillin present during growth but not during the measurement procedure. 3) A control where ampicillin was not present neither during growth nor during the measurement procedure.

Results: Figure 2 shows the motility of a λ -receptor in a metabolically competent cell (population 3) and in a cell treated with ampicillin (population 1). Insets show corresponding histograms and scatterplots. Treatment with ampicillin significantly decreases λ -receptor motility. The numbers resulting from the analysis are summarized in Table 2.

	Population 1	Population 2	Population 3 (control)
Growth	+ Ampicillin	+ Ampicillin	No Ampicillin
Experiment	+ Ampicillin	No Ampicillin	No Ampicillin
n (# datasets)	38	28	24
$\sigma \pm \text{SEM}$ [nm]	3.43 ± 0.32	10.25 ± 0.69	11.32 ± 0.85

Table 2: Results of ampicillin treatment.

The standard deviation of populations 1 and 3 characterizing the motility of the λ -receptor significantly decreases upon treatment with ampicillin (Students T-test gave $p = 2.1 \times 10^{-14}$). Also, a comparison of populations 1 and 2 showed a significant difference ($p = 8 \times 10^{-15}$). But populations 2 and 3 are indistinguishable. Hence, the λ -receptor mobility significantly decreases upon ampicillin treatment, but if the cells are transferred to ampicillin free growth media, the original λ -receptor motility can be restored [8]. The standard deviation characterizing the motility of the ampicillin control is slightly higher than that of the vancomycin controls. This could be due to the change in index of refraction caused by the presence of sucrose in the measurement chamber (which, in turn, changes the properties of the optical trap).

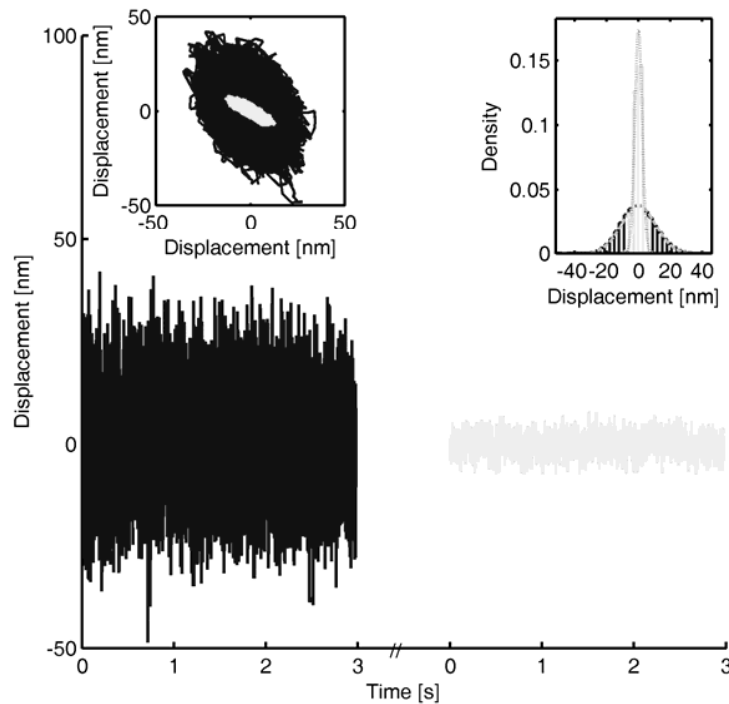


Figure 2: Effect of ampicillin treatment. The left part of the time series (black) shows the positions visited of a λ -receptor in a metabolically competent cell (population 3), the right part (grey) in a cell treated with ampicillin (population 1). The right inset shows a histogram of positions visited without (broad histogram) and with (narrow) ampicillin treatment. The left inset shows a scatterplot of positions visited without (black) and with (grey) ampicillin treatment.

Antimicrobial peptides:

The two antimicrobial peptides investigated in the present study are polymyxin B (PMB) and its truncated derivative polymyxin B-nonapeptide (PMBN). Figure 3 shows the chemical construction of PMB, and if a cut is made at the arrow the left part of the structure is PMBN. PMB increases the permeability of both the inner and outer membranes of gram negative bacteria [9]. This renders the bacterium unable to maintain an electrochemical gradient across its cell membrane and causes cell death. PMBN, on

the other hand, only makes the outer cell wall more permeable (does not cause cell death).

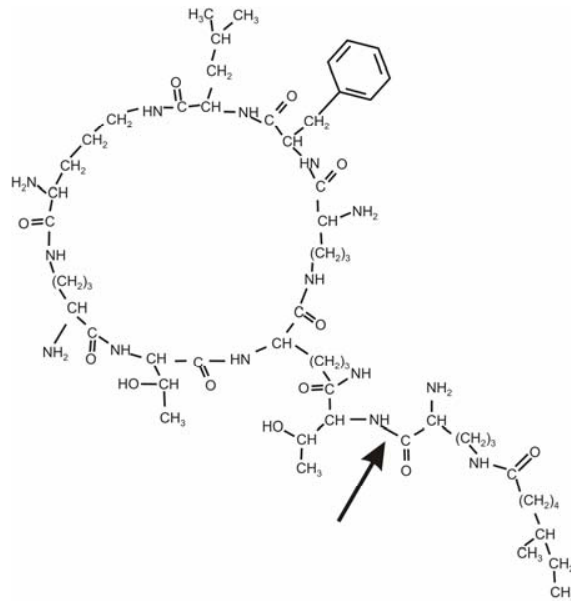


Figure 3: Schematic drawing of the chemical structure of PMB. If a cut is made at the arrow the left part of the structure is the truncated derivative PMBN.

Strains: The bacterial strain used is the same as in the ampicillin experiments.

Methods: As for vancomycin experiments. In the experiments with PMB first the motion of an individual λ -receptor was first measured in an untreated cell. Then the chamber was flushed with 5×10^6 μl buffer containing $100 \mu\text{g/ml}$ PMB and the motility of the same λ -receptor was measured after treatment with PMB. In the experiments with PMBN, $125 \mu\text{M}$ PMBN was flushed into the chamber before flushing with heparin and the chamber was left for 30 minutes with PMBN. The reason for this particular point of the procedure is that PMBN is known to bind electrostatically to the membrane, and heparin might thus shield this binding [21]. This concentration of PMBN is well above the concentrations which are reported to have an effect [9].

Results: Treatment of cells with the toxic PMB significantly decreases λ -receptor motility. This is shown in Figure 4 which shows a time series of the motility of the same λ -receptor before (black) and after (grey) treatment with PMB. The histograms of positions visited were well fitted by Gaussian functions as shown in the right insert. The left inset shows a scatter plot of positions visited.

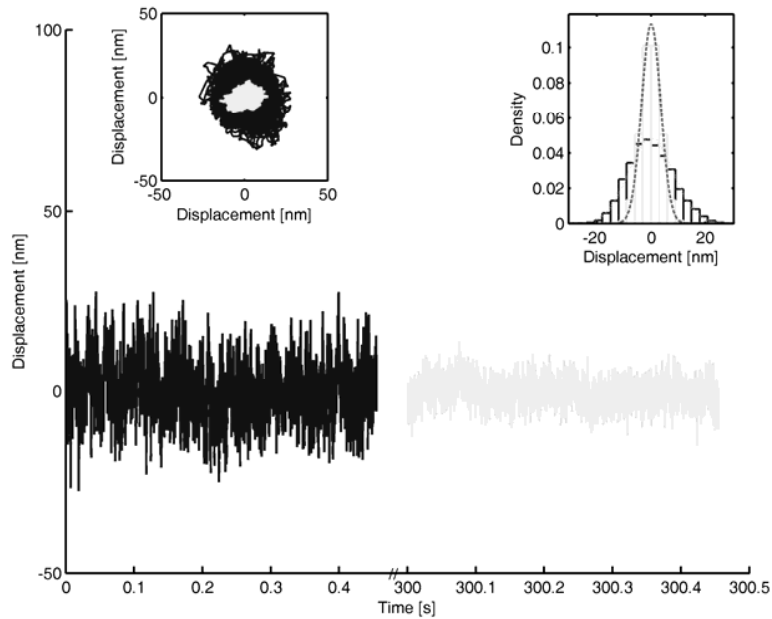


Figure 4: Effect of PMB treatment. Time series of positions visited by an individual λ -receptor before (black) and after (grey) vancomycin treatment. The right inset shows a histogram of positions visited before (broad histogram) and after (narrow) PMB treatment. The left inset shows a scatterplot of positions visited before (black) and after (grey) PMB treatment.

Again, λ -receptor motility was quantified by the standard deviation of the position histograms, and the results were $\sigma_{\text{before}} = (9.13 \pm 0.59)$ nm, and $\sigma_{\text{after}} = (3.32 \pm 0.67)$ nm, $n = 12$. These numbers are significantly different ($p = 0.00003$).

Treatment with PMBN did not give rise to a change in λ -receptor motility upon comparison with a control: $\sigma_{\text{PMBN}} = (9.53 \pm 0.41)$ nm, $n = 34$, and $\sigma_{\text{control}} = (9.68 \pm 0.53)$ nm, $n = 18$.

Discussion

Our results show that the motility of individual λ -receptors in the outer membrane of *E. coli* is strongly influenced by antibiotics and antimicrobial peptides because treatment with vancomycin, ampicillin and PMB significantly reduced λ -receptor motility. To investigate the effect of vancomycin treatment we cloned a strain with increased outer membrane permeability (*imp*). A comparison of the vancomycin control to the PMB, PMBN, and antibiotics controls show that λ -receptor motility is unaffected by the *imp* modification.

A strength of single molecule investigations is the ability to follow temporal behaviors masked in ensemble experiments. This, we utilized here to follow the temporal evolution

of the action of vancomycin on λ -receptor motility. Though vancomycin rapidly (within 0-3 minutes) decreased λ -receptor motility, the motility decreased significantly further after 30 minutes. This could give clues about the detailed action of vancomycin [22]: Vancomycin binds to intermediates in peptidoglycan synthesis. Therefore rapid action of vancomycin may be simply steric rather than compromised structural integrity. On longer time scales, the action might be compromised structural integrity caused by the hindered peptidoglycan synthesis.

A physical model of the attachment of the λ -receptor in the outer membrane of *E. coli* was put forward [4]. Later this model was expanded to include possible causes of energy depletion, which is also known to cause a significant decrease in λ -receptor motility [8]. Basically, the expanded model assumes the λ -receptor to perform a diffusive motion within the cell wall structure, the diffusive motion being mediated by thermal fluctuations and possibly also by active (ATP consuming) movement. Alternatively, the observed decrease in motility upon energy depletion could be caused by a change in the membrane structure, e.g., by an aggregation of proteins which could mediate a stiffening of the effective potential felt by the protein in the membrane [8]. The λ -receptor is firmly attached to the peptidoglycan layer [7], and in [8] it was proposed that the observed motility of the λ -receptor was mediated by the constant, dynamic, and energy consuming re-construction of the peptidoglycan layer.

Figure 5 shows a schematic drawing of the effect of the antibiotics and antimicrobial peptides used in the present investigation. The upper part shows the situations before treatment, the lower part the situations after. In an untreated cell, the λ -receptor performs an 'active' motion (visualized by the truck in Figure 5). Vancomycin and ampicillin both hinder peptidoglycan synthesis and are observed to decrease motility. PMB increases permeability of both the inner and outer membranes, destroys the electrochemical gradient across the inner cell wall and kills the cell. This also decreases λ -receptor motility. As PMB destroys the electrochemical gradient across the inner cell wall its biological action is somewhat similar to that of azide and arsenate, as reported in [8]. Hence, the results of PMB support the results and hypothesis put forward in [8].

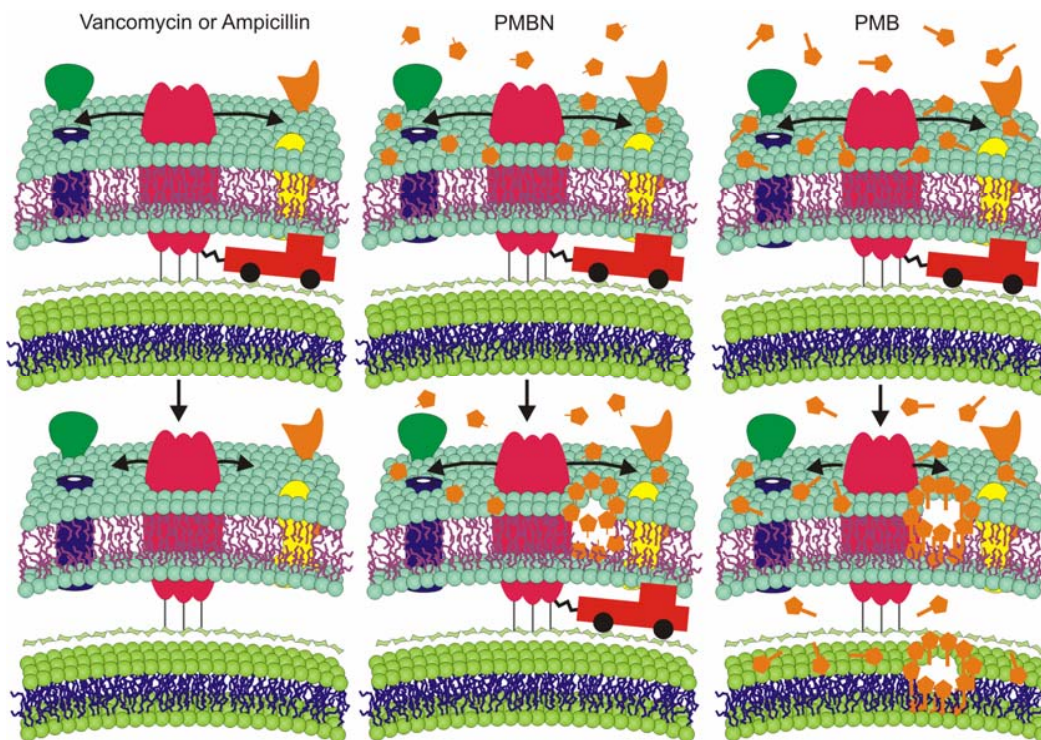


Figure 5: Schematic drawing of the action of vancomycin, ampicillin, PMBN, and PMB on the membrane structure, and hence on the motility of the λ -receptor. The upper row shows the situation before treatment, the lower row after treatment. An active motion of the λ -receptor is illustrated by the truck and the larger side-wards arrows. The λ -receptor is the pink tri-mer, the outer membrane is light blue, the peptidoglycan light grey, the inner membrane green, and both PMB and PMBN are colored orange.

We did not see an effect of PMBN treatment. This is probably because PMBN does not effect λ -receptor motility. PMBN was added during preparations but not in the final chamber. As its interaction is known to be strong and electrostatic PMBN is assumed to be firmly attached to the membranes also during the position measurements. However, there is a small risk that the bacteria resumed 'normal' protein motility when the drug was not abundantly present.

Altogether, the results of the present investigation show that a hindering of peptidoglycan synthesis, either by vancomycin or by ampicilling, decreases λ -receptor motility. The same effect is seen by treatment with PMB, which targets both the outer and inner membranes and kills the cell. No effect was seen with PMBN which only targets the outer membrane. Also, the *imp* modification of the bacteria which affected the outer membrane permeability had no effect. These observations strongly support the hypothesis put forward in Ref. [8] that the motility of the λ -receptor is mediated through its firm connection to the peptidoglycan layer. In other words, constant 'earthquakes' in the peptidoglycan layer give rise to the observed motility of the λ -receptor. Perturbations of the outer membrane had no effect on λ -receptor motility.

Conclusion:

We investigated the effect of antibiotic treatment on the motility of a single protein, the λ -receptor, in the bacterial outer membrane. An *E. coli* strain with increased outer membrane permeability thus allowing for transport of vancomycin was cloned. Treatment of this strain with vancomycin significantly decreased λ -receptor motility, this effect being present both at 22°C and at 37°C. A strength of the measurements was that the motility of an individual λ -receptor was observed for an extended period of time, both before and after exposure. This allowed us to observe a temporal evolution in the action of vancomycin: Vancomycin rapidly decreased the motility of the receptor, but after 30 minutes there was a significant further decrease of motility. Treatment with ampicillin also decreased λ -receptor motility. The same effect was observed after treating cells with PMB, an antimicrobial peptide, which increases permeability of both the inner and outer membranes and kills the cells. PMBN, which only targets the outer membrane, had no effect on λ -receptor motility. Altogether, we observed that if the re-construction of the peptidoglycan layer is hindered by vancomycin or ampicillin, or if the cell is killed by PMB, the motility of the λ -receptor decreases. This supports the hypothesis put forward in Ref. [8] that the λ -receptor is firmly attached to the peptidoglycan layer, and that its motility originates from the energy consuming motion of the peptidoglycan layer. Apart from providing detailed information on the biological causes of bacterial membrane protein motility, this investigation also paves the way for future investigations on the temporal evolution of the action of antibiotics and antimicrobial peptides on a single molecule level.

Acknowledgements:

We acknowledge discussions with S. Brown and financial support from BioNET, sponsored by the Villum Kann Rasmussen Foundation.

- [1] Wang, M. D.; Schnitzer, M. J.; Yin, H.; Landick, R.; Gelles, J.; Block S. M. (1998) *Science*, **282**, 902-907.
- [2] Shaevitz, J. W.; Abbondanzieri, E. A.; Landick, R.; Block, S. M. (2003) *Nature*, **426**, 684-687.
- [3] Ritchie, K. and Spector J. (2007) *Biopolymers*, **87**, 95-101.
- [4] Oddershede, L.; Dreyer, J. K.; Grego S.; Brown S.; Berg-Sørensen, K. (2002) *Biophysical Journal*, **83**, 3152-3161.
- [5] Oddershede, L.; Flyvbjerg, H.; Berg-Sørensen, K. (2003) *J. Phys.: Condens Matter*, **15**, 1737-1746.
- [6] Gibbs, K. A.; Isaac, D. D.; Xu, J.; Hendrix, R. W.; Silhavy, T. J.; Theriot, J. A. (2004), *Molecular Microbiology*, **53**, 1771-1783.
- [7] Gabay, J.; Yasunaka, K. (1979) *European Journal of Biochemistry*, **104**, 13-18.

- [8] Winther T.; Lei, X.; Berg-Sørensen, K.; Brown S.; Oddershede, L. (2009) *Submitted*.
- [9] Sahalan, A. Z. and Dixon R. A. (2008) *Antimicrobial*, **31**, 224-227.
- [10] Brown, S. (1997) *Nature biotechnology*, **15**, 269-272.
- [11] Rasmussen, M. B.; Oddershede, L.; Siegumfeldt; H. (2008) *Applied and Environmental Microbiology*, **74**, 2441-2446.
- [12] Jauffred, L.; Callisen, T.H.; Oddershede, L.B. (2007) *Biophysical journal*, **93**, 1-8.
- [13] Sampson, B. A.; Misra, R. and Benson S. A. (1989) *Genetics*, **122**, 491-501.
- [14] Ruiz, N.; Falcone, B.; Kahne, D. and Silhavy T. J. (2005) *Cell*, 307-317
- [15] Wu, T.; Malinverni, J.; Ruiz, N.; Kim, S.; Silhavy, T. J. and Kahne, D. (2005) *Cell*, **121**, 235-245.
- [16] Brown, S. (1992) *PNAS*, **89**, 8651-8655.
- [17] Brown, S. (1987) *Cell*, **49**, 825-833.
- [18] J. H. Miller (1972), *Experiments in Molecular Genetics*, Cold Spring Harbor Laboratory Press, New York.
- [19] Pardee, A; Jacob F.; Monod, J. (1959) *J. Mol. Biol.*, **1**, 165-178.
- [20] Eggert, U. S.; Ruiz, N.; Falcone, B. V.; Branstrom, A. A.; Goldman, R. C.; Silhavy, T. J. and Kahne, D. (2001) *Science*, **294**, 361-364.
- [21] Gutschmann, T.; Hagge, S. O.; David, A.; Roes, S.; Böhling, A.; Hammer, M. U.; Seydel U. (2005) *Journal of Endotoxin Research*, **11**, 167-73.
- [22] Loll, P.J.; Axelsen P.H. (2000) *Annu. Rev. Biophys. Biomol. Struct.*, **29**, 265-89.